a.y. 2012-2013

University of Padova – Department of Civil Engineering ICEA

Laboratoired'Etude des Transferts en Hydrologie et Environnement (LTHE)

Master Thesis

BEHAVIOUR OF TOP COVER OF A LANDFILL FOR RADIOACTIVE WASTE SUBJECTED TO SETTLEMENTS

Supervisors

Prof. Paolo CARRUBBA Prof. Jean-Pierre GOURC

Emilia Capecchi

Index

Abstract

Radioactive waste is currently disposed in specific facilities world-wide. The safety of these facilities relies on the use of engineered barriers, such as a cap liner, to isolate the waste and protect the environment. Generally, the materials used in the barrier layer should offer low permeability and should retain this property over long timescales (beyond a few decades normally required for facilities containing non-radioactive wastes). This report focuses on a disposal facility for radioactive waste placed in France and subjected to some differential settlements occurred on the top cover. The cap barrier in exam is a coupling of different means, including geomembrane and a sandy-silt layer. The deformation behaviour of the cap barrier of hazardous waste containment system is the subject of this rapport, relatively to the risk of barrier bending for differential settlements.

After a brief introduction to radioactivity decay, hazardous waste and its disposal facilities are presented: three main examples of radioactive waste disposal facilities give a general idea of different word-wide approaches to the subject; afterwards, the French site in exam in this report is described. Following chapters deal with a deep study on the top cover of a French disposal facility for low and intermediate radioactive waste. In particular, at first, geomembrane strain is considered: through a given altitude data-set, sections of deformed top soil and geomembrane were plotted; then sections before settlements were supposed, on the base of less-deformed section data-set. From this information linear elongations were evaluated, comparing the deformed and non-deformed trends. Particular evaluations on two deformed samples in a biaxial traction test validates previous results. The values observed lead to claim that a damage in geomembrane could be occurred. Moreover, a study on the volumes involved in the settlement, is carried out: an increase of volume is observed. Hypothesis on this unexpected increasing volume were made. The second aspect of this study concerns deformability of sandy-silt liner, placed above the geomembrane. From different tests (oedopermeability, unconfined compression test, bending test with PIV analysis), too high permeability and cracking damage are gathered.

The developing of the upper part of the sandy-silt liner could help geomembrane keeping the top cover waterproof and could limit damages caused by settlements. Thus, some hypothesis were suggested, in order to improve deformability and permeability properties of the soil of the site to deal with occurred deformations and cooperate with geomembrane.

Introduction

Radioactive decay, or radioactivity, represents all that atomic or nuclear processes which make an instable atomic nucleus decays into a lower energy nucleus, to achieve an higher stability, with emission of radiations (atomic particles). The daughter nucleus could be instable, thus radioactive decay lasts until stability is accomplished. In some decays, emission of particles implies a chemical transformation (transmutation), sometimes it implies loosing positive/negative charge (ionising potential).

Radiations originated in atomic or nuclear processes are categorised in four general types as follows (Knoll, 2010):

- Fast electrons
- Heavy charged particles
- Electromagnetic radiation
- Neutrons

Fast electrons include beta particles emitted in nuclear decay, as well as energetic electrons from any other process. Heavy charged particles include alpha particles, protons, fission products, or the products of every nuclear reaction. Electromagnetic radiation includes X-rays and gamma rays, as energy in an excited nucleus. Neutrons originated in various nuclear processes. Every category is characterised by different properties and degree of danger. The energy range spans between 10 eV to 20 MeV (Knoll, 2010). In 1975 , the General Conference on Weights and Measures (GCPM) claimed that the standard units for activity of a radioisotope is *Becquerel*, defined as one disintegration per second [s^{-1}]. Another characterizing parameter is the half-life, defined as the time taken for the activity of a given amount of radioactive substance to decay to half of its initial value.

The main emission of every category is reported in Table 0.1, coupled with distance covered in air, infect different behaviour were observed. Alpha and beta rays are composed by particles with an electric charge, so they easily interact with surrounding materials and they are soon adsorbed. On the contrary, gamma rays and neutrons do not have an electric charge: they can be adsorbed only by collision between atoms, as a consequence, they cover higher distances.

Emission	Covered distance in air	Covered distance in thick material
Beta rays	5-7m	micrometres
Alpha rays	6-7cm	millimetres
X and gamma rays	(Supposed, some km)	centimetres
Neutrons	(Supposed, some km)	

Table 0. 1 comparisons with adsorption capacity in air of the principal radioactive emissions.

Because of this “hardness” or ability to penetrate thicknesses of material, it is necessary to choose a proper shielding material in order to stop radiation transmission. For alpha and beta rays the use of shield some millimetres thick is sufficient, whereas for the other emissions a thicker and denser shield is required: lead is widely used thanks to its high density; iron or steel are also common shielding materials; also concrete is often used because of its low cost. Sometimes, a coupling solution of different material is used.

According to the International Atomic Energy Agency, “*radioactive contamination* is the deposition of, or presence of radioactive substances on surface or within solids, liquids or gases (including human body), where their presence is unintended and undesiderable” (IAEA, 2007). Radioactive decay is naturally occurring on Earth’s atmosphere or crust, due to cosmic rays. Furthermore, it can be produced artificially in many fields: in medicine (tomography, imaging, sterilising method for medical equipment, processes tracing); in food preservation; in industry (analysis of minerals and fuels, nuclear reactors, particle accelerator); in archaeology (measuring ages of rocks). Radioactive decay presents an high risk of contamination because of ionising radiation and transmutation power. Biological effects on human beings are dangerous in function to exposition, they can lead from nausea and vomiting to DNA and molecular structures mutations, to death.

Managing and preventing high hazard connected to radioactive decay is a fundamental issue in a world-wide perspective.

1.

Landfill for non-hazardous and hazardous waste

1.1. Hazardous and non-hazardous wastes

The huge increase of waste registered during the recent years, led to an higher and higher importance of waste treatment. Acting in order to prevent or limit negative effects, as environmental contamination (pollution of water tables, of soil and air), is fundamental. To that scope protection with landfill top and bottom layers, recycling, production of biogas and energetic valorisation, are all factors that play a key role.

Waste production could be divided in two categories:

- *hazardous wastes;* which need specific treatment (radioactive waste from hospitals, industries, as well as the nuclear reactors).
- *non-hazardous wastes*; in this category are placed every kind of waste not included in the previous category (some as inert materials and municipal solid waste are for the majority recyclable).

Non-hazardous wastes, are collected after treatment in non-dangerous disposal facility. The structure and the aim of this disposal facility have been sensibly developed in this last 30 years.

In the 80's, to safe environment from landfill pollution, leachate was let free to pass through different layers before reaching the ground. This method does not avoid pollution, but merely delay it. Further developments bring to isolation of the wastes, with neither water (from the top) nor leachate (to the ground) filtration through the barriers. This is the concept of "dry-tomb" disposal facility. On the contrary, the facilities of "new generation" permit a controlled water penetration, restrained with different semi-permeable layers of membrane and soil. The advantage related to water penetration is a faster degradation of the waste, stimulated by biological activity. Reducing degradation time yields also to a minor production of biogas.

Differently, *hazardous wastes* are settled in specific disposal facilities, which are still under study. Besides, barriers preventing water penetration and water infiltration are required features.

In these perspectives, top cover and bottom liner of a landfill are a fundamental part and different layer set-ups are studied to control or avoid water and gas penetration.

1.2. General elements of a landfill

A landfill is a carefully designed structure. Environment and public health preserving, affects landfill setting-up: distance to town centres and systems of underground and air protection are required. Moreover, a site requires proximity to an appropriate net of transport. In addition, hydro-geological evaluations are carried out on the site to evaluate permeability of the substratum, watertable level and its variability. A monitoring program is also designed, for the life of the landfill and for the post-operational period.

Figure 1.1 indicates the general issues associated with landfills and protection of the surrounding environment. One on the main aspect to deal with is gas breakthrough for its pollutant potential and, besides, for its disagreeable odour. In addition, infiltration of rainwater into a landfill, coupled with the biochemical decomposition of the wastes, produces leachate. If the leachate infiltrates surface or groundwater before sufficient dilution, serious pollution consequences can happen. If leachate enters groundwater or shallow aquifers, the problems are highly intractable. The pollution of shallow aquifers with high concentrations of chemicals can contaminate the soil and make an area uninhabitable. Consequently, the establishment of sophisticated leachate containment facilities in landfill site is critical issue, in order for reducing the impacts caused by the landfill on the surrounding groundwater (Inazumi, 2003).

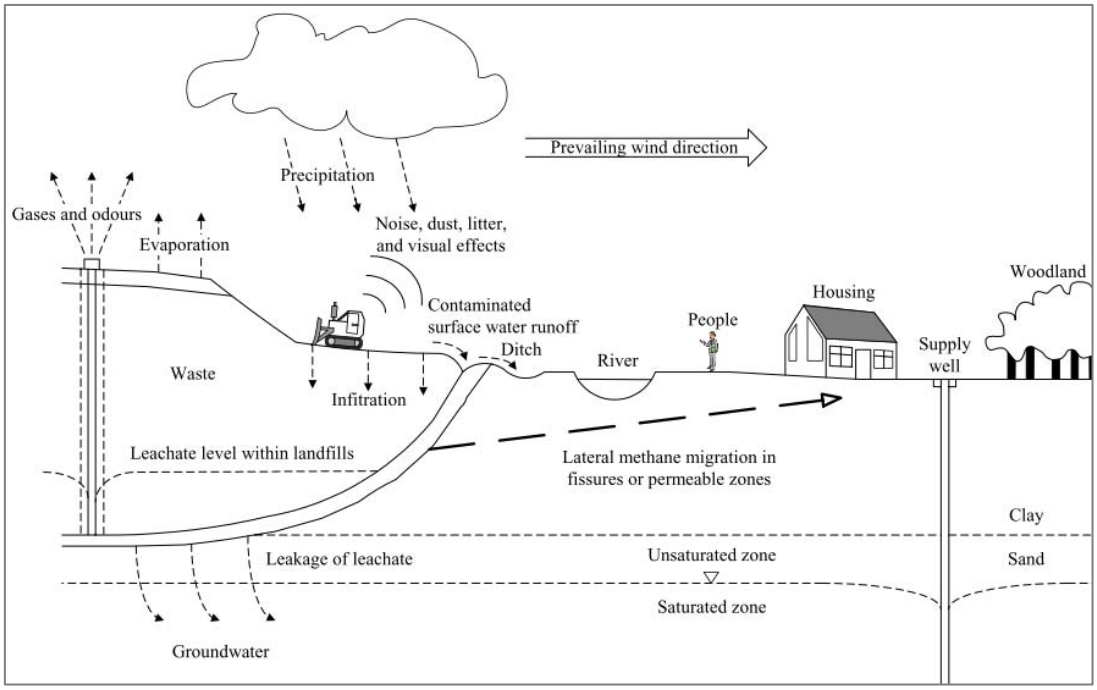

Figure 1. 1 General issues associated with landfills (Inazumi, 2003).

The practical installation of wastes is done step by step in different layers, compacted in order to assure stability to the waste body. A general layout section of a landfill for municipal solid waste is shown in Figure1.2.

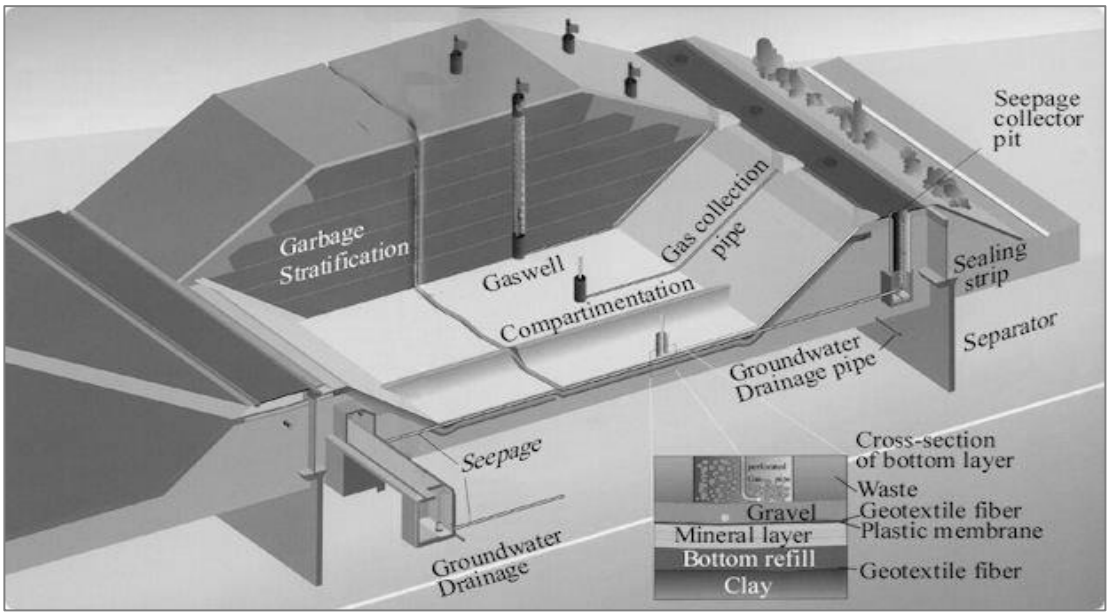

Figure 1. 2 Example of a municipal solid waste landfill layout (2g-cenergy.com).

The landfill's *base and sides liner system* consist of a mineral and synthetic layers which have to satisfy precise requirements of permeability and thickness. If the naturally occurring soils do not have the prescribed conditions, the barrier can be completed by other means, giving equivalent protection. Specific prescriptions for different cases arise to avoid water and gas infiltration, which could pollute underground and groundwater.

The *final cover system* consists on different protective layers of soil and geomembrane. The top cover, as well as the bottom liner, follows precise requirements of thickness and permeability. The primary purposes of final landfill cover systems are: to control the infiltration of rainwater after the landfill has been completed, to limit the uncontrolled release of landfill gases, and moreover to provide a suitable surface for vegetation.

The *drainage system*, combined with top cover and base and side liner systems, completes the landfill scheme. This apparatus is composed by geodrains, high permeability geocomposite and liner of soil characterised by high permeability. Water and gas production is collected by these devices, and it is led to appropriate sites: water in a basin where it can settle, gas to valorisation or combustion centre.

Fluid production continues at least 30 years after closure of the landfill, during this period a monitoring program is set.

1.2.1. General bottom layer

The bottom liner consists of a biological barrier which satisfies the following requirements (Figure 1.3):

- Landfill for hazardous waste:

  $k < 1 \times 10^{-9}$m/s; thickness > 5m

- Landfill for non-hazardous waste:

  $k < 1 \times 10^{-9}$m/s; thickness > 1m

  $k < 1 \times 10^{-6}$m/s; thickness > 5m

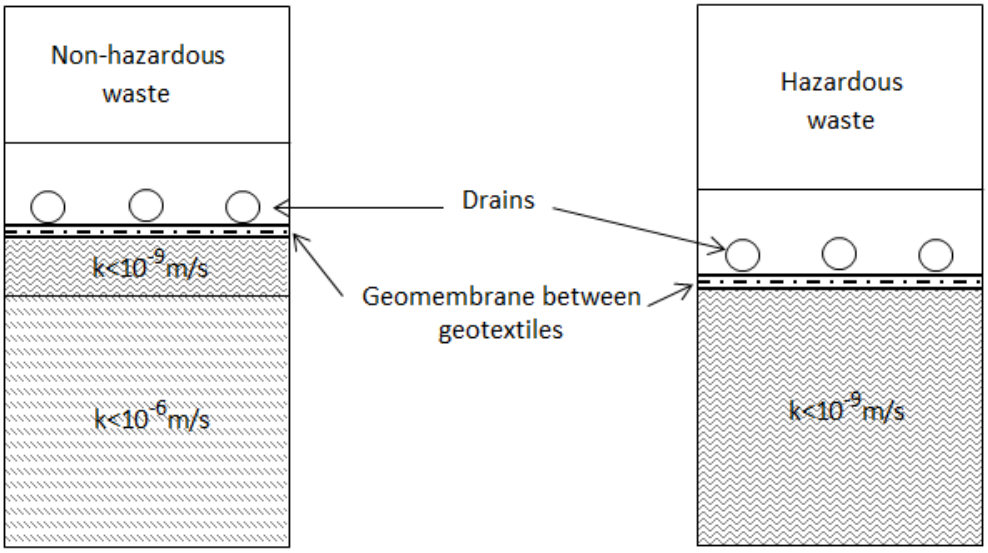

Figure 1. 3 General bottom layer of disposal facility for non-hazardous (left) or hazardous (right) waste.

Where the geological barrier for non-hazardous waste does not naturally meet the above conditions, a barrier of at least 0,5 m thick must be artificially established with other means (i.e. geosynthetic clay liner), giving equivalent protection. Geomembranes and compacted materials with sufficiently low permeability ought absolve the same assignment (Cuevas, 2009). The required geological barrier for hazardous waste is compulsory, it could not be replaced with other means.

A geomembrane is placed above the geological barrier, for its property of impermeability; it is included between two geotextiles which have the role of protecting geomembrane from damage.

Above the low permeability layers, a drainage system deals with collection of fluids. The apparatus is placed in a high permeability liner for two reasons: to facilitate collection of fluids and to give mechanical support to the waste body.

1.2.2. General top cover and lateral barrier

Landfill final cover systems must be able to deal with different conditions without deteriorating their properties. They have to tolerate climatic excursions (e.g., hot/cold, wet/dry, and freeze/thaw), to avoid water/wind erosion, to maintain stability against slumping, cracking, slope failure, and creep, to resist differential landfill settlement, and to resist deterioration caused by plants and animals avoiding thir intrusion. These features are reached with the coupling of different liners, everyone with a specific function (Figure 1.4).

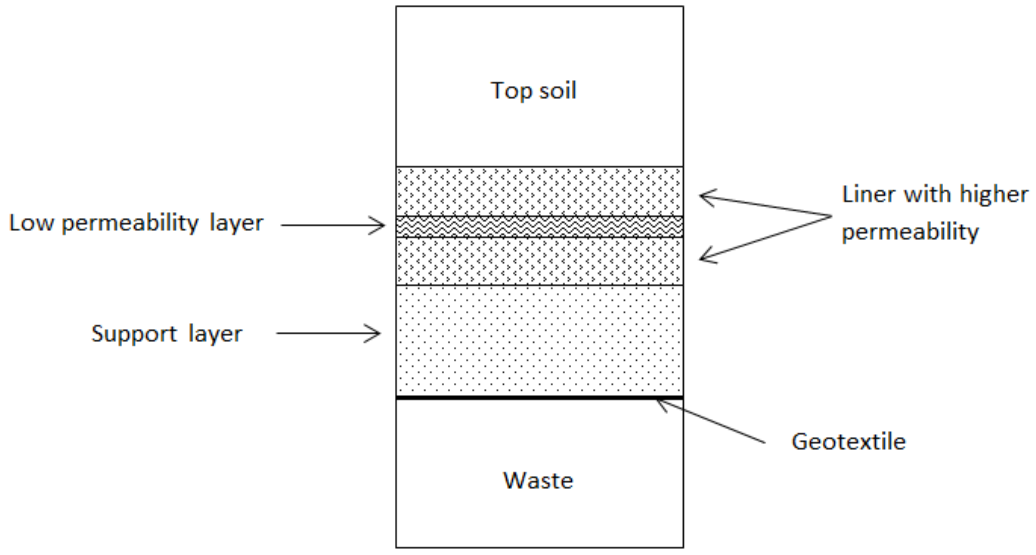

Figure 1. 4 Top cover layout.

Top soil liner is made of simple soil material that isolates the landfill body from the ambient, facilitates growing of vegetation, avoids erosion and animals/plants intrusion; the surface is set up with minimum slope of 3% that facilitate the movement of water from the surface towards the drainage system.

A first high permeability layer collects the water eventually infiltrated through the top soil and leads it to drains; the second high permeability layer, instead, collects the gas coming from the inner body. The collection efficiency of biogas is regardless of variations in gas permeability: the permeable layer reduces preferential gas flow through cracks in the cover material and O_2 intrusion (Jung et al., 2011).

The role of controlling water infiltration is awarded to low permeability layer, usually made of compacted clayey soil with a minimum thickness of 0,5m and a permeability of 10^{-9}m/s.

Finally, a geotextile isolates the wastes and a support layer gives support to the top cover and prevents damage from differential settlements.

1.3. Disposal facility for radioactive wastes

Despite the fact that the amount of hazardous waste is sensibly smaller if compared with the volume of non-hazardous waste, the treatment of the first one results more complex than the second one. The reasons lay in the high degree of danger both for environment and for human life, in the strict isolation requirements and in the operational period of the landfill, longer than the one for non-hazardous wastes.

According to the International System of Units, the level of radioactivity is measured by the Becquerel (Bq). It is defined as the activity of a quantity of radioactive material in which one nucleus decays per second, in other words it is the number of disintegration per seconds: 1 Bq = 1 disintegration per second (McNaught and Wilkinson, 1997). The Bq unit is therefore equivalent to an inverse second, s^{-1}.

Hazardous waste classification varies widely at international level: a conventional classification of radioactive waste remains a challenge of the International Community and for the International Atomic Energy Agency, (IAEA). Infect implementing a common classification scheme would facilitate communication among Member States, which has not yet been fulfilled. (IAEA, 2005). Guidelines in the classification of every state are similar: a general classification could be the following (www.word-nuclear.org):

- *Low-level waste (LLW)* “is generated from hospitals and industry, as well as the nuclear fuel cycle. It does not require shielding during handling and transport and is suitable for shallow land burial. To reduce its volume, it is often compacted or incinerated before disposal. It comprises some 90% of the volume but only 1% of the radioactivity of all radioactive waste.”
- *Intermediate-level waste (ILW)* “contains higher amounts of radioactivity and some requires shielding. It typically comprises resins, chemical sludge and metal fuel cladding, as well as contaminated materials from reactor decommissioning. Smaller items and any non-solids may be solidified in concrete or bitumen for disposal. It makes up some 7% of the volume and it has 4% of the radioactivity of all radioactive waste.”
- *High-level waste (HLW)* “arises from the 'burning' of uranium fuel in a nuclear reactor. HLW contains the fission products and transuranic elements generated in the reactor core. It is highly radioactive and hot, so requires cooling and shielding.”

An important concept in the perspective of radioactive waste managing is waste processing. The IAEA defines waste processing as any operation that changes the characteristics of waste, including pre-treatment, treatment and conditioning (IAEA, 2005). The importance of waste processing lies in how this processing could deal with people and environment protection. The choice of processes used is at first dependent on the level of activity and the type of waste. Secondly, it is also relied to each country's policy and regulations. According to INSC (International Nuclear Societies Council), each year, nuclear power generation facilities worldwide produce about 200000 m^3 of low- and intermediate-level radioactive waste, and about 10000 m^3 of high-level waste (about 300 million tonnes of hazardous wastes per year), but processed radioactive waste amounts to only 81000 m^3 per year (www.world-nuclear.org).

The *IAEA* defines (IAEA, 2005):

- *Pre-treatment*: “any or all of the operations prior to waste treatment, such as collection, segregation, chemical adjustment and decontamination”
- *treatment*: “operations intended to benefit safety and/or economy by changing the characteristics of the waste. Three basic treatment objectives are (a) volume reduction, (b) removal of radionuclides from the waste, and (c) change of composition of the waste”
- *conditioning*: “operations that produce a waste package suitable for handling, transport, storage and/or disposal. Conditioning may include the conversion of the waste to a solid waste form, enclosure of the waste in containers and, if necessary, providing an overpack.”

Through the last decades the problem of hazardous waste disposing has been widely studied, in relation to radioactive level of the waste, to the amount of its volume and its consistency. Generally, LLW, after packaging, is sent to a land-based disposal; besides, ILW and HLW are at first placed in a land-based disposal, waiting to be set in a more safety facility. Long term disposal facilities for ILW and HLW are still under study: many options have been investigated worldwide.

The International Atomic Energy Agency (IAEA) has defined commonly accepted management options, described below (www.iaea.org) :

- *Near-surface disposal facilities at ground level*. These facilities are on or just below the surface, the thickness of the covering amounts to few metres. Constructed vaults host waste containers, their stability is assured by backfilling. They could be covered with an impermeable membrane and top soil. These facilities may be provided of drainage system of water and gas. Near-surface disposal facilities currently in operation: UK (Low Level Waste Repository at Drigg in Cumbria); Spain (El Cabril for low and intermediate level radioactive waste); France (Centre de l'Aube); Japan (Low-Level Radioactive Waste Disposal Center at Rokkasho-Mura); USA (three low-level waste disposal facilities at: Barnwell, South Carolina; Richland, Washington; and Clive, Utah).

- *Near-surface disposal facilities in caverns below ground level*. Facilities built approx. 10 meters below ground level. This type of facilities is currently in use in: Sweden (the SFR final repository for short-lived radioactive waste at Forsmark), Finland (Olkiluoto and Loviisa power stations).

These facilities could be affected by long-term climate changes (such as glaciation) and this effect must be taken into account. This type of facility is therefore typically used for LLW and ILW with short half-life (up to about 30 years).

- *Deep geological disposal.* Stable geological formations (absence of water tables, seismic activity, etc.) could host radioactive waste in the deep underground, providing high isolation of the waste with natural (rock, clay, etc.) and engineered barriers (mostly provided by concrete).

Deep geological disposal remains the best option for ILW and HLW (especially if characterized by long life time) in several countries, including Argentina, Australia, Belgium, Czech Republic, Finland, Japan, Netherlands, Republic of Korea, Russia, Spain, Sweden, Switzerland and USA.

- *Interim waste storage.* Specially designed interim surface or sub surface storage waste facilities currently used in many countries. At first they were used for temporary storage, waiting for the availability of a long-term disposal mean; at the moment they became disposal facilities but it is necessary to highlight it is not a final solution.

Other ideas for disposal have been considered worldwide without success:

- *Long-term above ground storage*: investigated in France, Netherlands, Switzerland, UK and USA. They are conventional storage means requiring replacement and repackaging of waste every 200 years, or requiring high resistance performance for thousands of years.

-*Disposal in outer space:* investigated in USA, proposed for wastes that are highly concentrated. Investigations are now abandoned due to cost and potential risks of launch failure.

-*Deep boreholes:* investigated by Australia, Denmark, Italy, Russia, Sweden, Switzerland, UK and USA for HLW but not implemented anywhere mostly for economical reasons. Solid radioactive wastes would be placed in deep boreholes at several kilometres of depth, coupled with bentonite or concrete.

-*Disposal at subduction zones*: investigated by USA, not implemented anywhere because not permitted by International Agreements.

-*Sea disposal*: implemented for LLW and ILW by Belgium, France, Germany, Italy, Japan, Netherlands, Russia, South Korea, Switzerland, UK and USA, not permitted anymore by International Agreements. Packed radioactive waste has to be dropped into the sea and to sink to the seabed intact.

-*Sub seabed disposal*: investigated by Sweden and UK, not implemented anywhere because not permitted by International Agreements. In the perspective of this option, a suitable geological site has to be identified, after, by drilling or penetration, packed radioactive waste would be buried under the seabed. This option has been suggested for every level of radioactive waste.

-*Direct injection*: only suitable for liquid wastes, investigated by Russia and USA. It has been implemented in Russia for 40 years and in USA. This option consists in injecting radioactive waste, in liquid form, deep underground into a layer of rock, which has to have high porosity and permeability.

The measures or plans that various countries have in place to store, reprocess and dispose high level nuclear wastes are summarised in the following Table 1.1.

Country	Policy	Facilities and progress towards final repositories
Belgium	Reprocessing	Central waste storage at Dessel

		Construction of repository to begin about 2035
Canada	Direct disposal	Deep geological repository confirmed as policy, retrievable Repository site research from 2009, planned for use 2025
China	Reprocessing	Central used fuel storage at LanZhou Repository site selection to be completed by 2020; Underground research laboratory from 2020, disposal from 2050
Finland	Direct disposal	Posiva Oy set up 1995 to implement deep geological disposal Underground research laboratory Onkalo under construction Repository planned from this, near Olkiluoto, open in 2020
France	*Reprocessing*	*Underground rock laboratories in clay and granite* *Parliamentary confirmation in 2006 of deep geological disposal, containers to be retrievable* *Bured clay deposit is likely repository site to be licensed in 2015, operative in 2025*
Germany	Reprocessing but moving to direct disposal	Repository planning started in 1973 Used fuel storage at Ahaus and Gorleben salt dome Geological repository may be operational at Gorleben after 2025
India	Reprocessing	Research on deep geological disposal for HLW
Japan	Reprocessing	Underground laboratory at Mizunami in granite since 1996 Used fuel and HLW storage facility at Rokkasho since 1995 Used fuel storage under construction at Mutsu, start up 2013 • NUMO set up 2000, site selection for deep geological repository to 2025, operational from 2035, retrievable
Russia	Reprocessing	Underground laboratory in granite or gneiss in Krasnoyarsk region from 2015, may evolve into repository Dry storage for used RBMK and other fuel at

		Zheleznogorsk from 2012
South Korea	Direct disposal, maybe change	Waste program confirmed in 1998, KRWM set up in 2009 Central interim storage planned from 2016
Spain	Direct disposal	ENRESA established 1984, its plan accepted 1999 Central interim storage at Villar de Canas from 2016 (volunteered location) Research on deep geological disposal, decision after 2010
Sweden	Direct disposal	Central used fuel storage facility – CLAB – in operation since 1985 Underground research laboratory at Aspo for HLW repository Osthammar site selected for repository (volunteered location)
Switzerland	Reprocessing	Central interim storage for HLW and used fuel at ZZL Wurenlingen since 2001 Underground research laboratory for high-level waste repository at Grimsel since 1983 • Deep repository from 2020, containers to be retrievable
United Kingdom	Reprocessing	Low-level waste repository in operation since 1959 HLW from reprocessing is vitrified and stored at Sellafield Repository location to be on basis of community agreement New NDA subsidiary to progress geological disposal
USA	Direct disposal but reconsidering	DoE responsible for used fuel from 1998, accumulated $32 billion waste fund Considerable research and development on repository in welded tuffs at Yucca Mountain, Nevada The 2002 Congress decision of geological repository to be at Yucca Mountain was countered politically in 2009 • Central interim storage for used fuel

Table 1. 1 Waste management for used fuel and HLW from nuclear power reactors (www.world-nuclear.org).

This study focuses on *waste disposing* for low and intermediate radioactive waste in *surface disposal facility,* in order to describe the storage of the larger amount of radioactive waste. In the following chapters, at first some international models are described; after, a French disposal facility is studied.

In order to delineate the type of facility this report focuses at, in the following lines a general radioactive surface disposal facility is described.

A disposal cell for hosting nuclear waste is set generally as schematised in Figure 1.5. It is covered by a shelter building during the disposal of the waste. After the final exploitation of the first cell, it is covered by a geomembrane and the following cell is exploited, and so on. When all the storage volume is used, a final cover is set. Every disposal cell is isolated from the geological site through specific barriers (Camp, 2008). The requirement of global isolation of the waste are compulsory but the way in which it is reached could be different.

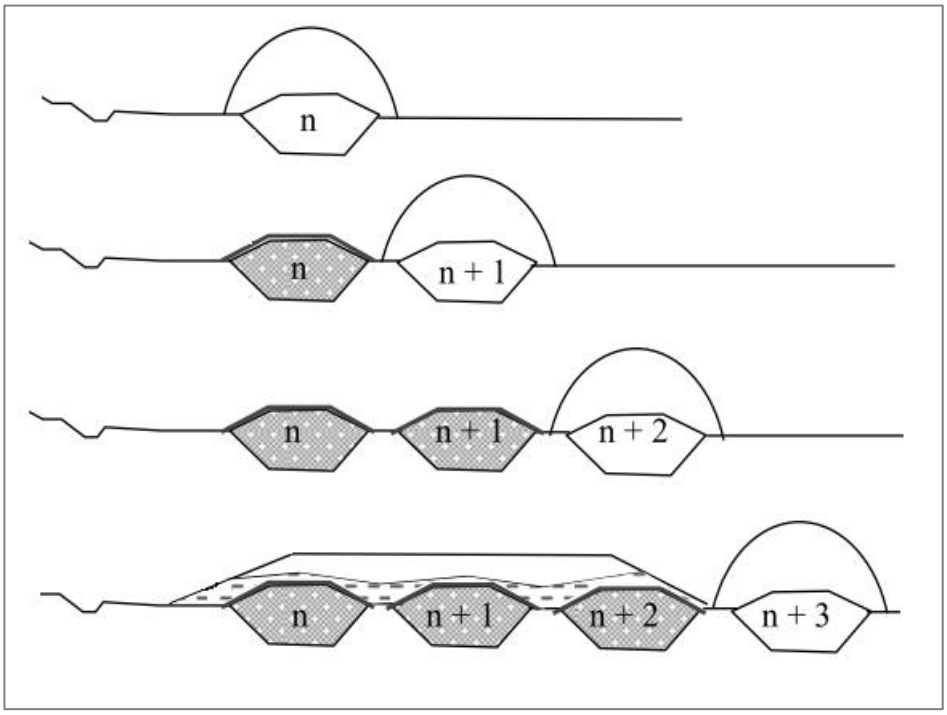

Figure 1. 5 Surface disposal facility outline (Camp, 2008).

1.3.1. USA disposal facilities

The three federal agencies in charge to regulates radioactive waste in the United States of America are: the Nuclear Regulatory Commission (NRC) that deal with commercial radioactive waste resulting from the production of electricity and other non-military uses of nuclear material; the Department of Energy (DoE), responsible for radioactive waste related to nuclear weapons production and research activities; and the Environmental Protection Agency (EPA), which handles with human and environmental aspects.

The Nuclear Waste Policy Act of 1982 has defined United States policies concerning the disposal of High Level Waste (HLW). This Act specifies that HLW has to be disposed in a *deep geologic repository*. The Yucca Mountain, Nevada, would be the single candidate site as a potential geologic repository (www.nrc.gov). “Although high contestations, the location was approved in 2002 by the United States Congress. However, under the Obama Administration, funding for development of Yucca Mountain waste site was terminated. The US Government Accountability Office (GAO) stated that the closure was for political, not technical or safety reasons” (“GAO: Death of Yucca Mountain Caused by Political Manoeuvring”. New York Times. May 9, 2011).

Currently, there are no permanent disposal facilities in the United States for high-level nuclear waste. There are three low-level disposal facilities for low-level wastes: they are located in Barnwell, South Carolina, in Richland, Washington and in Clive, Utah. Four former low-level radioactive waste disposal sites are closed ; they are located in or near Sheffield, Illinois; Morehead, Kentucky; Beatty, Nevada; and West Valley, New York (Radioactive Waste: production, storage, disposal. U.S. Nuclear Regulatory Commission).

The three low-level waste disposal facilities in the United States (www.nrc.gov) still working are:

- *EnergySolutions Barnwell Operations, located in Barnwell, South Carolina.* Currently, Barnwell accepts waste from all U.S. generators except those in the Rocky Mountain and Northwest Compacts. Beginning in 2008, Barnwell only accepts waste from Connecticut, New Jersey, and South Carolina.

- *U.S. Ecology, located in Richland, Washington.* Richland accepts waste from the Northwest and Rocky Mountain compacts.

- *EnergySolutions Clive Operations, located in Clive, Utah.* Clive accepts waste from all regions of the United States.

In the following Table 1.2 are reported volumes of LLW disposed in the United States.

Site	Volume (m^3)	Activity (Bq)
Clive	57740	$1,74 \times 10^{11}$
Barnwell	630	$2,8 \times 10^{13}$
Richland	645	$6,09 \times 10^{11}$
TOTAL	**59015**	**$2,90 \times 10^{13}$**

Table 1. 2 Volume and activity by disposal facility at 2008 (www.nrc.gov)

Barnwell Disposal Facility, operative since the 70's, is now discussed as model of U.S. Disposal Facility for Low Level Waste. It is represented in Figure 1.6.

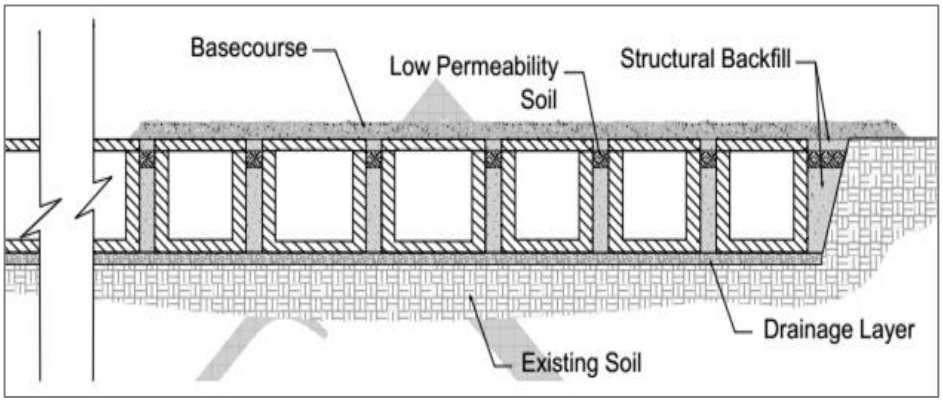

Figure 1. 6 Cross section of disposal unit of Barnwell disposal facility (Baird et al., 2007).

Structural elements of this facility are steel-reinforced concrete units or vaults; after excavation of the disposal area, the natural existing clay stratum at the bottom has been scarified and compacted in order to improve its properties of hydraulic barrier; a drainage layer is placed above. Then, the concrete units are set in one layer only, so that the upper part could be at the same altitude of the ground. They are spaced

out approx. 30cm between them, in order to have enough space to place backfill. This improves structural stability of the cover system. As indicated in Figure 1.8, a low permeability soil liner is set on the backfill between the disposal units walls. This is an interim clay cover installed during the setting-up period, aiming to avoid water infiltrations.

Once disposal operations have been completed, the low permeability cover system is built. It has been crowned to encourage water run-off. “The characteristics of the entire cover system will be such that radiation levels at the top surface of the final cover system will not exceed limits stated in the regulations” (Baird et al., 2007).

1.3.2. Spanish model

Since 1984, the Empresa Nacional de Residuos Radioactivos (ENRESA) is the public company in charge of the safe management, storage and disposal of radioactive wastes produced in Spain.

Figure 1. 7 El Cabril disposal facility site (ENRESA, 2009).

The only Spanish installation for disposal of low and intermediate level radioactive wastes is El Cabril (Figure 1.7), situated in the province of Còrdoba, in the foothills of the Sierra Albarrana. In the 90’s, it has been designed to satisfy all the disposal needs for this type of wastes, including those arising from the dismantling of nuclear power plants. At the end of 2008 it hosted 28218m^3 of nuclear waste (ENRESA,

2009). The disposal system is based fundamentally on the incorporation of natural and engineered barriers safely isolating the materials disposed in, for the time necessary for them to be converted into harmless substances (www.enresa.es).

El Cabril is one of the most modern disposal facility, above all for two reasons: it is an anti-seismic construction and it disposes of an automatic system for storage, so a minimum number of workers is required. Moreover, waste itself is stocked in bins in a solid mean of concrete, avoiding production of fluid and gas; sub-cells host 18 bins of wastes. Twenty-eight storage concrete cells (with a base of 24m x 19m, height of 9m) gather each one 320 sub-cells. Every row of cells is connected to a drainage system and is covered with an alternation of impermeable and permeable layers, finally covered with vegetative soil (ENRESA, (2009), Figure 1.8).

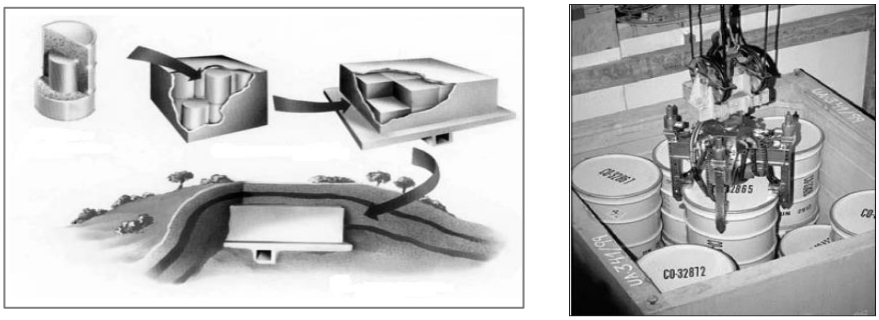

Figure 1. 8 Disposal phases of wastes in El Cabil Disposal Facility (ENRESA, 2009)

1.3.3. Swedish model

In the 1970s', the construction of Ringhals nuclear power plant, the largest power plant in Scandinavia, began. It is situated on the west coast of Sweden, 60 kilometres south of Gothenburg. Ringhals is part of Vattenfall Agency, which supplies energy to some Nordic countries and in northern Europe (Vattenfall, 2009). The Swedish Nuclear Fuel Handling Company (SKB) deals with the task of managing radioactive waste from Swedish nuclear power plants.

In Ringhals plant, radioactive wastes are treated differently in function of their radioactivity. High-level radioactive waste is stored at Ringhals for at least one year. After, it is shipped to the Central intermediate storage facility for spent nuclear fuel, at the Oskarshamn nuclear power plant, where waste is stored for 40 years.

Intermediate level waste is mixed with concrete and it is cast into steel plate or concrete containers, which are transferred to the terminal storage facility for radioactive operating waste (SFR) located at the Forsmark nuclear power plant. The low-level radioactive waste is buried in the Ringhals underground storage facility. This facility consists of two main parts the waste storage body and the infiltration bed (Figure 1.9).

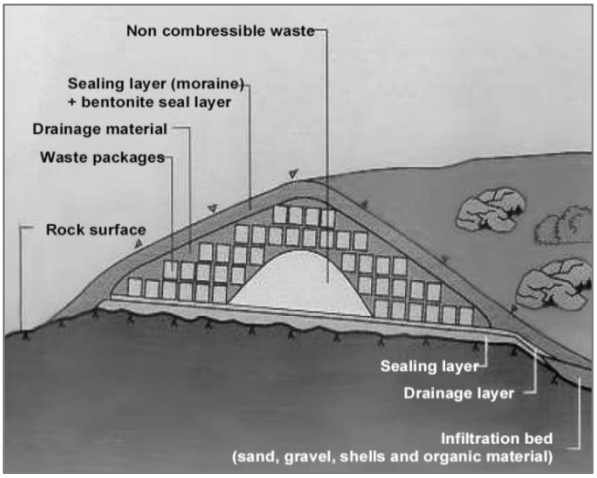

Figure 1. 10 Schematic views of the Ringhals landfilll (Shallow lnd repositories for very low level waste, Dr D.Aronsson).

Figure 1. 10 Installation of Rhingals landfill (Shallow lnd repositories for very low level waste, Dr D.Aronsson).

Waste is packed in different ways; in particular non-compressible waste is placed in the central main body, and over it the compressible waste in plastic-wrapped bales is set, giving the facility an hill shape (Figure 1.10). The entire body is covered with a draining material; in addition it is covered with a top layer of moraine. The purpose of the cover is to keep the storage facility dry and provide effective shielding of any radiation. A drainage layer is set under the waste body to collect and to direct leachate in the infiltration bed. It consists of a mixture of sand, shells and organic materials. The leachate substances are in this manner restraint and their transport to the sea is thus delayed. A monitoring program assures the armless radioactive level of leachate.

1.4. Disposal facility for radioactive wastes: France

ANDRA “Agence Nationale pour la gestion des Déchets Radioactifs” is the agency in charge to manage all nuclear waste in France. It designed different methodologies for the storage of intermediate or low level radioactive waste. Moreover it controls waste repositories, defines the acceptance criteria for waste packages in these repositories and controls the quality of their production.

Since this report discusses a French disposal facility for radioactive waste, focussing on French nuclear policy and conventions about this subject seems a suitable remark. In this perspective, in the following lines, nuclear waste classification in France outline is analysed.

Nuclear wastes are classified according to two main criteria: the activity and the half-life time (Verstaevel et al., 2012). The activity criteria are:

- Very low level (VLL), the initial activity of this type of nuclear wastes is from 1 to 100 Bq/g,
- Low level (LL), the initial activity is from 100 to 100,000 Bq/g
- Intermediate level (IL), the initial activity is from 100 000 to 1,000,000 Bq/g
- High level (HL), the average initial activity is about 10,000,000,000 Bq/g.

The half-life time criteria are:

- Very short life time (VSL), the half-life time is less than 100 days,
- Short life time (SL), the half-life time is between 100 days and 31 years
- Long life time (LL), the half-life time is longer than 31 years.

Finally, French nuclear wastes are classified as follow:

1. Very low level waste (VLL)
2. Low level short life waste (LL-SL)
3. Intermediate level short life waste (IL-SL)
4. Low level long life waste (LL-LL)
5. Intermediate level long life waste (IL-LL)
6. High level waste (HL)

Main producers of nuclear wastes in France are EDF (Electricité de France), Cogema (Companie Generale des Matieres Nucleaires) and CEA (Commisariat à l'énergie atomique). They must notify their production of nuclear waste to ANDRA every year. This an important issue that could help to design disposal facilities and to avoid storage complications. Table 1.3 reports distribution of radioactive waste in storage or disposal facility.

Wastes	**Volumes [m^3]**
VLL	360 000
LL-SL and FL-SL	830 000
LL-LL	87 000
IL-LL	41 000
HL	2 700
Total	1 320 000

Table 1. 3 Volumes of radioactive waste in storage or disposal facility at the end of 2010 (ANDRA, 2012).

Besides, Table 1.4 reports different storage systems in function to the activity and the half-life of nuclear waste. It comes out that surface disposals facilities host the major volume of radioactive waste, including low and intermediate level waste with a short life time. Very low level waste are generally stored in the production site to allow radioactive decay. Instead, for high level waste or intermediate level but with long lifetime waste, a proper disposal facility is still under study.

<table>
<tr><th>Half-life
Activity</th><th>VSL</th><th colspan="2">SL</th><th>LL</th></tr>
<tr><td>VLL</td><td rowspan="4">Stored to allow radioactive decay on the production site, then disposed in conventional disposals.</td><td colspan="3">Surface disposal facility for VLL waste</td></tr>
<tr><td>LL</td><td rowspan="2">Surface disposal facility for LL and IL waste</td><td colspan="2">Near surface disposal facility studied in accordance the Planning Act (art.4, June 28th, 2006) on the suitable management of radioactive material and waste</td></tr>
<tr><td>IL</td><td colspan="2">Deep disposal facility studied in accordance with art. 3 of the Planning of Act of June 28th, 2006 on the sustainable management of radioactive materials and waste</td></tr>
<tr><td>HL</td><td colspan="3">Deep disposal facility studied in accordance with art. 3 of the Planning of Act of June 28th, 2006 on the sustainable management of radioactive materials and waste</td></tr>
</table>

Table 1. 4 Characteristics of France existing disposal facilities (ANDRA, 2012).

The three existing French surface disposal facilities are: CSTFA (disposal facility for very low level short life and very low level long life wastes); CSFMA (disposal facility for intermediate and low level short life wastes); CSM (disposal facility for low and intermediate level short life wastes). The CSM (Centre de Stckage de la Manche) was the first French surface disposal facility and it is now in a post-closure monitoring phase; the CSFMA, hosting the same CSM classes of waste, and CSTFA, hosting very low level short and long time wastes, are still in operative phase (www.andra.fr). In Table 1.5 volumes of radioactive waste hosted at the present time in France are reported.

Name	Place	Waste class	Opening	Volume (2009) (m^3)	Volume at closure (m^3)
CSM	Manche	LL-SL & IL-SL	1969-1994	527,225	527,225
CSFMA	Aube	LL-SL & IL-SL	1992	231,046	1,000,000
CSTFA	Aube	VLL-SL & VLL-LL	2003	142,990	650,000

Table 1. 5 Existing French superficial disposal facilities (Versaevel and Gourc, 2012).

Every single component of a radioactive disposal facility is designed to be safe throughout all the lifetime of the wastes. In Table 1.6 some time-references of radioactive wastes are reported.

Site	Waste class	Period	Activity after 300years	Time to reach 80 Bq
CSTFA	VLL-SL	100days÷31years	0÷0,1 Bq	30 years
	VLL-LL	>31years	-	-
CSM and CSFMA	LL-SL	100days÷31years	<100 Bq	360 years
	IL-SL	100days÷31years	<100 Bq	450 years

Table 1. 6 Time references, useful to understand radioactive disposal facility requirements.

1.4.1. Presentation of a French low and intermediate level short life waste disposal facility: CSM, Centre de Stockage de la Manche.

The first French disposal facility for nuclear waste was the Centre de Stockage de la Manche (CSM), opened in 1969 for intermediate and low level short life waste; it closed in 1994. A volume of 527 225 m^3 of radioactive waste is stored in. Figure 1.11 provides an outlook of the 15 ha site.

Figure 1. 11 Outlook of the CSM site (ANDRA, 2012).

During the operational life of this site, four successive phases can be considered (Verstaevel and Gourc, 2012). The first phase (1969-1979) passed through three different options: the first one consisted in burying the wastes in earth trenches (Figure 1.12a); secondly, the process changed into concrete cells (Figure 1.12b) and after into storage stack of barrels laterally on a concrete raft (Figure 1.12c).

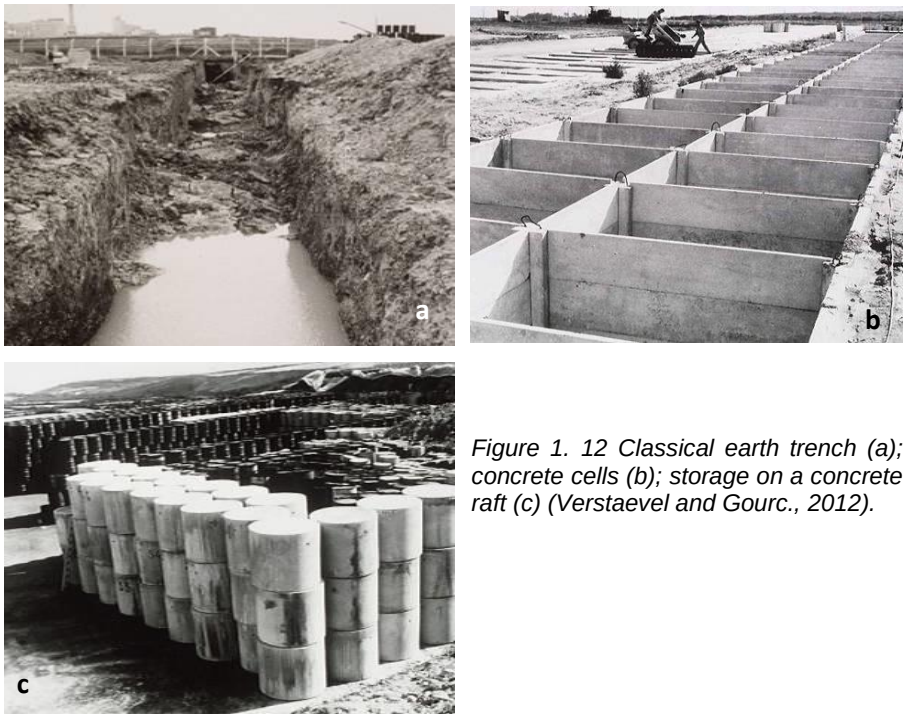

Figure 1. 12 Classical earth trench (a); concrete cells (b); storage on a concrete raft (c) (Verstaevel and Gourc., 2012).

In the second phase (1979-early 90's) the process changed again: waste was stored in monolith (Figure 1.13, a) and tumulus (Figure 1.13, b). This process was used until site closure; the wastes which were previously stored in earth trenches have been put in tumulus.

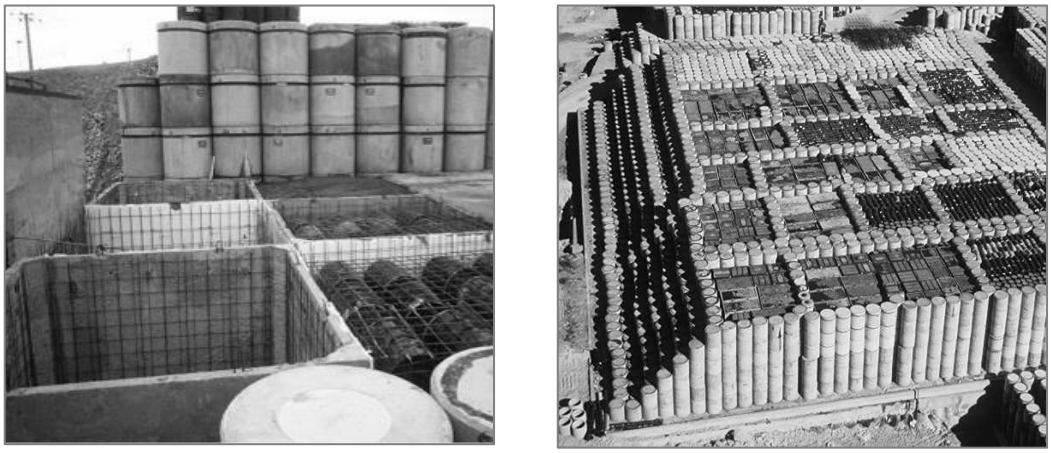

Figure 1. 13 CSM monolith process (a) and tumulus process (b) (Verstaevel and Gourc., 2012).

Finally, during this period the site was filled and at the same time the cover was set up. The following figure (Figure 1.14) shows a schematic section of a storage cell.

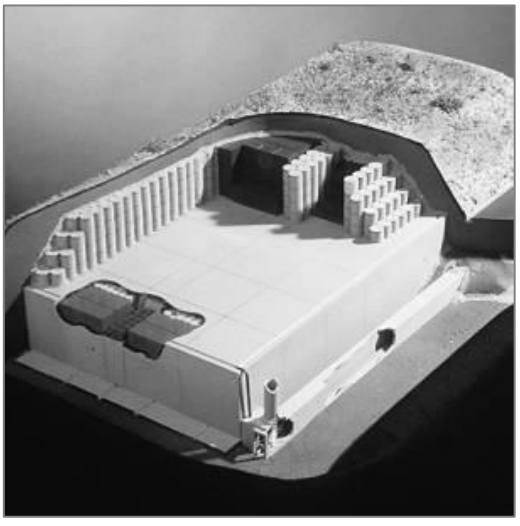

Figure 1. 14 CSM, storage cell section (Verstaevel and Gourc., 2012).

2.

Materials and tests for a top cover

2.1. Different means for a top cover

Modern landfills, both during their active operation and after closure, should be isolated by a combination of natural and artificial sealing systems to restrict their negative effects on the environment to an acceptable level. A cover system should limit the uncontrolled release of landfill gas and pollutants, as well as the infiltration of water into the landfill main body. It is very important to maintain physical, mechanical and hydraulic characteristics of the cap barriers throughout the designed life of the facility.

In the 90's, first national guidelines, ordinances and regulations were introduced in the United State of America (Nuclear Waste Policy Act, 1982) and Germany (Act for Promoting Closed Substance Cycle Waste Management and Ensuring Environmentally Compatible Waste Disposal, 1996) in order to manage waste disposal in landfills. In these regulations, the importance of bottom layer and cap cover sealing was highlighted, so that precise requirements were introduced. Both the layers have to control fluid infiltration and emission through different means, natural (e.g. clay layer) or artificial (e.g. geomembrane). In 1999, the first worldwide survey of landfill liner and cover systems was carried out by the Geosynthetic Research Institute (GRI); it turned out that 37 countries had already established regulations for landfill sealing systems (Heerten and Koerner, 2008).

In the perspective of the topic of this report, as the cover system of a landfill for radioactive waste, some aspects are now treated: from the description and analysis of different means for top cover, to different useful tests to characterise and study these means themselves.

2.1.1. Clay

Clays are aluminum-silicate minerals, they are formed by the superimposition of elementary very thin sheets (7-14nm); every sheet is made by two or three units (Barral, 2008), forming (Figure 2.1):

- Tetrahedron with four atoms of oxygen and one of silicon or aluminum

- Octahedron with six atoms of oxygen or hydrogen and one of aluminum or magnesium

Different compositions of sheets give different types of clay. Every sheet has an electric charge that could be different in intensity and origin, and that influences the behaviour of the different type of clay (e.g. hydration and swelling). Clays could be divided in 3 groups: smectite, illite and kaolinite. In the geotechnical outlook, a specific type of clay is often used: bentonite. It is a clayey material formed mostly by montmorillonite, and in less part by calcium or sodium. In bentonite, free pore water could freely move through hydraulic gradient. Instead, adsorbed water is tied at sheet molecules through strong connections (Van der Waals and electrostatic one). Here, the relation between the electronegative charge of the water and the positive ions on the surface of the sheets is the driving force of adsorbed water movement. (Barral, 2008).

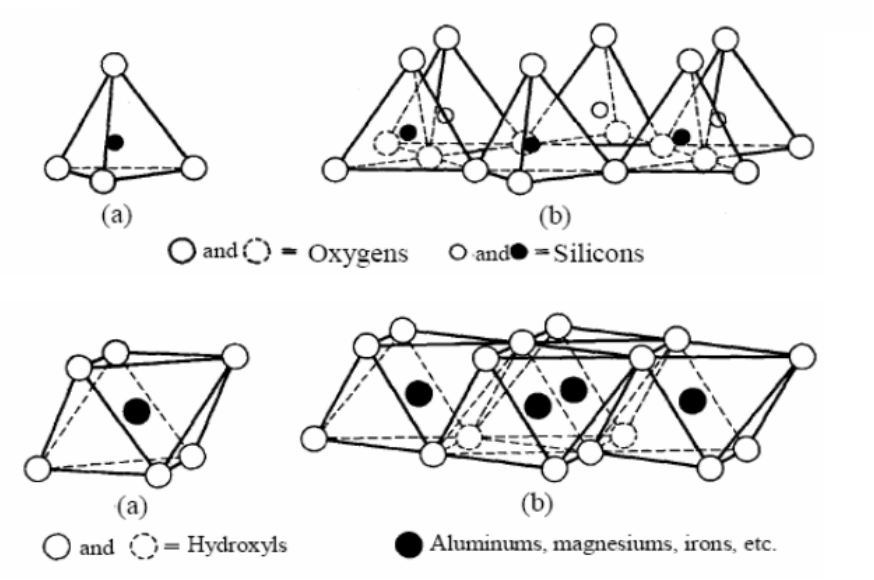

Figure 2. 1 Tetrahedron and octahedron (Barral, 2008).

A layer of compacted clay is often used as part of top cover of a landfill. The purpose of an low permeability layer in the form of clay barrier in closure system, is to facilitate water run-off, limit infiltration of water, provide gas control and serve as an erosion barrier (Viswanadham and Rajesh, 2008). According to Heerten and Koerner (2008) “the use of a classic clay liner over a body of waste (i.e. in the cover or surface seal of a landfill) is a challenge in view of the long-term sealing effect for critical water-content parameters of the clay liner, and in view of the uneven

settlement and subsidence associated with the body of waste." The selection of the better type of clay and the better installation way are still under study.

The most important aspect that has to be taken in account is permeability of clay layer, both permeability to water and permeability to gas. It should be noted that the generally accepted maximum permeability coefficient of clay liner is $k<1\times10^{-7}$cm/s, corresponding to 32 mm/year of seepage (Heerten and Koerner, 2008). This topic, as permeability in clay liner (CL), could be approached from two sides: cracks formation and swelling. Occurring of cracks in a clay layer could compromise permeability; clay swelling acts on the opposite side: voids present in the soil-clay matrix of the layer could be refilled by clay. Though, an excessive swelling could imply an higher distance between grains and so water movement, with the consequence of increasing permeability. Moreover, an excessive dependence of swelling on water content could imply an high influence of atmospheric conditions. These aspects are now considered.

Desiccation is a cause of occurrence of cracks, that could cause a change on mechanical properties (Tang et al., 2011). The evaporation of soil water results in volume shrinkage and differential movement. Water evaporation starts from the surface of the top cover; as the water-air interface reaches the layer gradually, a water–air meniscus between clay particles starts to form. Capillary suction is therefore developed. As water evaporation proceeds, the curvature of capillary meniscus increases and is accompanied by an increase in capillary suction and effective stress between clay particles. Consequently, the clay layer consolidates and shrinks. A tensile stress field is set-up in the layer. Once the rising tensile stress exceeds the tensile strength of clay layer, cracking occurs on the surface. Cracking significantly influences the hydraulic properties and the transport processes that occur in the soil, these imply high potential infiltration rates and low storage capacities, due to this preferred flow. For example, it take place preferential flow and faster movement of gas, water, solutes and particles, than would be expected from the soil matrix properties. It is shown that most cracking is during desiccation, when water content is decreasing. (Tang et al., 2011).

On an other hand, cracking potential is highly influenced by differential settlements of landfill cover. The forced deformation in the surface sealing system, combined with surface seal crack-formation and dehydration, can lead to increased system

permeability beyond tolerable limits. Heerten and Koerner (2008) report very strict limitation on clay liner deformation at ε=2‰.

Deformation behavior of the clay layer is put in comparison with overburden and thickness in a centrifuge test (Viswanadham and Rajesh, 2008). It has been seen that the water breakthrough takes place over a certain deformation, when the crack has a sufficient width. In Figure 2.2, it can be seen a steep variation of the ratio V/V_0 (volume of water on initial volume of water) after a deformation ratio a/a_0 (curvature of the sample on its initial curvature) of min 60%. Moreover, we can see how thickness of the layer positively influences occurrence of cracks. Confirmation of this could be found in the study of Gourc et al. (2010). Furthermore, presence of overburden sensibly delays cracking.

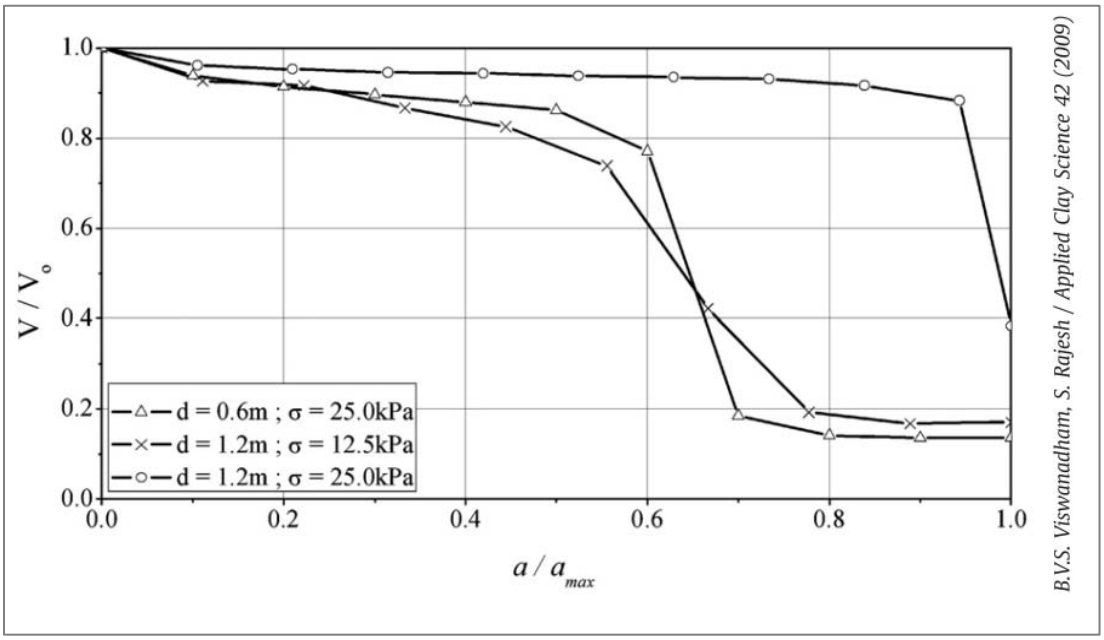

Figure 2. 2 Trends of water volume ratio on deformation ratio for different layer thickness and different overload (Viswanadham and Rajesh., 2008).

According to Rajesh et al. (2011), the occurrence of cracks are also influenced by moisture content. Its increase leads to a significant delay in crack initiation and gas breakthrough, with a reduction in the flexural tensile strength. Soil compacted at optimum moisture content tends to be more rigid if compared with soil compacted in the wet side of the optimum. Plè et al. (2011) confirms this statement: the higher the moister content, the lower the tensile strength and the higher the deformability.

About swelling capacity, it is necessary to distinguish between free swelling and confined swelling. Free swelling is a property of a mean made of clay (mostly bentonite) and soil not confined; the second one, on the contrary, considers a confined behaviour. Mainly two are the factors that influence free swelling (Mishra, 2011). One is the exchangeable sodium percentage (ESP): as it can be seen in Figure 2.4b, free swell increases with ESP, till 30% of content. Moreover, Figure 2.4a shows the increasing of free swelling with the increasing of the percentage of the bentonite in the clay fraction. Finally Figure 2.4c shows how hydraulic conductivity decreases with the increasing of swelling.

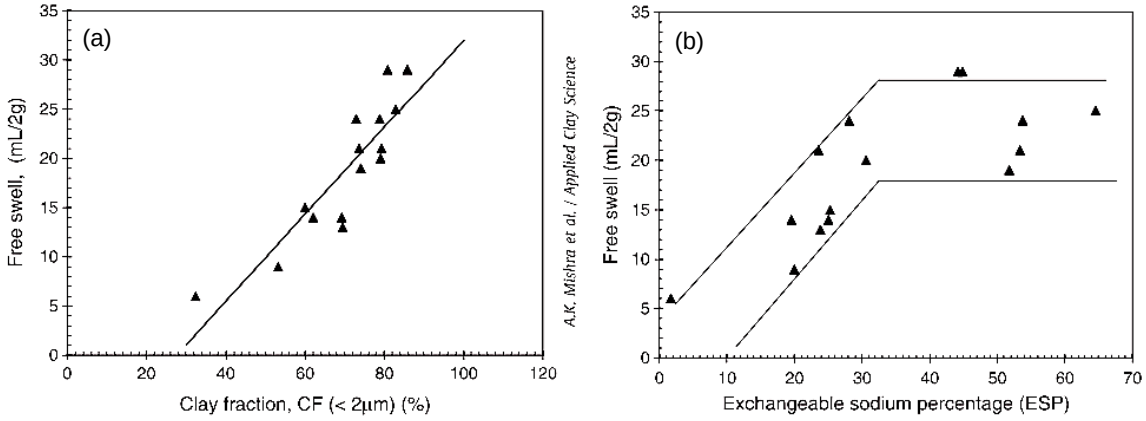

Figure 2. 4 (a) Trend of free swell in function of clay fraction and (b) of exchange sodium percentage (Mishra, 2011)

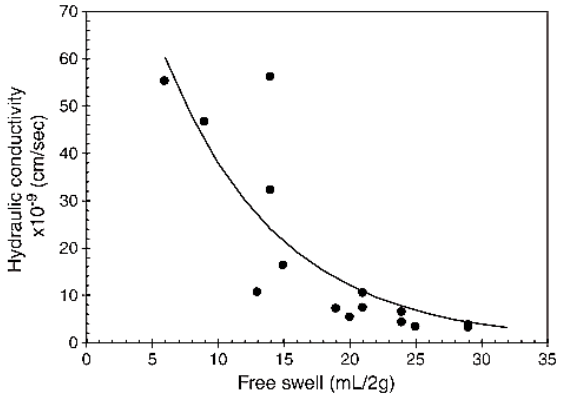

Figure 2. 4 Trend of free swell in function of hydraulic conductivity (Mishra, 2011)

About confined swelling, according to Villar and Lloret (2008), it can be distinguished between swelling pressure (SP, pressure that the soil practices on the confinement, while hydration) and swelling capacity (SC, deformation capacity of the sample not confined on one side). SP is dependent to dry density (the higher it is, the higher is the SP), and almost independent by initial water content of bentonite; SC is influenced by the entity of a possible overburden and by dry density of bentonite (the

higher it is, the higher is the SC); moreover, for a particular vertical pressure, the influence of initial water content is more noticeable for highest initial dry densities and, for a given dry density, the swelling capacity decreases with water content of bentonite. In Figure 2.5 relationship between vertical load and dry density are compared for SP and SC.

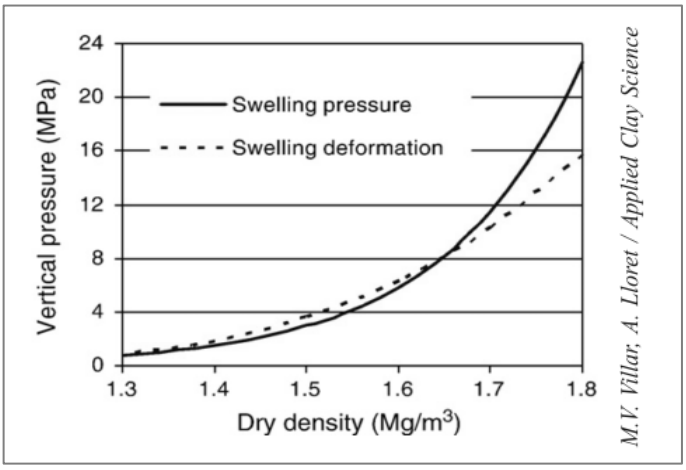

Figure 2. 5 Relationship of SP and SC with vertical pressure and dry density (Villar and Lloret, 2008).

In the last few decades, always higher performances are required for materials, especially in a field such as landfill. Among different improving solutions, reinforcement with randomly distribute polyester fibres in a clay layer gives good results (Gourc et al., 2010; Rajesh et al., 2011, Viswanadham et al., 2011). A reinforced soil barrier enhances tensile strength, in particular the rapport between

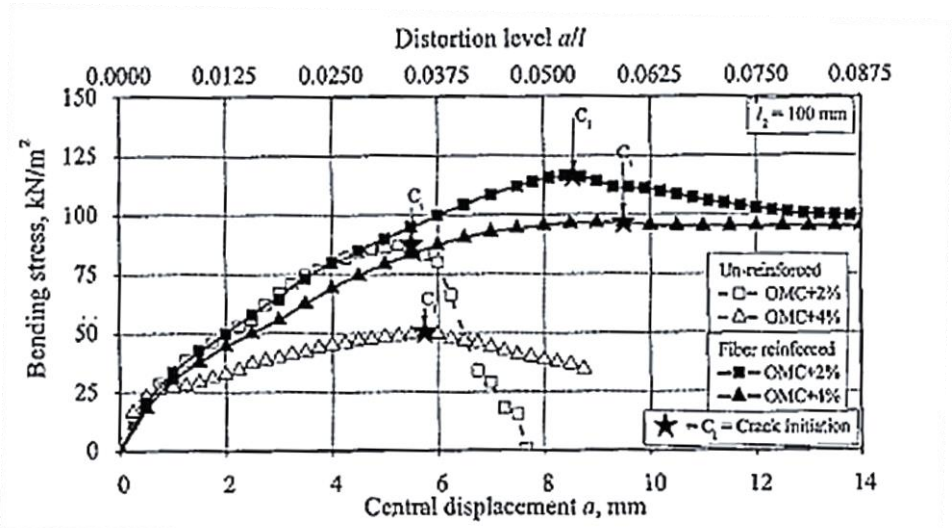

Figure 2. 6 Variation of bending stress of soil beams with and without fiber reinforcement against central displacement and distortion level (Rajesh et al., 2011)

tensile strength and strain behaviour. Figure 2.6 shows the results of bending tests on soil beams at different moisture contents, with or without polyester fiber reinforcement.

It can be seen how reinforcement sensibly delays the occurring of cracks; moreover for both moister contents the behaviour is very similar, so we can claim that with a fibre reinforcement, moister content does not influence tensile strength. Polyester fibres, in conclusion, provide an improvement in the integrity of a clay layer and in consequence, avoiding occurrence of cracks, in the waterproofness of gas and water (Figure 2.7).

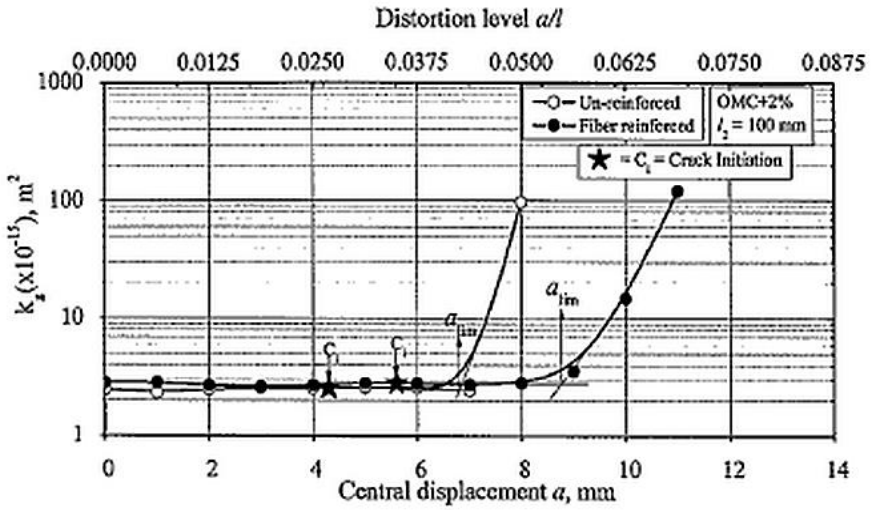

Figure 2. 7 Variation of gas permeability of the soil beam, with and without fiber reinforcement during a gas-permeabilty bending test (Rajesh et al., 2011).

2.1.2. Geosynthetics

Whereas the mineral components of a landfill's sealing system are built and constructed to a high standard, their actual long-term effectiveness is still not satisfying. In this outlook geosynthetics could deal with long-term required properties.

The geosynthetic family includes various products of textile, rubber and plastics industries as well as bitumen-polymer membranes and bentonite industries. They are prefabricated and furnished in rolls or panels. The main types of polymers used are polyethylene (PE), polypropylene (PP), polyester (PET) and polyvinyl chloride

(PVC). In the geosynthetic family we can find different type of them with different functions (www.geosyntheticssociety.org):

- Geotextiles are continuous sheets of woven, nonwoven, knitted or stitch-bonded fibres or yarns. The sheets are flexible and permeable and generally have the appearance of a fabric. Geotextiles are used for separation, filtration, drainage, reinforcement and erosion control applications.

- Geogrids are geosynthetic materials that have an open grid-like appearance. The principal application for geogrids is the reinforcement of soil.

- Geonets are open grid-like materials formed by two sets of coarse, parallel, extruded polymeric strands intersecting at a constant acute angle. The network forms a sheet with in-plane porosity that is used to carry relatively large fluid or gas flows.

- Geomembranes are continuous flexible sheets manufactured from one or more synthetic materials. They are relatively impermeable and are used as liners for fluid or gas containment and as vapour barriers.

- Geocomposites are geosynthetics made from a combination of two or more geosynthetic types. Examples include: geotextile-geonet; geotextile-geogrid; geonetgeomembrane; or a geosynthetic clay liner (GCL). Prefabricated geocomposite drains or prefabricated vertical drains (PVDs) are formed by a plastic drainage core surrounded by a geotextile filter.

- Geocells are relatively thick, three-dimensional networks constructed from strips of polymeric sheet. The strips are joined together to form interconnected cells that are infilled with soil and sometimes concrete. In some cases 0.5 m to 1 m wide strips of polyolefin geogrids have been linked together with vertical polymeric rods used to form deep geocell layers called geomattresses.

General long-term characteristics for a geomembrane are (Heerten and Koerner, 2008): (a) long-term protection against UV radiation, (b) withstanding a large range of forced deformation without damage, (c) resistance to the effects of frost, fluctuations in water content or water tension in the overlying layers, (d) barrier against roots and rodents, (e) permanently water- and gas-tightness. These imply

an high expected life-time for this mean. HDPE geomembrane long-term effectiveness has been studied in junction with temperature, confirming precedent statement. Results are shown in Table 2.1.

Temperature (°C)	Long-term effectiveness (years)
20	400-1000
25	250-600
30	150-400
35	100-250
40	60-80

Table 2. 1 Long-term effectivness in junction with different temperatures for a HDPE geomembrane (Heerten and Koerner, 2008).

Most commonly used geosynthetics in the landfill top cover are geosynthetic clay liners (GCLs): they are geocomposites prefabricated with a bentonite clay layer typically incorporated between a top and bottom geotextile layer, or bentonite bonded to a geomembrane or single layer of geotextile. Geotextile-encased GCLs are often stitched or needlepunched through the bentonite core to increase internal shear resistance.

The waterproofness is assured by bentonite; the confinement of the bentonite is necessary to limiting swelling, to assure functions of separation, reinforcement and protection (Barral, 2008,). GCLs are widely used because of its important advantages: its hydraulic conductivity is very low ($10^{-10} \div 10^{-12}$m/s) (Bouazza, 2002), and it has a self-healing capacity thanks to its swelling property (the more swelling, the more self-healing) that implies it could support differential settlements. Kang et al. (2011) noticed that a consolidation load could enhances GCL behaviour. The most important problems could occur with this geocomposite are:

- chemical alterations, due to organic matter, of the clay composition;
- iones exchange, that decreases the pore water fraction, forming empty canals and increasing the permeability (Bouchelaghem, 2009);
- limited thickness, for damage during installation and for bentonite inner distribution that could become not homogeneous (Barral, 2008);

- durability, that could lead to an increasing of hydraulic conductivity of $10^3 \div 10^4$ times in 10 years (Benson et al., 2010).

Although this negative aspects, Heerten and Koerner (2008) quantify that the internal shear strength of the geosynthetic components alone, when used in landfill surface seals, in the bentonite mats investigated, is sufficient to ensure the structural stability of the sealing system over at least centuries (>>100 years).

2.1.3. Sand-Bentonite-Polymers layer

In the '90s, in Netherland at first and after diffused in almost all Europe, a possible outer reach came out. It is called SBP layer. It is used as impermeable layer, consisting in three components (www.trisoplast.nl):

- Granular material (e.g. sand)
- Bentonite (12%)
- Polymer (1,9%)

It is supposed to give advantages, especially if compared with clay liner and GSC, it is characterized by the following properties:

- φ=30°, c'=50÷100 kN/m^2: friction angle proper of granular material, cohesion of both granular material and cohesive one.
- both permeability to gas and to water are very low: $10^{-11} \div 10^{-12}$m/s for a saturation S≥60%, estimated fall in permeability: 16% in 100 years;
- high durability: little affection to desiccation, no influence of temperature, high resistance to acid ambient thanks to polymers;
- high deformability: no problem of cracks and differential settlements;
- swelling does not influence performances.

2.2. Tests on top cover materials

In the outlook of this report, focussing on disposal facility for radioactive waste, some tests are now briefly treated. In particular, since that the top cover plays an important role in this study, tests for delineate properties and mechanical strength of soil and geomembrane are described.

Proctor test

Proctor compaction test is a laboratory method for determining the optimal moisture content at which a soil achieve its maximum dry density. The test consists in hydrate the soil at different moisture content and in compacting the sample with a precise procedure described in the standard NF P 94 093, according to one of the two different procedures: Standard Proctor test or Modified Proctor test (Figure 2.8). After compaction, the dry density is evaluated after drying it in oven.

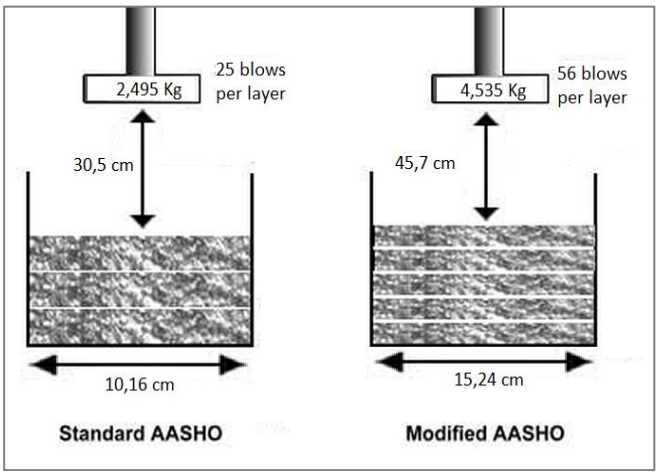

Figure 2. 8 Trend procedure for Standard Proctor and Modified Proctor.

Coupling different values of moisture contents with the relative dry density, a Proctor curve is set. The maximum value of the curve identifies the optimum moister content for the maximum dry density. The side of the curve where $w>w_{opt}$ is called *wet*, otherwise is called *dry*. The Proctor curve is more or less convex, in function of the sensibility of soil to water, and tends asymptotically to saturation curve of the soil. Applying different compaction energies E_i in Proctor tests, the Proctor curve moves up (Figure 2.9); linking all the optimum condition, the optimum curve is set.

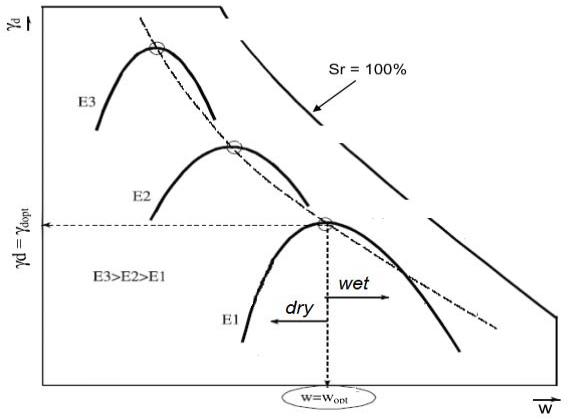

Figure 2. 9 Proctor curves, optimum and saturation curves (Camp, 2008).

In Figure 2.10, there are a compaction curve and two curves representing the variability of permeability in function of moister content, at two different confining pressure. It can be notice that in the wet side of the proctor curve, permeability is not highly affected by confining pressure and moisture content, whereas in the dry side it is. In the outlook of our study, the preferred moisture content for a low-permeability soil for a top cover is in the wettest part of the curve. In this way, variation of moister content do not sensibly affect permeability.

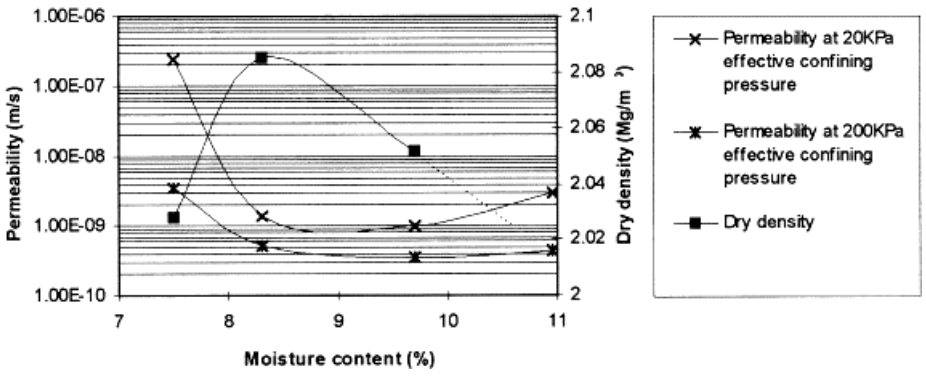

Figure 2. 10 Effect of moisture content on compaction and permeability (Smith et al., 1999).

The Bureau de Recherches Géologiques et Minières (BRGM) fixes a domain in which the compromise between mechanical stiffness and permeability is achieved for a daily landfill: a moisture content included between w_{opt} +2% and w_{opt} + 6% (Camp, 2008).

Oedometer and oedo-permeameter test

According to the standard XP P 94-090-1, the goal of this test is calculate the compressibility of fine and fine coherent soils. Applying load steps to a cylindrical sample of soil, vertical displacements are measured, whereas lateral deformation are avoided. Vertical displacement in time is recorded. Hence, coupling void ration in function of vertical stress, a compressibility curve is designed (Figure 2.11). The slope of the e-log(σ') curve is fairly flat until the preconsolidation pressure (σ'_p) is reached. Beyond this point, the slope of the curve becomes steeper: the soil becomes more compressible. The first portion of the line represents the recompression loading, then the effective loading. Finally, the unloading is seen. This test is useful to find compression (C_c) and recompression (C_a) indexes.

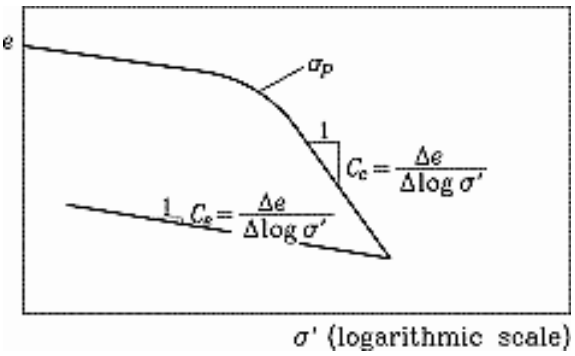

Figure 2. 11 Typical oedometer curve with definitions of C_c and C_r (Turc et al., 2001).

The same apparatus can be used to evaluate permeability. The sample is placed between two porous stones. In a first phase the sample is saturated, then a an hydraulic gradient is applied. The hydraulic charge in function of time is evaluated; through Darcy law, the permeability k [m/s] is found, with the equation (2.1):

$$k = 2{,}3\frac{sH\log\frac{h_0}{h_1}}{A(t_1 - t_0)} \qquad (2.1)$$

Where (see Figure 2.12):

- s alimentation tube section area (m^2)

- H height of the sample (m)
- h_0 and h_1 height of the water in the alimentation tube at times t_0 and t_1
- A sample area (m^2)

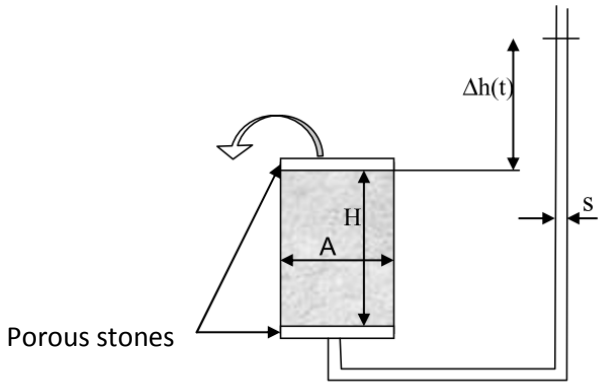

Figure 2. 12 Oedopermeameter scheme (Camp, 2008).

Unconfined compression test

This test consists in applying an axial load to a cylindrical sample with diameter 2*R, with no lateral support. The load F is applied by an increasing displacement of 0,01 mm/s (NF P 94-077) of the moving plate where the sample is placed. It increased until the soil fails. The force F coupled with vertical displacement ΔH is recorded. The maximum vertical stress is given by equation 2.2:

$$\sigma_{c\max} = \frac{F_{\max}}{\pi R_{\max}^2} \tag{2.2}$$

Whereas, the strain ε_i during the test is evaluated through the ratio of the displacement at the moment *i* compared to the initial height of the sample H_0 (see equation 2.3):

$$\varepsilon_i = \frac{H_0 - H_i}{H_0} \tag{2.3}$$

In Figure 2.13 typical curves of unconfined compression test are shown. The tangent at the curve in the origin is the Young modulus E_y.

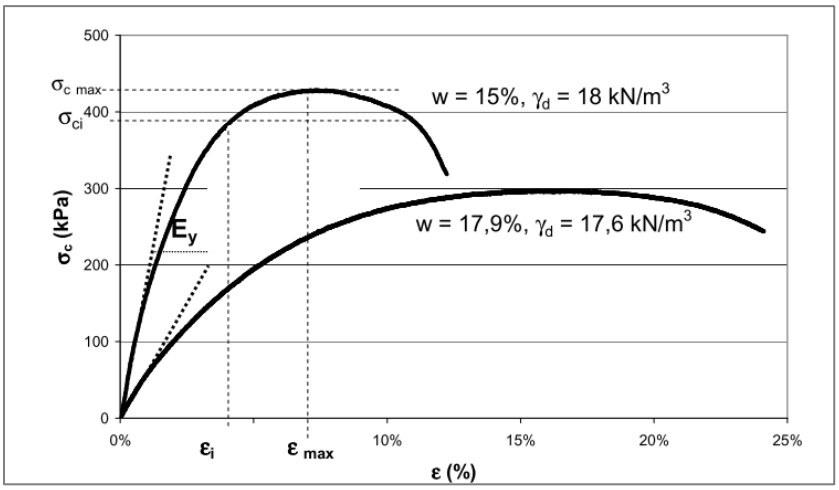

Figure 2. 13 Curves describing a unconfined compression test at different moisture content (Camp, 2008).

Bending test

Bending test is a flexion test that consist in applying pure flexion to a sample in the form of beam. It can be set with four or three point bending modes. The difference is the location of the maximum bending moment and the maximum fiber stress. In Figure 2. *14* is shown the tensile field. In our study a bending test with four bending point is chosen. Normally, this test is done with concrete beam, and less frequently with clayey soil. Laboratory bending test with soil beam well represents the tensile condition of a soil layer in a landfill top cover subjected to settlement of the submitted waste body. The soil beam of square section is prepared. The soil is mixed with the required moisture content and then sealed in a plastic bag for at least 48 hours to allow uniform hydration. Afterwards the soil is compacted by static double compaction to form the beam (L = 0,4m, a = 0,1m). The beam is symmetrically placed on the two movable supports, spacing L_2=0,3m (Figure 2.14); it is subjected of a continuous displacement rate (e.g. 0,2 mm/min), rising against the upper fix supports spaced L_1=0,1m, until breaking (Camp et al., 2010; Rajesh et al., 2011).

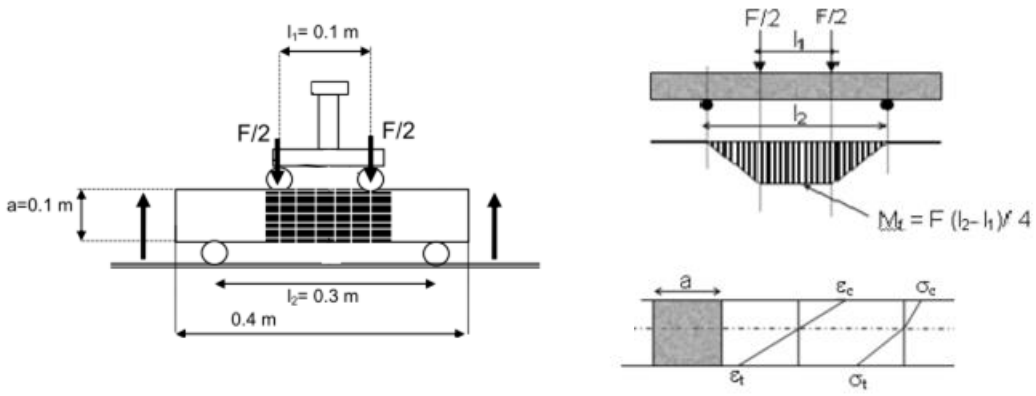

Figure 2. 14 (a) Four points bending test apparatus, (b) stress and strain field (Camp, 2008).

Particle Image Velocimetry method

Assessement of soil behaviour in element tests or phisycal models could be evaluated through stress-strain measurements. Precision to study a variety of geotechnical processes increased till small-strain range (0,001%) and it is studied with modern techniques; anyway, measurement techniques for the construction of planar deformation fields in geotechnical model tests remain less precise (Scholey et al., 1995).

Various image-based techniques have been used to measure planar deformation fields in geotechnical element and model tests: X-ray, stereo-photogrammetric methods, computer-based image processing techniques, i.e. centroiding. The latter relies on the presence of artificial targets within the deforming soil; these targets are reference points for the element or modeling test. Some drawbacks follow the assumption of targets: excessive density of markers can influence the behaviour of the soil, besides, a widely spaced gird provides sparse data, moreover trackers could be obscured during the experience.

Particle Image Velocimetry (PIV) method is an alternative technique for measuring the deformation of soil through a series of digitally captured images. It is a velocity-measuring technique that was originally developed in the field of experimental fluid mechanics, by Adrian (1991), and then it was applied to geotechnical testing. Since the PIV method operates on the image texture, intrusive target markers need not to be installed in the observed soil: natural soil (i.e. sand) has its own texture in the

form of different-coloured grains and of light and shadow formed between differently illuminated grains. Instead of using targets, digital photography is used to capture images of planar soil deformation. In digitalized form, colour images consist of three intensity (brightness) matrices (from 0 to 255), one for each colour channel (red, green and blue). In a monochrome image, there is only one colour channel, so the three intensity matrices are the same: a monochrome image is composed by a single matrix containing the intensity recorded at each pixel. This intensity matrix is defined as $I(\boldsymbol{U})$, where $\boldsymbol{U}=(u, v)$is the pixel coordinate (White et al., 2003).

In the paper of White et al. (2003), PIV method is explained. This measurement technique operates by processing digital images, captured from a digital camera Kodak DC280, (resolution: 1760x1168 pixels).

The displacement between two following images is processed as shown in Figure 2.15.

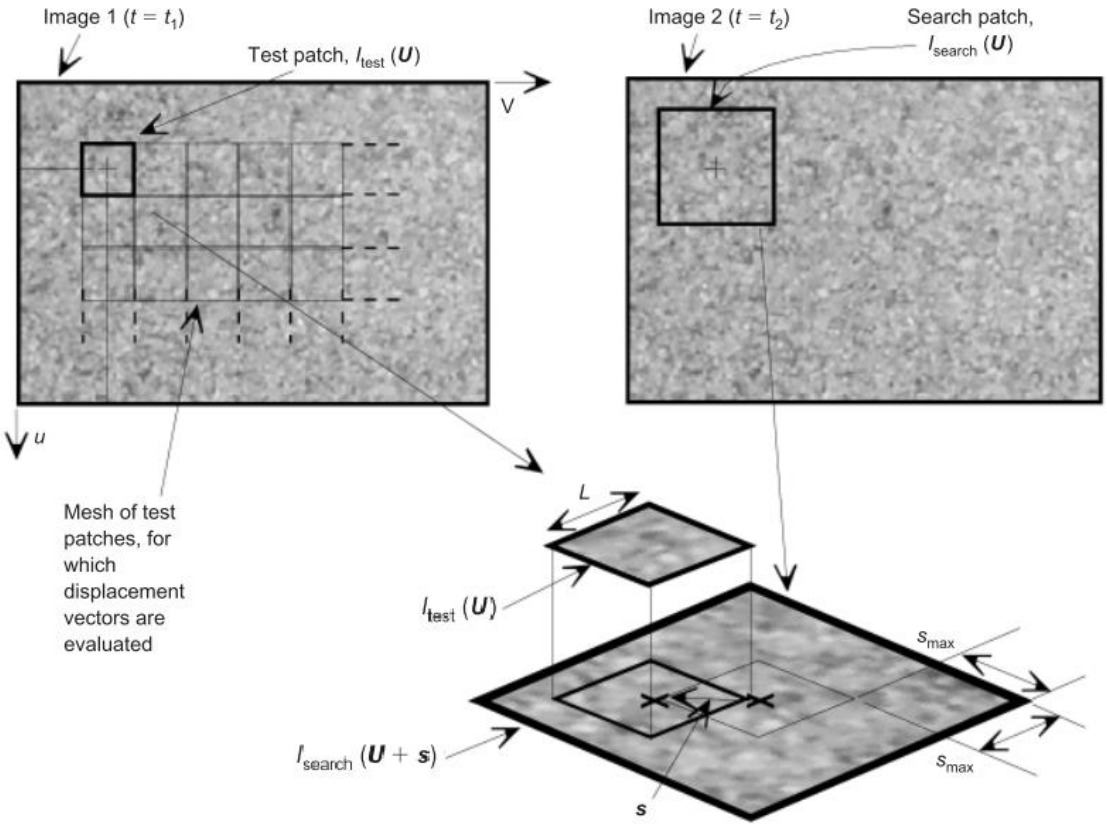

Figure 2. 15 Image manipulation during PIV analysis (White et al., 2003).

The first image (mesh) is divided into a grid of test patches. Each test patch, $I_{test}(\boldsymbol{U})$, consists of a sample of the image matrix, $I(\boldsymbol{U})$, of size L x L pixels. To find the displacement of the test patch between images 1 and 2, a search patch $I_{search}(\boldsymbol{U} + \boldsymbol{s})$ is extracted from the second image. This search patch extends beyond the test patch by a distance $\boldsymbol{s}_{max}$, in the *u* and *v* directions, defining the zone in which the test patch is to be searched for. The cross-correlation of $I_{test}(\boldsymbol{U})$ and $I_{search}(\boldsymbol{U} + \boldsymbol{s})$ is evaluated, and normalised by the square root of the sum of the squared values of $I_{search}(\boldsymbol{U} + \boldsymbol{s})$ over the range of $\boldsymbol{U}$ occupied by the test patch. The resulting normalised correlation plane $R_n(\boldsymbol{s})$ indicates the 'degree of match' between the test and search patch over the offset range in the domain of $\boldsymbol{s}$. The highest peak in the normalized correlation plane, $R_n(\boldsymbol{s})$, indicates the displacement vector of test patch, $\boldsymbol{s}_{peak}$.

This procedure is repeated for the entire grid of test patches, giving the displacement field between two images. The analysis continues comparing image 1 to image 3, and so on.

Precision plays an important role in this overview, it is defined as the random difference between multiple measures of the same quantity (White et al., 2003). PIV precision could be affected by: (a) test patch size, (b) appearance of the soil and (c) movement, meant as whole or fraction of a pixel. Different experiences at different patches sizes were carried out by the authors:

A. Comparison of an artificial image of soil, consisting of a matrix of randomly generated pixel intensities, with itself, without movement;

B. It use the same random image used in experience A, but enlarged: patch dimension is the same but 'grain' size is doubled;

C. Same experience but with a sand soil image, still without movement;

D. Sand soil image compared with itself, with integer movement of 1 pixel;

E. Sand soil image compared with itself, with movement of a fraction of pixel;

F. In this experience an artificial texture is imparted to clay.

From the results reported in Figure 2.16, some conclusions are taken: larger PIV patches produces less scatter, and therefore improved precision, over 8x8 pixel patch size; experienced B register less precision than A; a further reduction in

precision is registered with sand matrix, in fact errors could occur i.e. for lightening changes; from comparison between experiment D and E, precision is noticed to be reduced if movement is far from an integer value; finally results of artificial clay textured is comparable with experience C, so it is applicable. The curve UB (Figure 2.16) is an empirically derived upper bound on the precision error, and it is given by equation (2.4):

$$\rho_{pixel} = \frac{0{,}6}{L} + \frac{150000}{L^8} \tag{2.4}$$

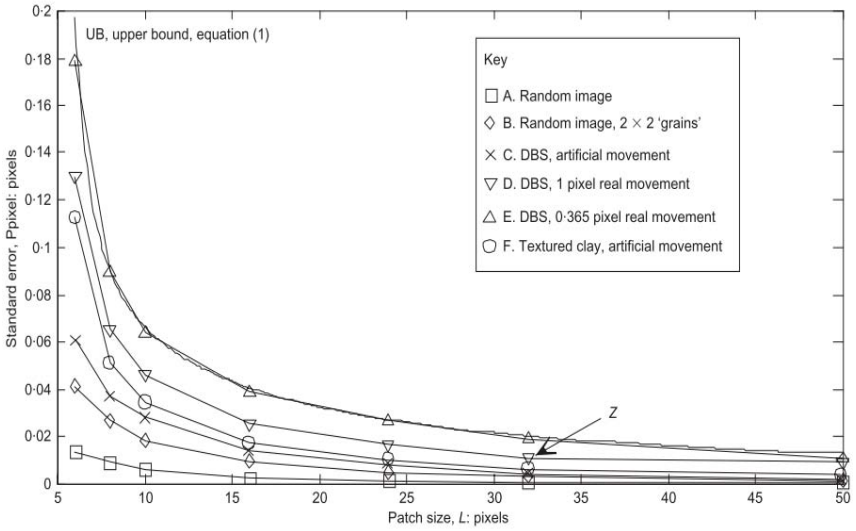

Figure 2. 16 PIV precision against patch size (White et al., 2003).

In conclusion, PIV method is a strong function of type and dimension of the texture (Figure 2. *16*6) and moreover of path size (Figure 2. *17*7): larger patches improve precision but on the other hand smaller patches allow a greater number of measurements. It has been demonstrated that the planar movement of sand can be detected using PIV to a precision of 1/15th of a pixel (White et al., 2001a).

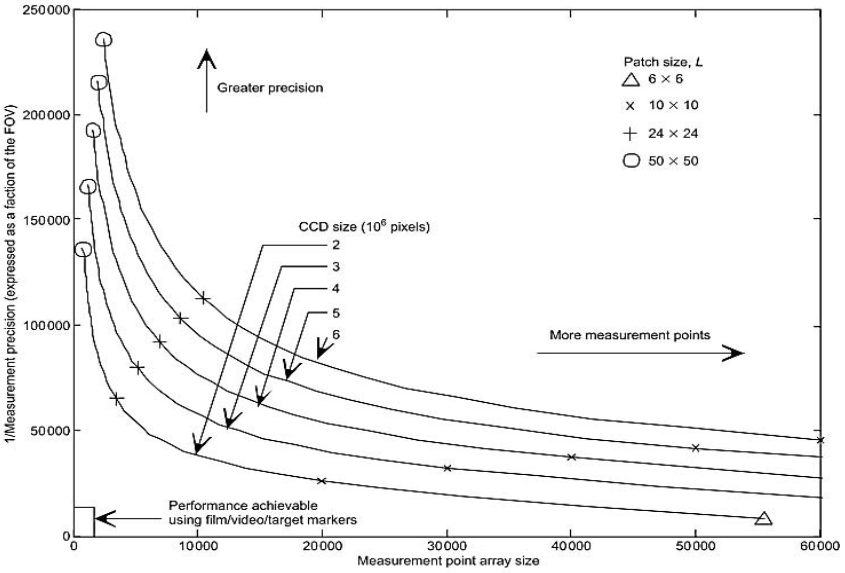

Figure 2. 17 Precision against measurement array size (White et al., 2003).

The following Figure 2.18 highlights the improving of precision in comparison with centroiding methods.

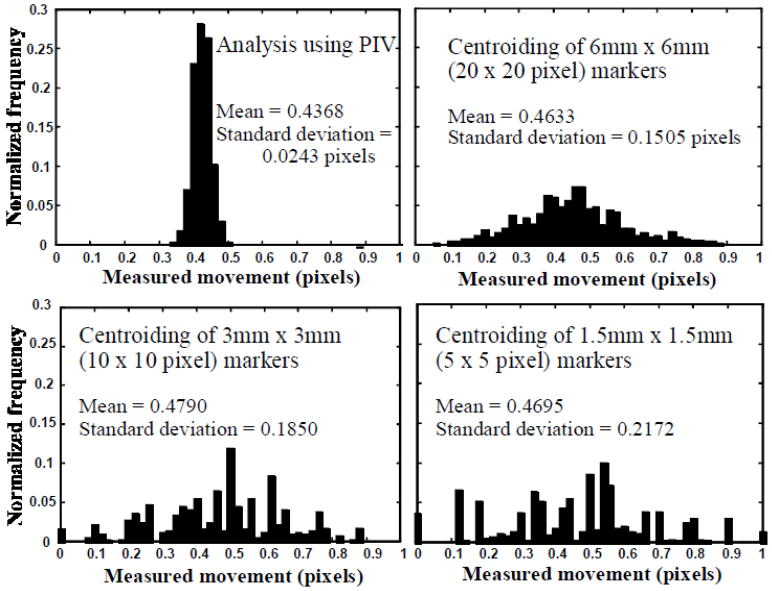

Figure 2. 18 Comparative precision of PIV and centroiding methods (White et al., 2001b)

Biaxial traction test

In this report, high attention is given to behaviour of geomembrane. Infect, limiting fluid intrusions, it plays a key role in sealing a landfill, so that its integrity affects the efficacy of a barrier. Moreover, the durability of the geomembrane throughout the life of the landfill is a required performance, still hardly achievable. In this outlook, studying deformability and strength is fundamental.

This test consists in anchoring a circular sample of geomembrane on the boundary and in applying a pressure from the bottom with injection of air. Deformation and tension on the geomembrane are calculated thanks to measurements of pressure applied (p) and height of the cap (e) (see Figure 2.19) .

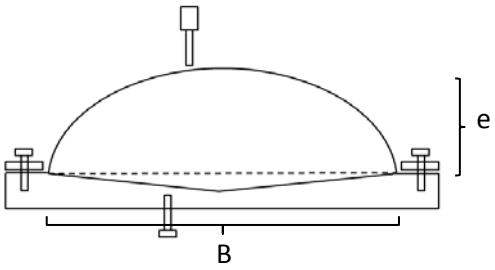

Figure 2. 19 Biaxial traction test apparatus

The hypothesis are: spherical and uniform deformation; geomembrane homogeneous and incompressible; tension on the geomembrane constant and homogeneous on the thickness, linear-elastic behaviour. The problem is solved through the theory of the symmetric hemispherical deformed geomembrane (Gourc, 1982).

At first, the parameter θ is iteratively determined through equation (2.5):

$$\frac{2e}{B} = \frac{1-\cos\vartheta}{\sin\vartheta} \tag{2.5}$$

In which:

- e = cap's height
- B = diameter of the sample, equal to 0,2m

In a second step, deformation ε is provided by equation (2.6):

$$\varepsilon = (1+\nu)\frac{\vartheta - \sin\vartheta}{\sin\vartheta} \tag{2.6}$$

In which:

- v = Poisson coefficient, assumed equal 0,5

Hence, the elastic modulus k si given by equation (2.7):

$$\frac{p}{k}\pi\frac{B^2}{4} = (1-\nu)(\vartheta - \sin\vartheta)\pi B \tag{2.7}$$

In which:

- p = pressure applied

In the end, tension T is provided by equation (2.8). T represents the tension on the geomembrane before the loss of resistance and permeability.

$$\varepsilon = \frac{T}{k} \tag{2.8}$$

3.

Study on CSM top cover deformation

This rapport focuses on a French disposal facility for a low and intermediate level short life nuclear waste, described in Section 1.4.1.. The importance of this report lies in the opportunity of carrying out a great quantity of observations of the behaviour of a top cover subjected to differential settlements.

The important role played by the cover system (limit infiltration of water, limit release of gas, avoid erosion, etc) implies a careful study and a precise design. The cover principle is a system of several different layers made of natural and synthetic materials, supposed to keep physical, mechanical and hydraulic features throughout the life of the disposal facility. The cap cover of the CSM disposal facility is described in the following lines (Figure 3.1).

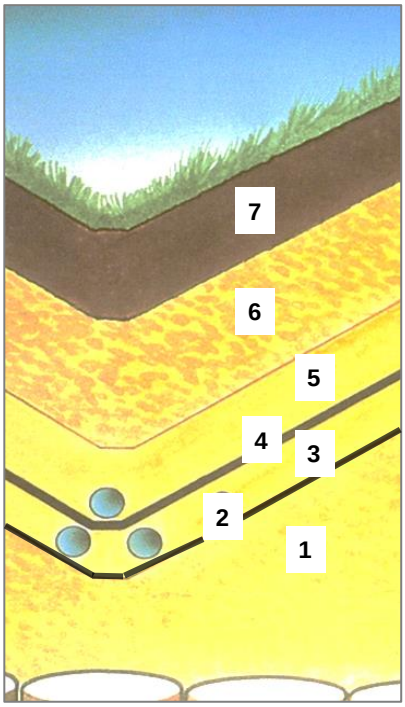

Figure 3.1 CSM cross section (Vervialle, 2011).

The upper layer (n.7), composed of vegetative soil, limits water infiltration with its retentive power, prevent degradation from climatic forces and gives to the facility a more attractive aspect. Even the following layer (n.6), made mostly of sandy silt and secondly of sandstone, limits infiltration; in addition it protects the geomembrane against animal and human intrusions. Figure 3.3 clearly shows this first two layers.

Below a layer of sand (n.5) has a function of drainage of the water directed to the pipes. The next layer (n.4) is the bituminous geomembrane, it prevents a water flow and directs it into the proper storage area. The choice of the bituminous geomembrane deals with the capability to sustain large deformations (see Table 3.2 and Figure 3.2). Layer n.3 is composed of sand to drain water in case of leakage of the geomembrane. Another layer (n.1) of clay and sand is set up to give the specific shape of the cover which is similar to a factory (Figure 3.2). This shape has been selected in order to collect the run-off following a shortened flow path.

Figure 3.2 CSM cover implementation.

Figure 3.3 CSM: view of the first two layers.

Actually there is another layer (n.2), between layer 3 and 1, that is an additional geomembrane with a function of alert, in order to assure with an higher level of certainty the waterproof condition of the cover system.

Grain size distribution	
<2μm	12%
<80μm	39%
Atterberg limits	
Plastic Index, PI	8
Plastic Limit, w_P	22%
Liquid limit, w_L	30%
Normal Proctor characteristics	
Optimum dry unit weight, $\gamma_{d,OPT}$	18,7 kN/m^3
Optimum water content, w_{OPT}	11,3%

Table 3.1 Geotechnical properties of sandy silt used for the CSM (Versaevel and Gourc, 2012).

Liner	Max Deformation (%)
Clay	0,2 – 1,5
GM HighDensity Polyethylene	15
Geosynthetic Clay Liner	20
GM bituminous	50
GM polypropylene	50
GM PolyVinyle Chlorure	300
GM Ethylene Propylene Diene	>300

Table 3.2 Comparison of extensibility of different available types of geomembranes (Versaevel and Gourc, 2012).

3.1. Study on geomembrane elongations

During the post-operational phase of the disposal facility, some settlements were registered: the more significant values were observed mainly on slopes and only locally on the top of the cap cover. The Figure 3.4 represents the field of total settlements in 2008.

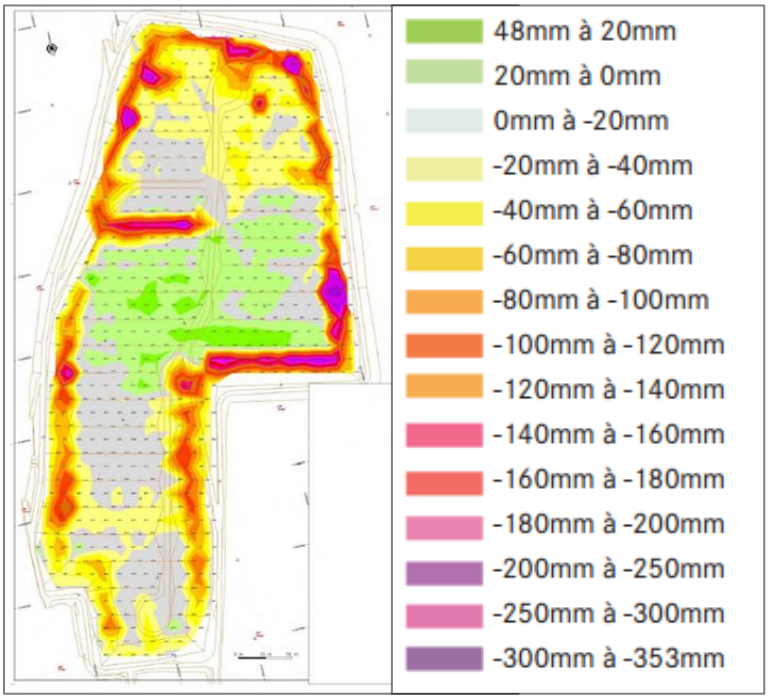

Figure 3.4 Field of settlements from installation to 2008, (ANDRA, 2008).

The settlements on slopes could be caused by the sliding of the cap cover on the geomembrane or by the sliding of the geomembrane on the leveling layer. The settlement on the top cover on the north-eastern part of landfill, seems to be connected with a local crushing of the waste body (Figure 3.5 and Figure 3.6). Finally, the settlement on the western part took place along the way used during operational phase, resulting an area more subjected to stress. The remedy for the settlements on slopes was to smooth the slide adding natural materials and building a bottom retaining wall.

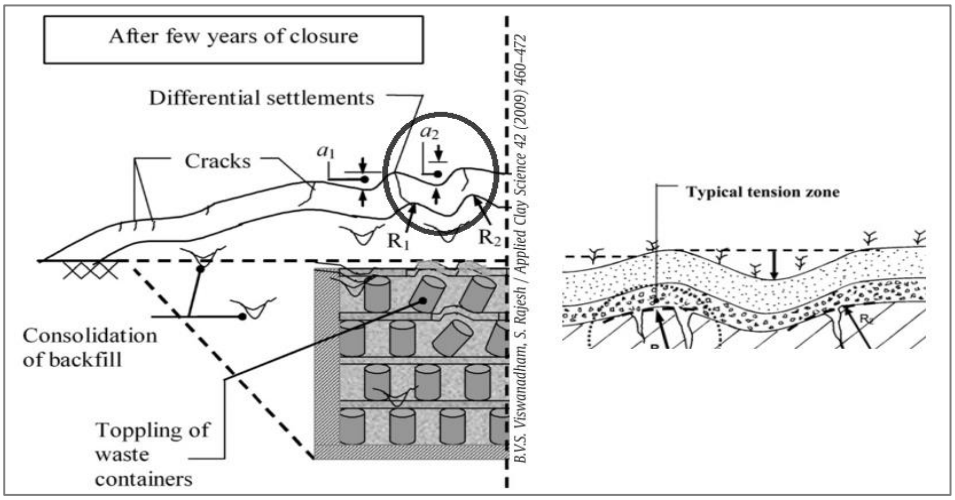

Figure 3.5 Schematic representation of distress in a closure system of low-level radioactive waste disposal site (Viswanadham, 2009).

In 2009, the N-E settlement area has been excavated. The aim of this excavation was to control if the geomembrane was damaged due to this differential settlement (Villard et al., 2000) and to find out the cause of this settlement.The excavation showed that the geomembrane was not evidently damaged. The reason of this settlement seems to be a local crushing of the waste body (Figure 3.5), maybe due to a cracking of the backfill.

Figure 3.6 View of the settlement from the top soil.

In general, the importance in studying effects of the settlements on the top cover lies in different factors. An excessive traction on the geomembrane could damage it (cracks, holes), and this could compromise characteristics for which it has been designed for (permeability, stiffness, deformability); moreover a study of the sandy silt layer itself under stress and deformation, and a study of volumes involved could help to better understand the top soil behaviour. In particular, in CSM disposal facility, waterproofness is accomplished by bituminous geomembrane, but, due to excessive deformation, occurred settlements could cause loss of permeability and tensile strength. It is for these reasons that studying elongation of the geomembrane is the key to evaluate its state.

The area taken into account corresponds to the area of the N-E settlement, reported in Figure 3.7. The maximum lowering registered on the top soil is 0,43m, whereas the relative lowering on the principal geomembrane is about 0,61m.

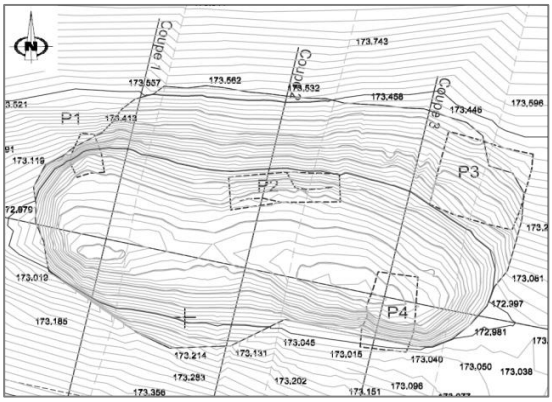

Figure 3.7 Topographic plan of the settlement and representation of the four samples of geomembrane: P1, P2, P3 and P4.

At first, through an accurate topographical work from the topographical data-set collected on the site in 2009, the entire area has been represented, through different sections: one section, sec. A (x=0÷24,6m), along east-west direction, and 26 sections along north-south side (every meter, except section 26 placed after 0,60m from section 25) (Figure 3.9). For every section, the trends of the top soil (TS), of the principal geomembrane (PG) and of the alert geomembrane (AG) were outlined

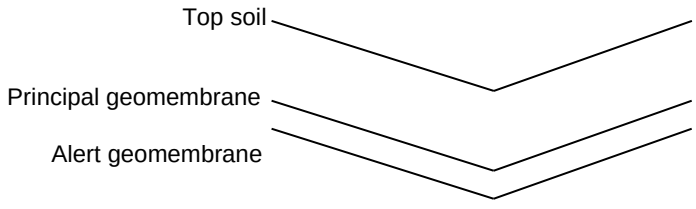

Figure 3.8 Scheme of the top layer.

(Figure 3.8) in the actual deformed outlook.

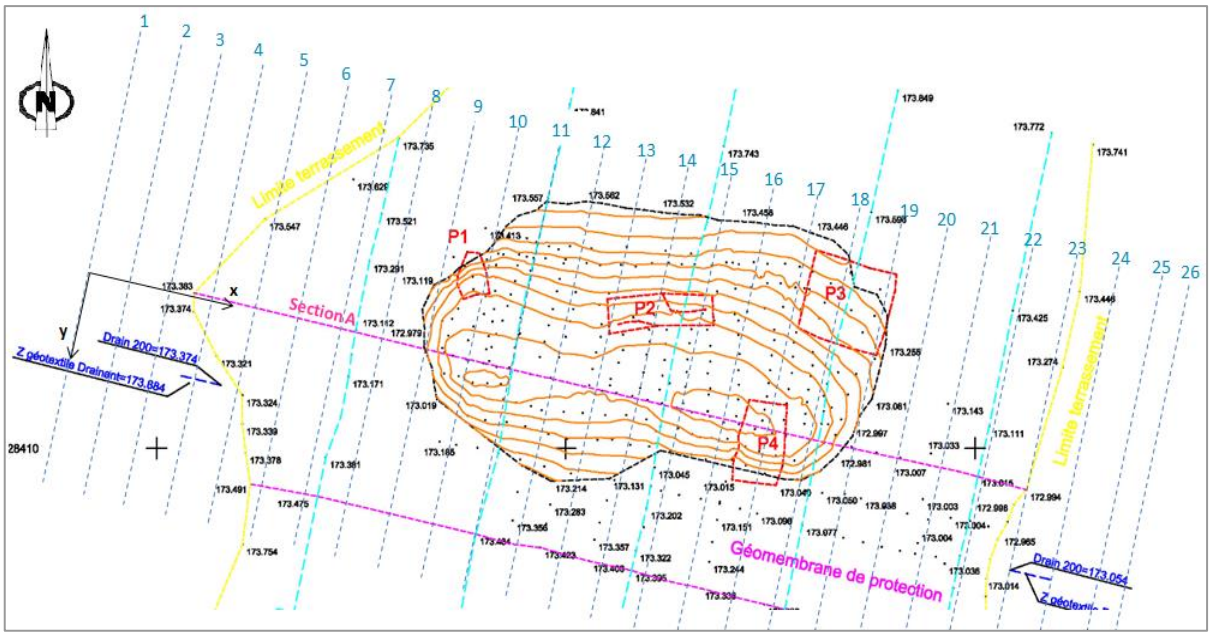

Figure 3.9 Topographic plan of settlement of the top soil.

Secondly, the trends of the three surfaces (TS, PG and AG) before settlement has been supposed.

Outer sections (sec. 1-7, sec 21-26) did not show deformations (Figure 3.9), thus they were used as sample to represent *top soil* in the deformed sections (S9÷19). For the northern part (y=0÷-6m) the average slope results to be 5°. The southern part (y=0÷6m) was characterized by two different slopes, steeper approaching section A; for this reason it has been calculate an average slope for every section, it results to be 9°.

Different suppositions were carried out in order to find the better surface that could approximate the *principal geomembrane*. At first, it has been taken the same slopes of the top soil and it gave good results. Then, the slopes were calculated with the same procedure used for the top soil: a slope of 5° was found for the northern part, and a slope varying between 7° and 8° for the southern one. At the moment of comparing the two surfaces supposed for the PG, before and after the settlement, it results more representative the second approximation.

For the *alert geomembrane*, it was decided to use the same slopes of the PG. This is a great estimation, but necessary: infect there were not enough data to

understand were the AG was precisely placed. This uncertainty affects also further studies.

Elongations of top soil (TS) and principal geomembrane (PG) were considered, in particular along section A and sections 5 ÷ 22; alert membrane has been excluded because of the uncertainty of its position.

As Table 3.3 and Table 3.4 report, along section A, PG shows an higher elongation than TS (0,20% and 0,72% respectively). Perpendicularly, for both the levels, highest deformation are registered between section 9 and section 19. Even in this direction, deformation of PG results sensibly more important, until 72% higher than TS's: 0,41% of TS versus 1,49% of PG. Then, focusing on geomembrane of section 16, on the most deformed part (y=-6÷1,5m; Figure 3.10 and Table 3.4), a deformation of 2,39% was registered.

TOP SOIL			
Sections	**L before settl. [m]**	**L after settl. [m]**	**Δε (%)**
SA x=4÷21m	24,62	24,67	**0,20**
S5 y=-6÷6m	12,08	12,08	**0,00**
S6 y=-6÷6m	12,08	12,09	**0,08**
S7 y=-6÷6m	12,08	12,1	**0,17**
S8 y=-6÷6m	12,08	12,11	**0,25**
S9 y=-6÷6m	12,08	12,12	**0,33**
S10 y=-6÷6m	12,08	12,14	**0,50**
S11 y=-6÷6m	12,08	12,14	**0,50**
S12 y=-6÷6m	12,08	12,14	**0,50**
S13 y=-6÷6m	12,08	12,13	**0,41**
S14 y=-6÷6m	12,08	12,13	**0,41**
S15 y=-6÷6m	12,08	12,13	**0,41**
S16 y=-6÷6m	12,08	12,11	**0,25**
S17 y=-6÷6m	12,08	12,1	**0,17**
S18 y=-6÷6m	12,08	12,1	**0,17**
S19 y=-6÷6m	12,08	12,08	**0,00**
S20 y=-6÷6m	12,08	12,08	**0,00**
S21 y=-6÷6m	12,08	12,08	**0,00**
S22 y=-6÷6m	12,08	12,08	**0,00**

Table 3.3 Elongation of the top soil.

PRINCIPAL GEOMEMBRANE			
Sections	**L before settl. [m]**	**L after settl. [m]**	**Δε (%)**
SA x=4÷21m	20,82	20,97	**0,72**
S5 y=-6÷6m	9,48	9,5	**0,21**
S6 y=-6÷6m	10,42	10,45	**0,29**
S7 y=-6÷6m	11,78	11,83	**0,42**
S8 y=-6÷6m	12,07	12,16	**0,75**
S9 y=-6÷6m	12,07	12,35	**2,32**
S10 y=-6÷6m	12,07	12,32	**2,07**
S11 y=-6÷6m	12,07	12,25	**1,49**
S12 y=-6÷6m	12,07	12,23	**1,33**
S13 y=-6÷6m	12,07	12,24	**1,41**
S14 y=-6÷6m	12,07	12,25	**1,49**
S15 y=-6÷6m	12,07	12,25	**1,49**
S16 y=-6÷6m	12,07	12,26	**1,57**
S17 y=-6÷6m	12,07	12,24	**1,41**
S18 y=-6÷6m	12,07	12,15	**0,66**
S19 y=-6÷6m	12,07	12,08	**0,08**
S20 y=-6÷6m	12,07	12,07	**0,00**
S21 y=-6÷6m	12,07	12,07	**0,00**
S22 y=-6÷6m	12,07	12,07	**0,00**
S16 y=-6÷1,5m	7,53	7,71	**2,39**

Table 3.4 Elongation of the principal geomembrane.

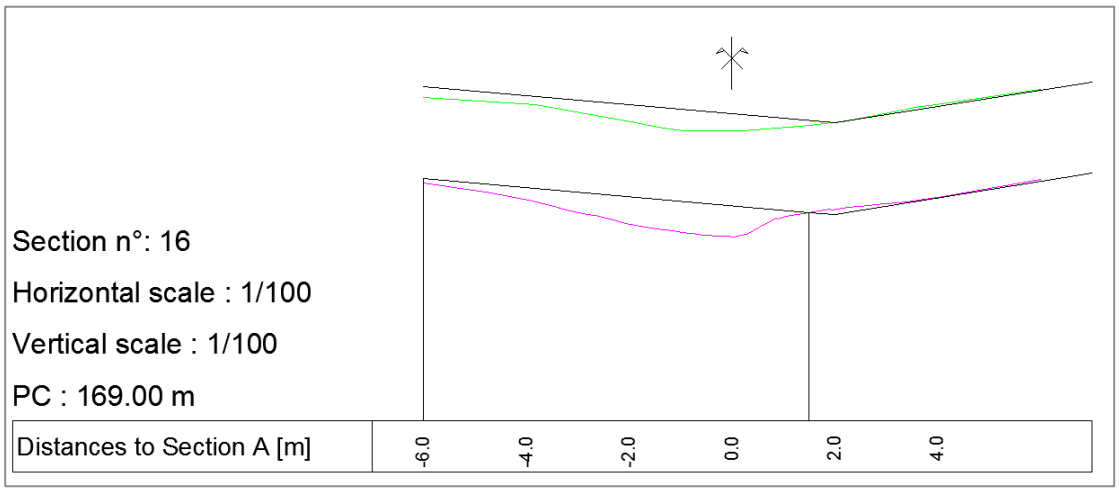

Figure 3.60 Particular of section 16, green coloured line represents top soil, pink coloured line represents principal geomembrane.

A further study of relative settlement and relative elongation has been carried out. Figures 3.11-16 report the results. On one hand, the two surfaces (green line for top soil and red line for geomembrane) were plotted in comparison with relative settlements (blue line), on the other hand relative elongations (every meter) of the top soil and principal geomembrane (relatively green and red dotted line) were plotted in comparison with their relative altitudes. Sections A, 10, 12, 16 and 18 have been represented, for their location on the main settled parts (Figures 3.11-16).

These comparisons support the previous results. In general, PG deformation is more important than TS one. From graphs in Figure 3.11b, Figure 3.12b, Figure 3.13b, Figure 3.14b, and Figure 3.15b, percentage elongation is observed to be higher in correspondence of flexion areas. This is noticed for both the surfaces but more sensibly for PG: the TS's trend is less brusque than the PG's; this fact confirms that PG settled more than TS. The local relative elongations shows values close to 10%, thus cracking of the soil is expected in these specific zones, since relative elongation is far than 0,5%, for low confinement condition (Gourc et al., 2010). Figure 3.11a, Figure 3.12a, Figure 3.13a, Figure 3.14a and Figure 3.15a, show that the relative settlement for every section is placed between y=-4÷2m. Along section A, we can see that settlement is placed between x=9m and x=19m.

In some graphs, it seems that a shortening occurs (percentage deformation is > 0), infect the elongation is positive. This is due to considering the deformation every meter. Arbitrarily, I decided to put value 0 instead all the negative values, claiming that it is not possible to have a shortening of the membrane (Figure 3.16).

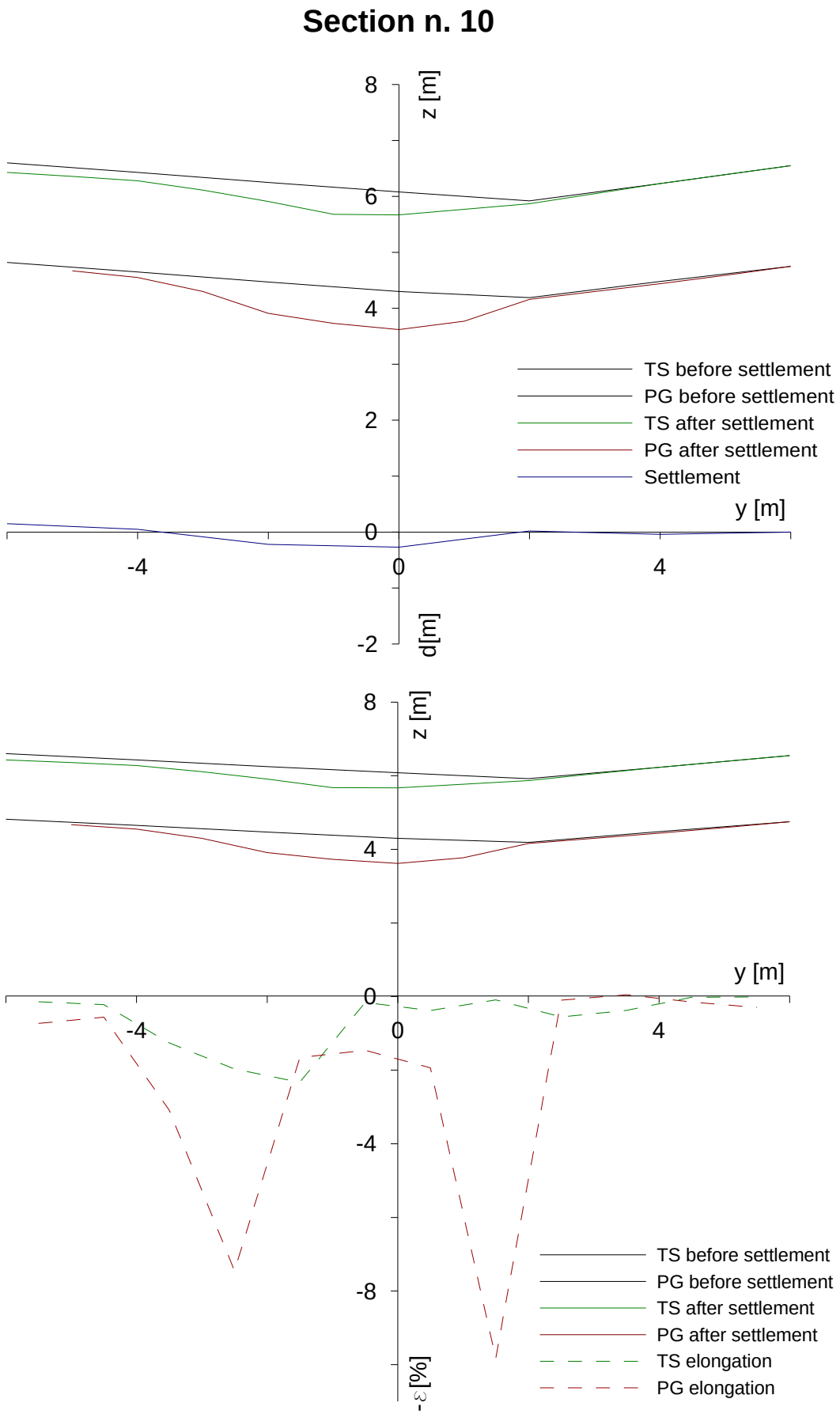

Figure 3.71 Section n. 10: (a) TS and PG altitudes plotted in comparison with the relative settlements; (b) relative elongations of TP and PG plotted in comparison with their relative altitudes.

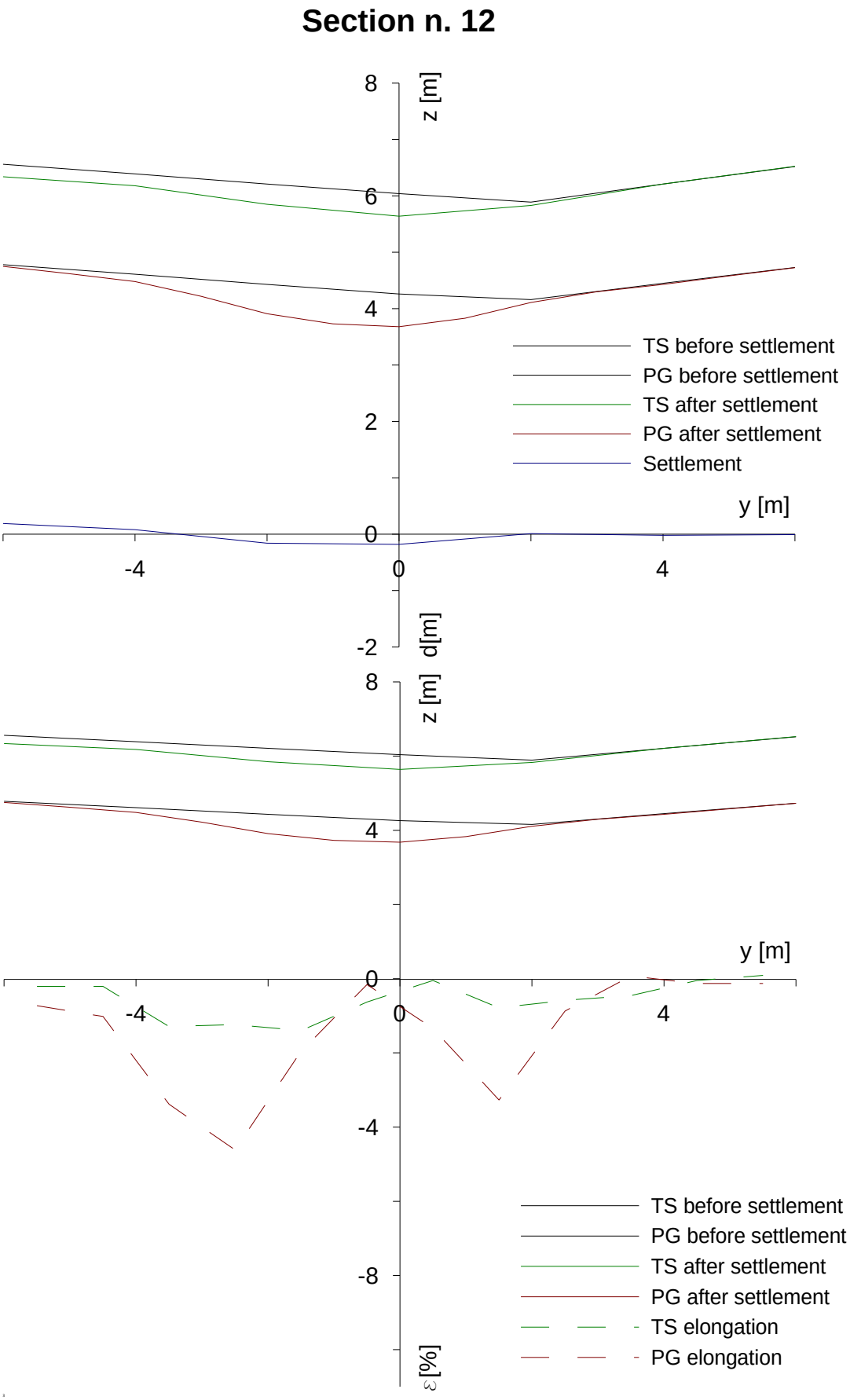

Figure 3.82 Section n. 12: (a) TS and PG altitudes plotted in comparison with the relative settlements; (b) relative elongations of TP and PG plotted in comparison with their relative altitudes.

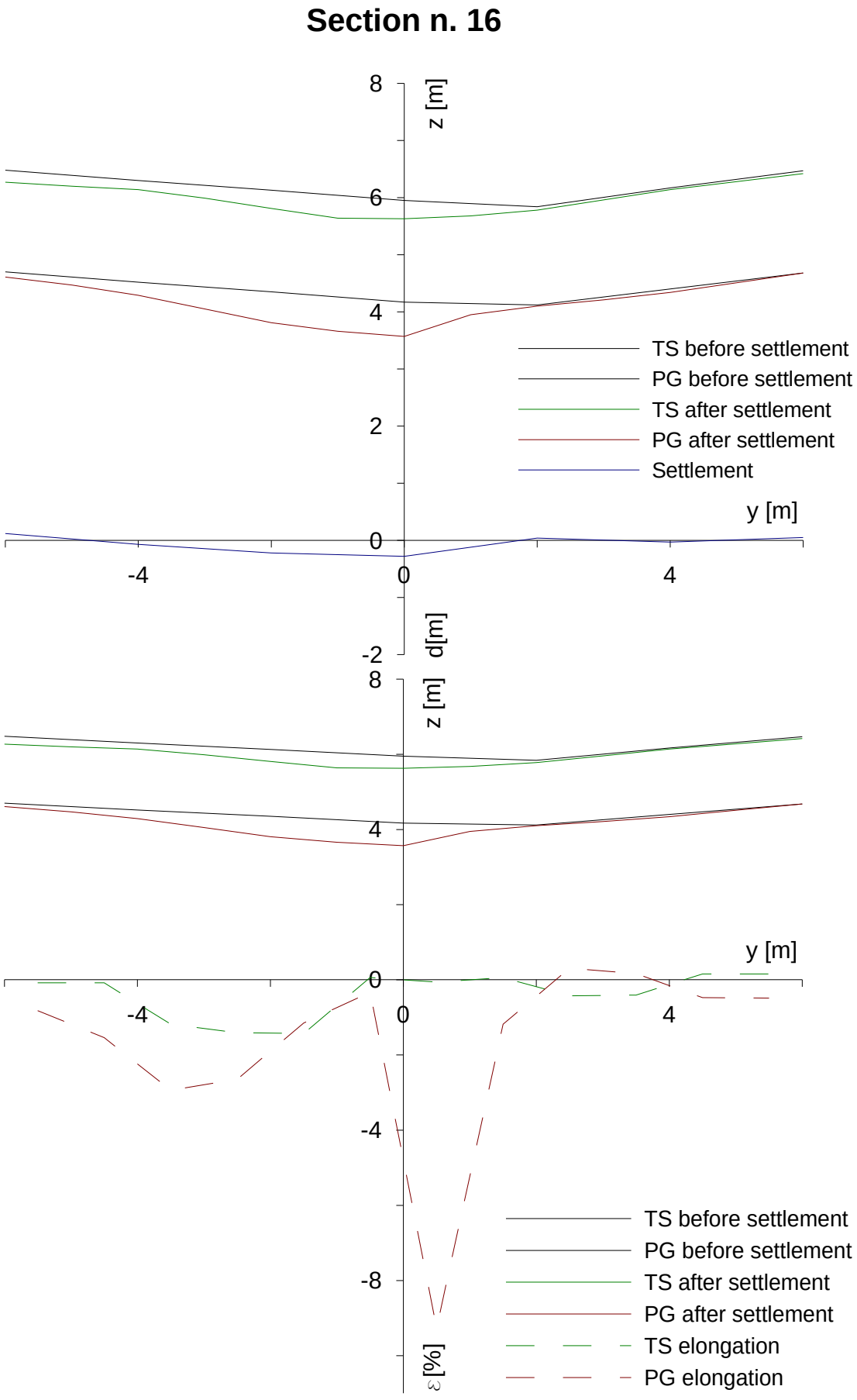

Figure 3.93 Section n. 16: (a) TS and PG altitudes plotted in comparison with the relative settlements; (b) relative elongations of TP and PG plotted in comparison with their relative altitudes.

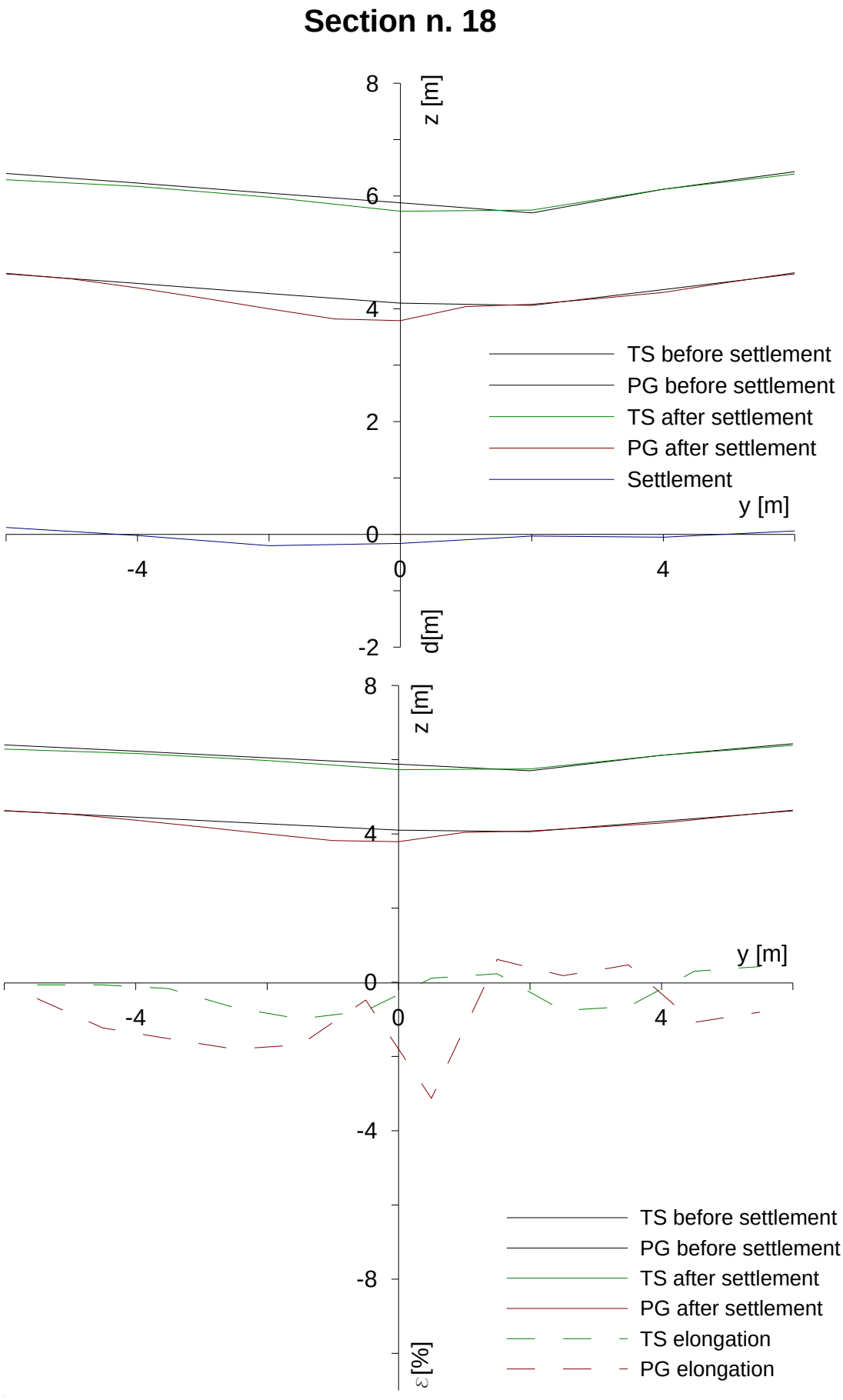

Figure 3.104 Section n. 18: (a) TS and PG altitudes plotted in comparison with the relative settlements; (b) relative elongations of TP and PG plotted in comparison with their relative altitudes.

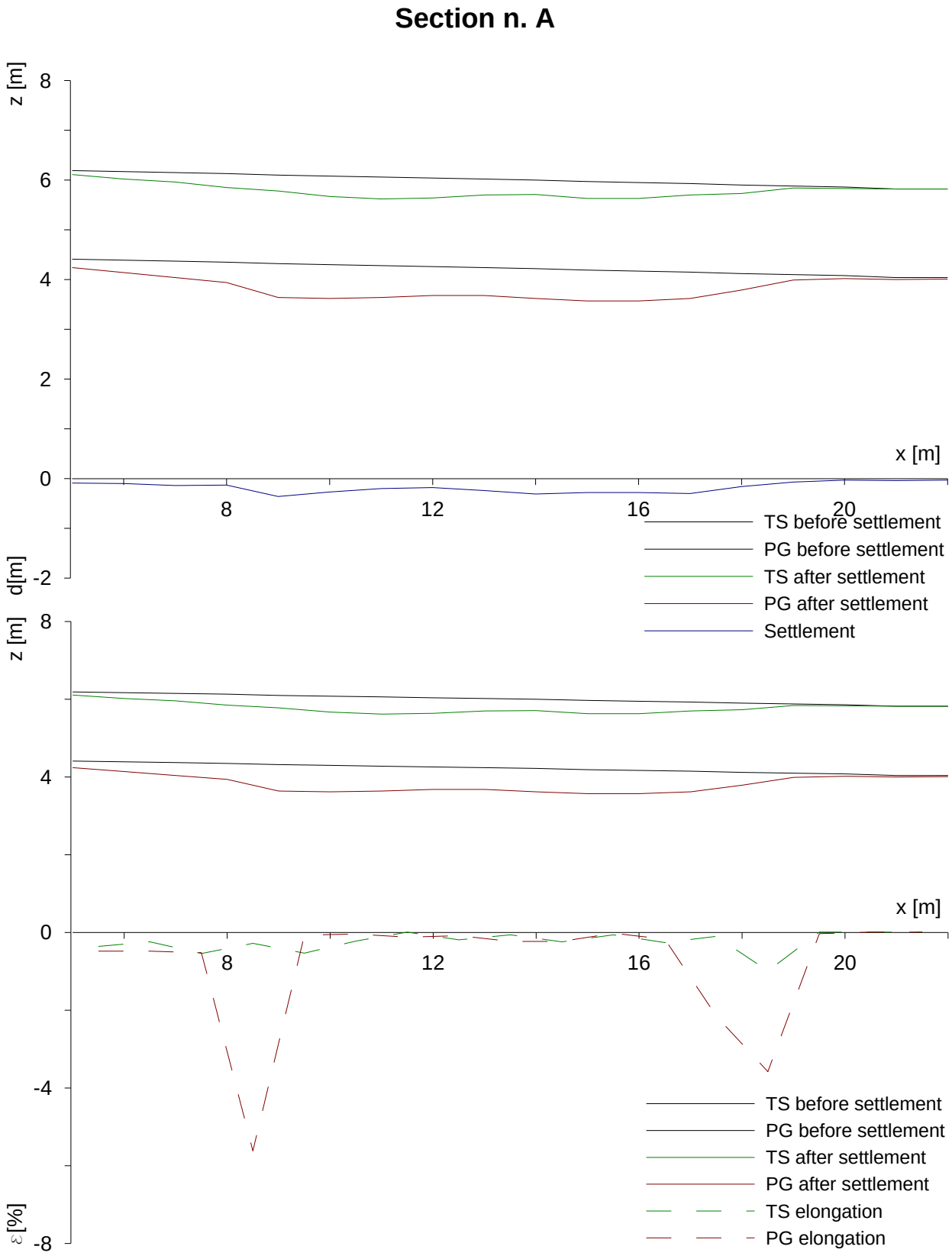

Figure 3.15 Section n. 10: (a) TS and PG altitudes plotted in comparison with the relative settlements; (b) relative elongations of TP and PG plotted in comparison with their relative altitudes.

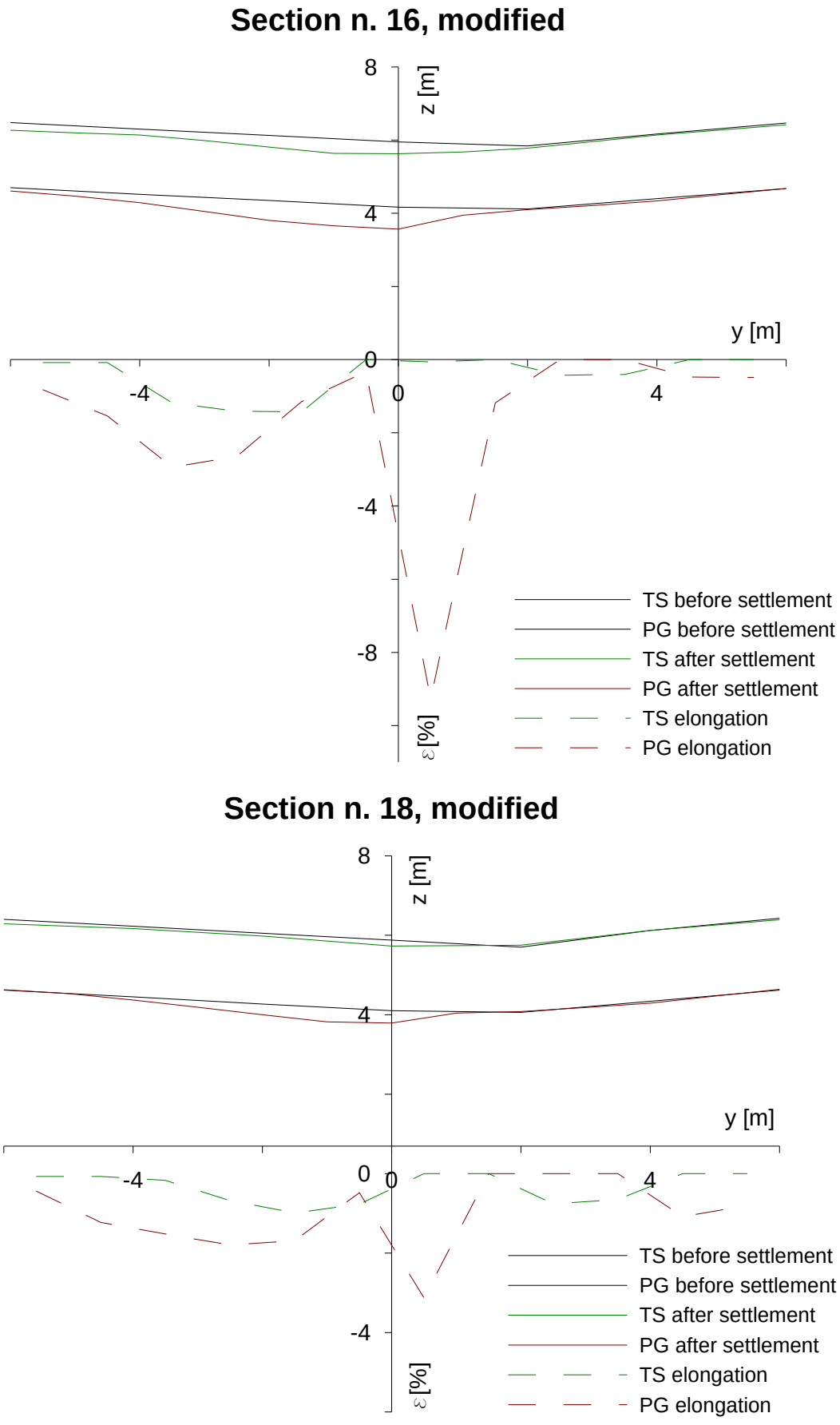

Figure 3.116 (a) Section 16: TS and PG altitudes plotted in comparison with the modified relative settlements; (b) Section 18: TS and PG altitudes plotted in comparison with the modified relative settlements.

3.1.1. Focus on samples

In January 2012 some samples of the deformed bituminous geomembrane were collected. Two samples (P3 and P4) were studied with a biaxial traction test, by the company CEMAGREF. Sample P3 was taken from an area less subjected to settlement, in comparison with P4 that came from a strained part (Figure 3.17). P1 and P2 are not taken in account for this study.

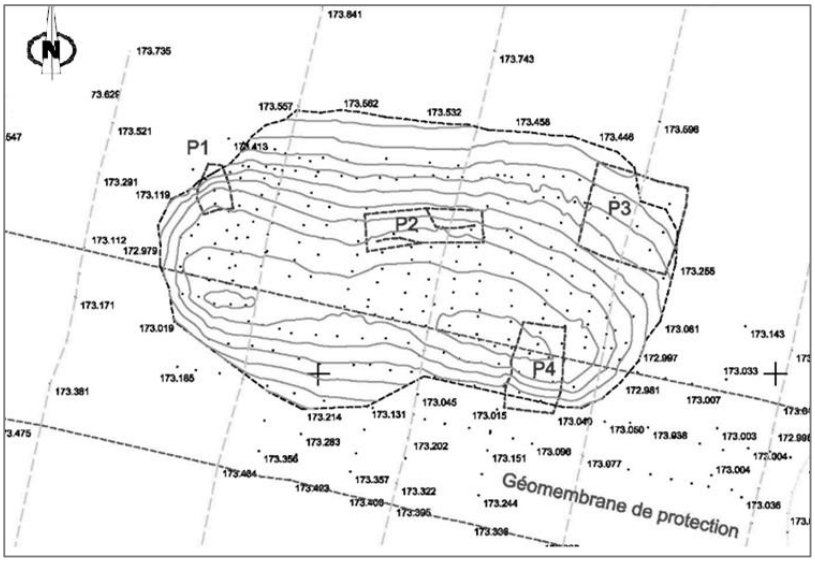

Figure 3.17 Area of the settlement. Topographic plan of the principal geomembrane.

From P3, four circular samples were taken (A1, A2, A3 and A4), with diameter of B=0,2m. From P4, was taken only a sample, A3, with the same diameter. A pressure (p) was applied and the height of the cap (e) was measured (Figure 3.18).

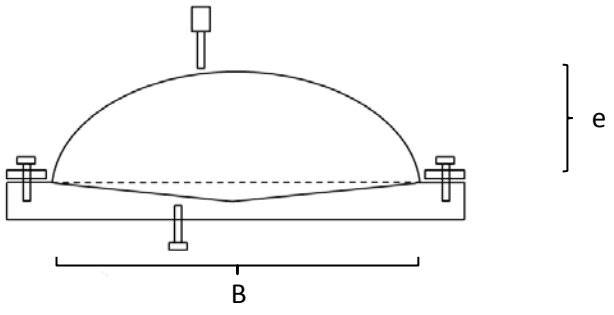

Figure 3.18 Scheme of the apparatus for a biaxial traction test.

From the biaxial test, we obtain the following information (Table 3.5): pressure applied and consequent cap's elevation.

Sample	p: pressure [kPa]	e: cap's height [m]
P3 - A1	142	0,032
P3 - A2	130	0,022
P3 - A3	151	0,031
P3 - A4	166	0,029
P4 - A3	40	0,026

Table 3.5 Results from laboratory biaxial traction test.

From this data, deformations and tensions on the geomembrane were calculated as described in Section 3.1. The hypothesis are: spherical and uniform deformation; geomembrane homogeneous and incompressible; tension on the geomembrane constant and homogeneous on the thickness, linear-elastic behaviour. The problem is solved through the theory of the symmetric hemispherical deformed geomembrane (Gourc, 1982).

The results are reported in Table 3.6. The value of the deformation is sensible for all the samples. The more significant data is the value of T for the sample P4, the tensile strength infect results to be substantially lower than the other samples. This means that the settlement damaged P4 considerably.

	P3 A1	P3 A2	P3 A3	P3 A4	P4 A3
θ [rad]	0,6194	0,5110	0,6093	0,5887	0,5566
ε [%]	10,0	6,7	9,7	9,0	8,0
k [kN/m]	121,8	197,5	136,0	165,5	47,1
T [kN/m]	12,2	13,3	13,2	14,9	**3,8**

Table 3.6 Results of the study and the samples of geomembrane, in evidence the sample placed in the most deformed area according to the topographic data.

To put in comparison these results, geomembrane percentage elongation of the samples is considered in two different directions (Figure 3.19). Thanks to the given altitude data, elongations of the samples P3 and P4 along section AA' and section BB' were estimated every meter (Table 3.7 and Figure 3.19). The deformation along section AA' in both the samples is higher than along BB', than the higher percentage of elongation is in N-S direction. Deformation is more important for P4 than P3, in both the directions. This support the fact that P4 was taken from the most deformed area.

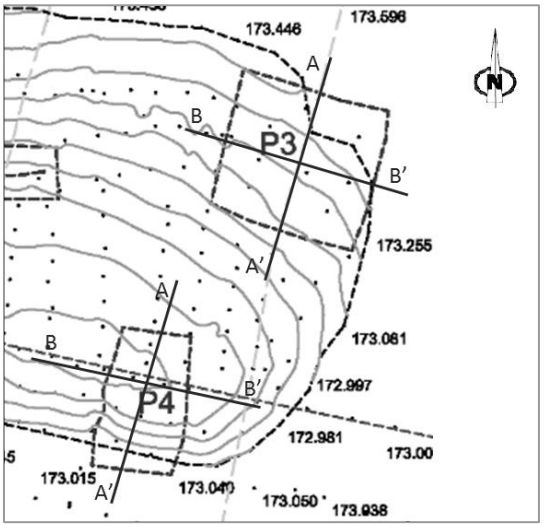

Figure 3.19 Particular of the section studied.

P4	**AA'** x=18	
	before	after
L [m] y=-1;1	2,0076	2,0866
ε [%]	*3,94*	

P4	**BB'** y=0	
	before	after
L [m] x=17;19	2,0005	2,0236
ε [%]	*1,15*	

P3	**AA'** x=19	
	before	after
L [m] y=-4;-2	2,0076	2,0354
ε [%]	*1,38*	

P3	**BB'** y=-3	
	before	after
L [m] x=18;20	2,0034	2,0128
ε [%]	*0,47*	

Table 3.7 Geomembrane sample elongations in two directions.

After that, elongation every 0,50 m was estimated (Table 3.8). The deformation along AA' of the sample P3 is more considerable than P4, except between y=0,5m and y=1m where P4 elongation is sensibly higher. In Figure 3.19, altitude curve confirm this trend. About deformation along BB', in both the sample the higher deformation is registered in the eastern portion. The more important value is registered in P4 again.

P4	**AA'** x=18	
	before	after
L [m] y=-1;-0,5	0,5019	0,5043
ε [%]	*0,48*	
L [m] y=-0,5;0	0,5019	0,5018
ε [%]	*-0,02*	
L [m] y=0;0,5	0,5019	0,5064
ε [%]	*0,90*	
L [m] y=0,5;1	0,5019	0,5741
ε [%]	*14,39*	

P4	**BB'** y=0	
	before	after
L [m] x=17;17,5	0,5001	0,5002
ε [%]	*0,34*	
L [m] x=17,5;18	0,5001	0,5017
ε [%]	*0,32*	
L [m] x=18;18,5	0,5001	0,5053
ε [%]	*1,04*	
L [m] x=18,5;19	0,5001	0,5164
ε [%]	*3,26*	

P3	**AA'** x=19	
	before	after
L [m] y=-4;-3,5	0,5019	0,5036
ε [%]	*0,34*	
L [m] y=-3,5;-3	0,5019	0,5043
ε [%]	*0,48*	
L [m] y=-3;-2,5	0,5019	0,5047
ε [%]	*0,56*	
L [m] y=-2,5;-2	0,5019	0,5047
ε [%]	*0,56*	

P3	**BB'** y=-3	
	before	after
L [m] x=18;18,5	0,5002	0,5005
ε [%]	*0,06*	
L [m] x=18,5;19	0,5002	0,5019
ε [%]	*0,34*	
L [m] x=19;19,5	0,5015	0,5012
ε [%]	*-0,06*	
L [m] x=19,5;20	0,5015	0,5092
ε [%]	*1,54*	

Table 3.8 Geomembrane sample elongations in two directions, every meter.

3.2. Study on volumes involved in the settlement

The sandy silt layer as part of top cover of CSM diposal facility for radioactive waste, is partially in charge of sealing wastes. This property could be affected by differential settlements of the cap cover, due to occurring of cracks in the layer of soil.

The settlement on the northern-east part of the landfill (Figure 3.20) has been studied.

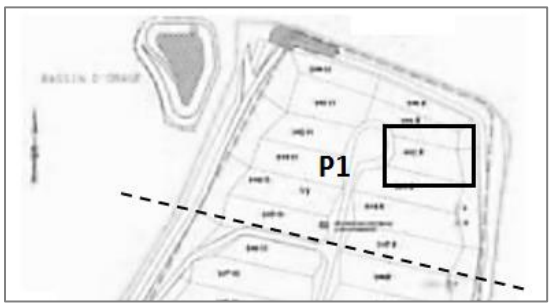

Figure 3.120 Particular of the area in study.

After surfaces' determination thanks to topographical work (Section 3.1), the software Surfer has been used to study the volumes. Different volumes were considered: V2 between top soil and first geomembrane, V1 between top soil and alert membrane, and V3 between the two membranes, as illustrated in Figure 3.21.

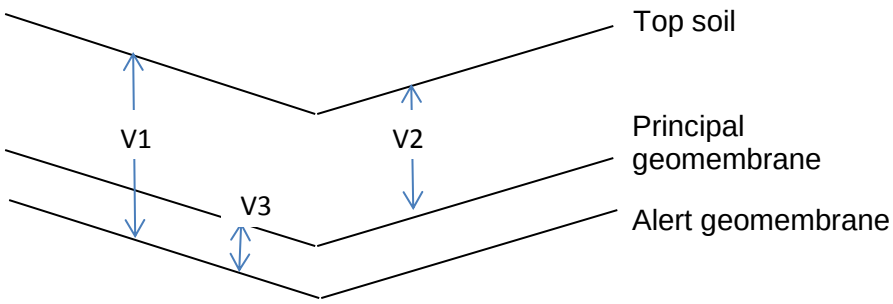

Figure 3.131 Scheme of the investigated volumes.

At first all the area was studied, from section 1 to 26. As it can be seen in Table 3.9, after settlements, volume 1 decreased of -1,7%; the higher decrease is of volume 3 (-27,4%) but the uncertainty of the position of the alert membrane did not permit to have relevant results for volume 3; volume2 increased of 2,8%. Globally, the volume decreased, but the one between top soil and principal membrane increased. The increasing of volume could be explained in this terms: a positive variation of the volume correspond to a dilatation of the soil, while crushing. The elongation of PG, higher than the one of TS, in any direction considered (Sections 3.1 and 3.1.1), remarks the behavior of volume increasing. This could lead to an increase on permeability of the layer.

VOLUME before settlement		
V1	422	m^3
V2	360	m^3
V3	62	m^3

VOLUME after settlement		
V1	415	m^3
V2	370	m^3
V3	45	m^3

ΔV1	-1,7	%
ΔV2	2,8	%
ΔV3	-27,4	%

Table 3.9 Measures of volume of the entire area.

The area of the settlements is now more particularly treated. The area counts a surface of approx. 10m x 12m, determined between sections 9 and 19. Five parts could be identified (Figures 3.22 and 3.23):

- A: x= 8 ÷ 10 m, y= -4 ÷ 3 m;
- B: x= 10 ÷ 12 m, y= -4 ÷ 3 m;
- C: x= 14 ÷ 16 m, y= -4 ÷ 3 m;
- D: x= 16 ÷ 18 m, y= -4 ÷ 3 m;
- TOT: x= 8 ÷ 18 m, y= -6 ÷ 6 m

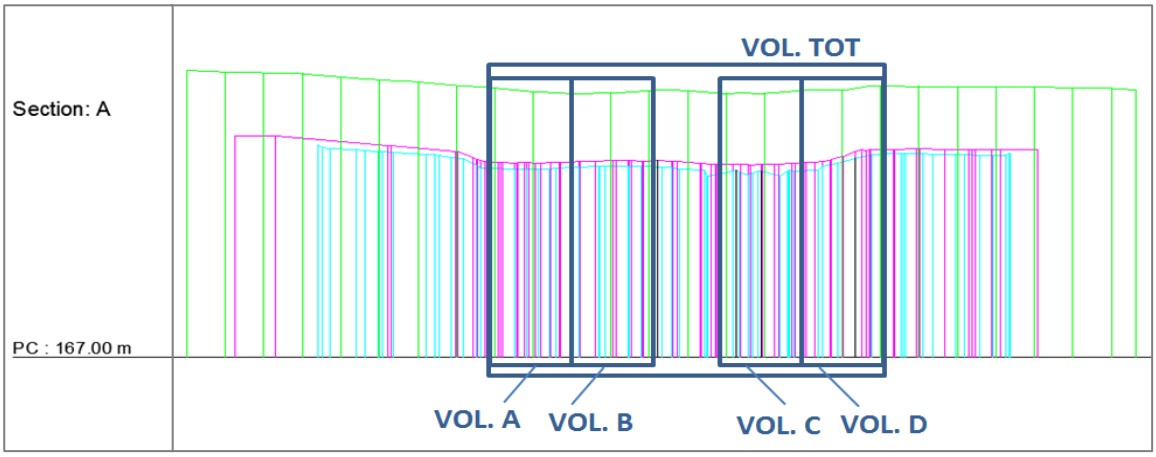

Figure 3.22 Sections of volumes studied.

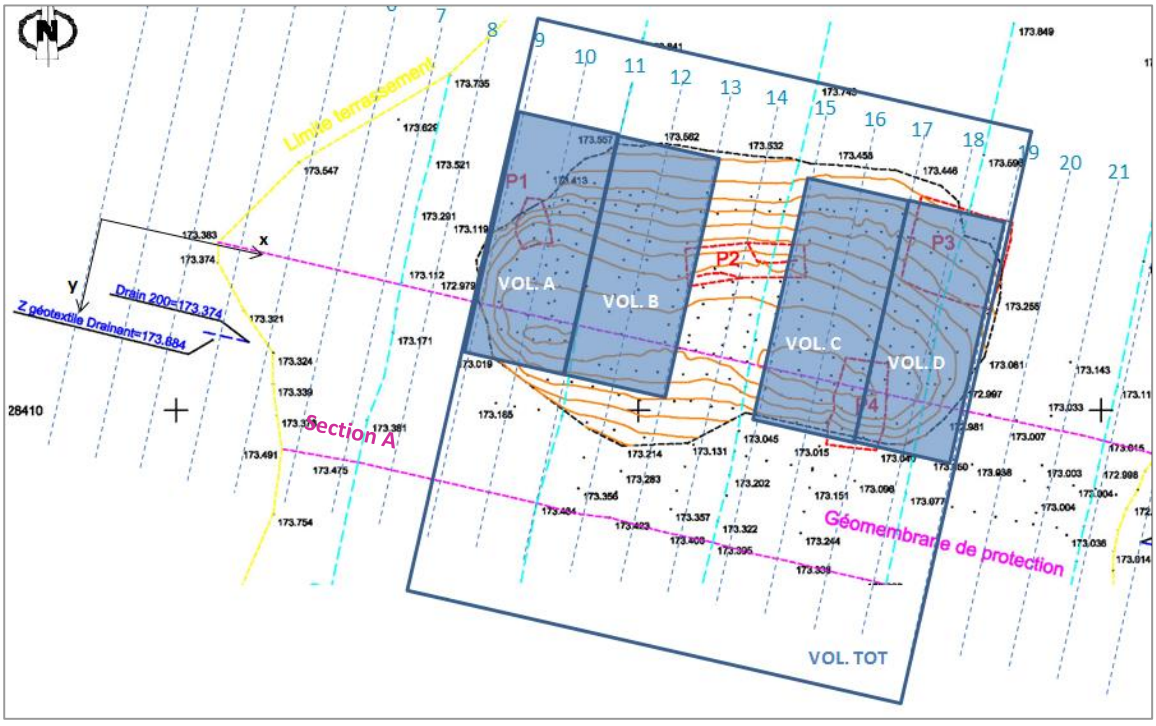

Figure 3.143 Plans of the volumes studied.

Volume TOT (Table 3.10) shows a global increase (ΔV1= 2,1%), in V2 the increase is more remarkable (6,4%), V3 shows a sensible decrease, but as already claimed, this results could not be taken into account. In all the other parts (Table 3.11), in general the volume V1 shows an increase, more accentuated for volume A (6,0%) and less for the other (B: 3,5%; C: 3,1%; D: 3,4%). We can see an increase of volume in V2, more significant in parts A and C (resp. 10,8% and 10,9%), in comparison with B (8,0%) and D (7,6%). The values given by V3 are not taken in account because the position of the membrane is not properly defined, in consequence it gives values not close to reality. Again, the reason of the increase of volume could be that during the settlement, the soil crushes and hence it increases its specific volume.

VOLUME TOT before settlement		
V1	145,3	m^3
V2	124	m^3
V3	21,3	m^3

VOLUME TOT after settlement		
V1	148,33	m^3
V2	131,99	m^3
V3	16,34	m^3

ΔV1	2,1	%
ΔV2	6,4	%
ΔV3	-23,3	%

Table 3.30 Measures of volume of the area VOL. TOT.

VOL. A (Sec. 9-11)			**VOL. B (Sec. 11-13)**			**VOL. C (Sec. 13-17)**			**VOL. D (Sec. 17-19)**		
Before settlement			**Before settlement**			**Before settlement**			**Before settlement**		
V1	20,76	m^3	V1	20,81	m^3	V1	20,8	m^3	V1	20,77	m^3
V2	17,72	m^3	V2	17,76	m^3	V2	17,76	m^3	V2	17,73	m^3
V3	3,04	m^3	V3	3,05	m^3	V3	3,04	m^3	V3	3,04	m^3
After settlement			**After settlement**			**After settlement**			**After settlement**		
V1	22,01	m^3	V1	21,53	m^3	V1	21,44	m^3	V1	21,47	m^3
V2	19,64	m^3	V2	19,18	m^3	V2	19,7	m^3	V2	19,07	m^3
V3	2,37	m^3	V3	2,35	m^3	V3	1,74	m^3	V3	2,4	m^3
ΔV1	6,0	%	ΔV1	3,5	%	ΔV1	3,1	%	ΔV1	3,4	%
ΔV2	10,8	%	ΔV2	8,0	%	ΔV2	10,9	%	ΔV2	7,6	%
ΔV3	-22,0	%	ΔV3	-23,0	%	ΔV3	-42,8	%	ΔV3	-21,1	%

Table 3.41 Differences of volumes of particulars A, B, C and D.

With the software Surfer, the surface of the top soil and principal geomembrane have been represented, before and after the settlement (Figure 3.24). It can be clearly seen the shape and the trend of the settlement.

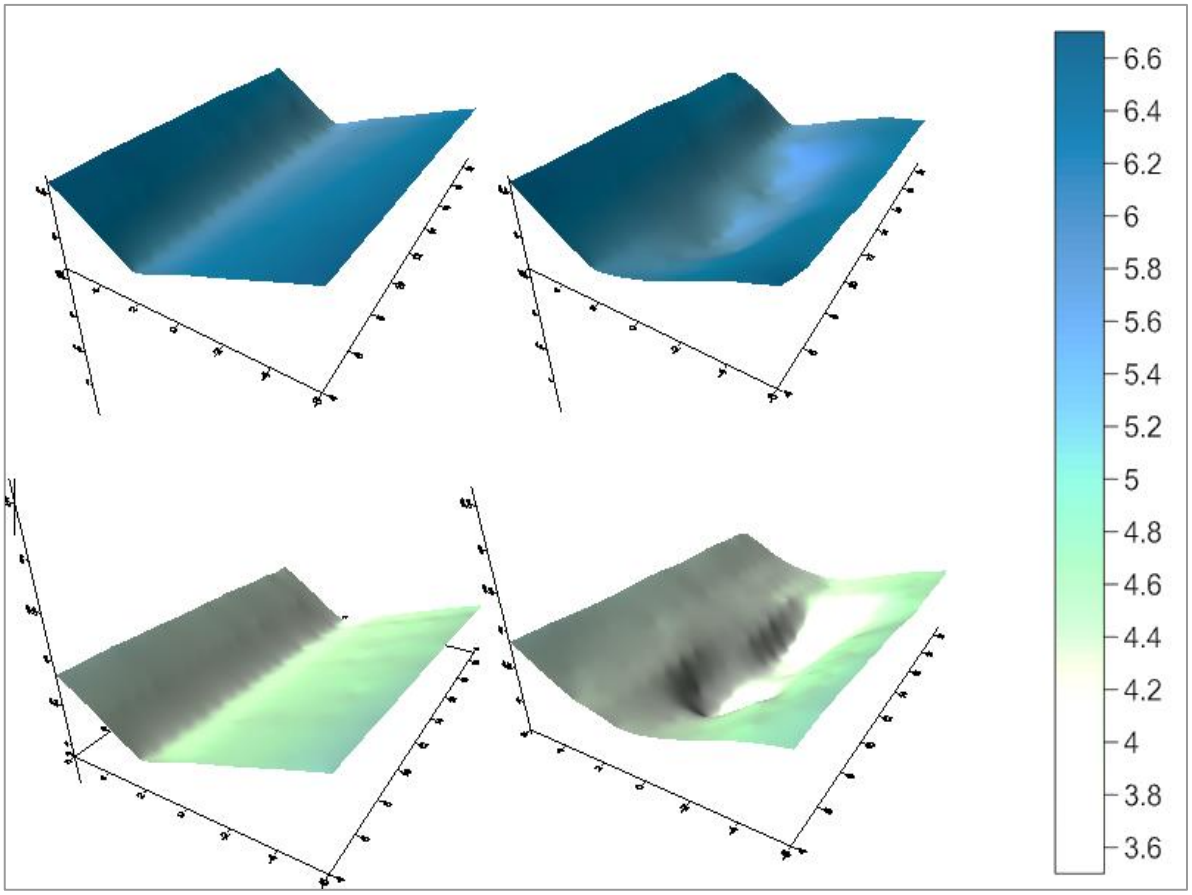

Figure 3.154 In the first row, top soil before (left) and after (right) settlements is represented; in the second row, principal geomembrane before (left) and after (right) settlements is represented. On the right, there is the scale in meter. The reference surface is placed at z=169m.

4.

Study on CSM top cover cracking potential

Geomembrane is supposed to keep its properties (waterproofness, deformability) for at least 300 years, but this is hardly achievable. The importance of sandy silt soil lies in the further role it could play: improving its characteristics could be helpful in sealing waste body, beside geomembrane. Camp (2008) led in situ and in laboratory tests to study the behaviour of a top silty soil after crushing of the waste body, focusing on the occurrence of cracks. Interesting points came out: high moister content and fiber reinforcement delay opening cracks.

Approaching our case, some samples of the first 0,30 m of sandy silt layer were studied. This choice is due to strict permission on managing soil coming from the proximity to the waste body. At first properties and mechanical characteristics were studied, after some suggestions to develop the layer are exposed.

4.1. Sandy silt layer characterization

In January 2012, 100 samples of soil (approx. 6 tons) have been collected from the site from the sixth layer (sandy-silt layer): 50 samples from the more superficial part (50-70 cm deep) of the layer, 50 samples deeper. The reason was defining one or two samples representative of the layer and studying their characteristics. On these samples some tests have been performed, in order to characterize the material, as discuss in the following lines.

Granulometry and sedimentometry

Granulometry test has the aim of determinate the relative mass distribution by different dimension of the grains; they are sieved until a dimension of 80 µm (NF P94-056), above this dimension the analysis is realised through sedimentometry (NF P94-057). These tests permit to design the granulometric curve. The percentage of fine part is the fraction with dimension < 80 µm; the fraction ≤ 2 µm identifies clay, silt grain dimension is between 2 µm and 20 µm and fine sand between 20 µm and 200 µm.

The resulting granulometric curves of the soil are reported in Figure 4.2. As it can be noticed, soil taken from the site can be divided into three different groups, according with their granulometry. These three groups correspond to three different part of the landfill (Figure 4.1).

Part 1 (P1), placed in the northern part, corresponding to blue curves in Figure 4.2, is quite similar to part 2 (P2), placed in the middle, corresponding to the green curves. The average lines have the same shape and are quite similar. The red curves that represent part 3 (P3), placed in the southern part of the landfill, show a sensible difference, compared with the other two.

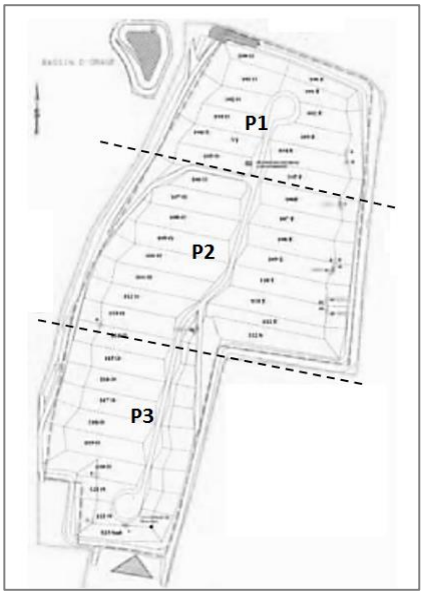

Figure 4. 1 Landfill site (Andra, 2011).

Besides, the results of sedimentometric test (Figure 4.3 and Table 4.1) confirm the results of granulometry: P1 and P2 are comparable, instead P3 results to have less content of fine part.

	P1	**P2**	**P3**
% passing at 80 µm	41,67	36,66	18,39
% passing at 20 mm	90,90	85,66	80,19

Table 4. 1 Results of sedimentometry for the three parts.

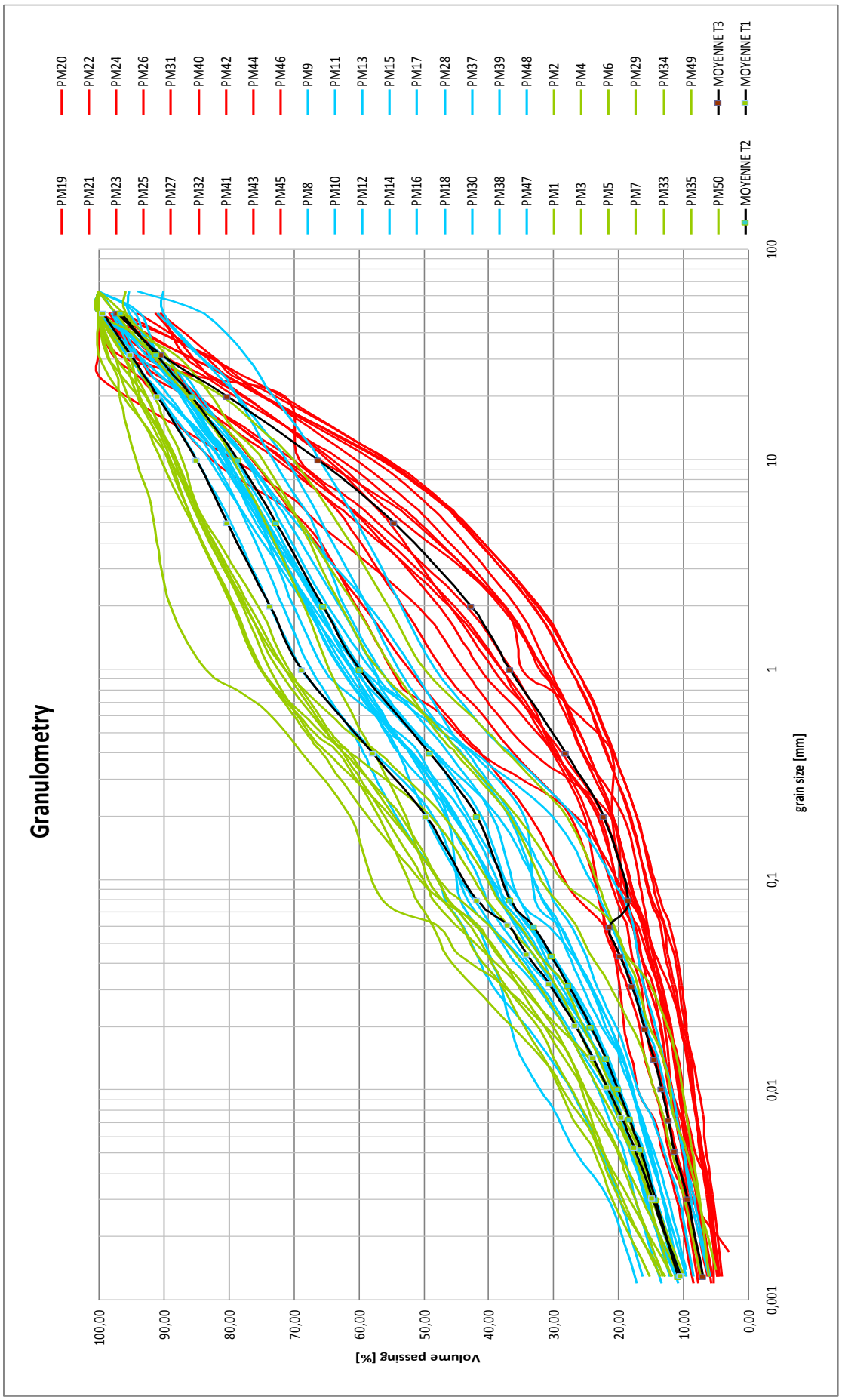

Figure 4. 2 Granulometry of the sandy silt layer.

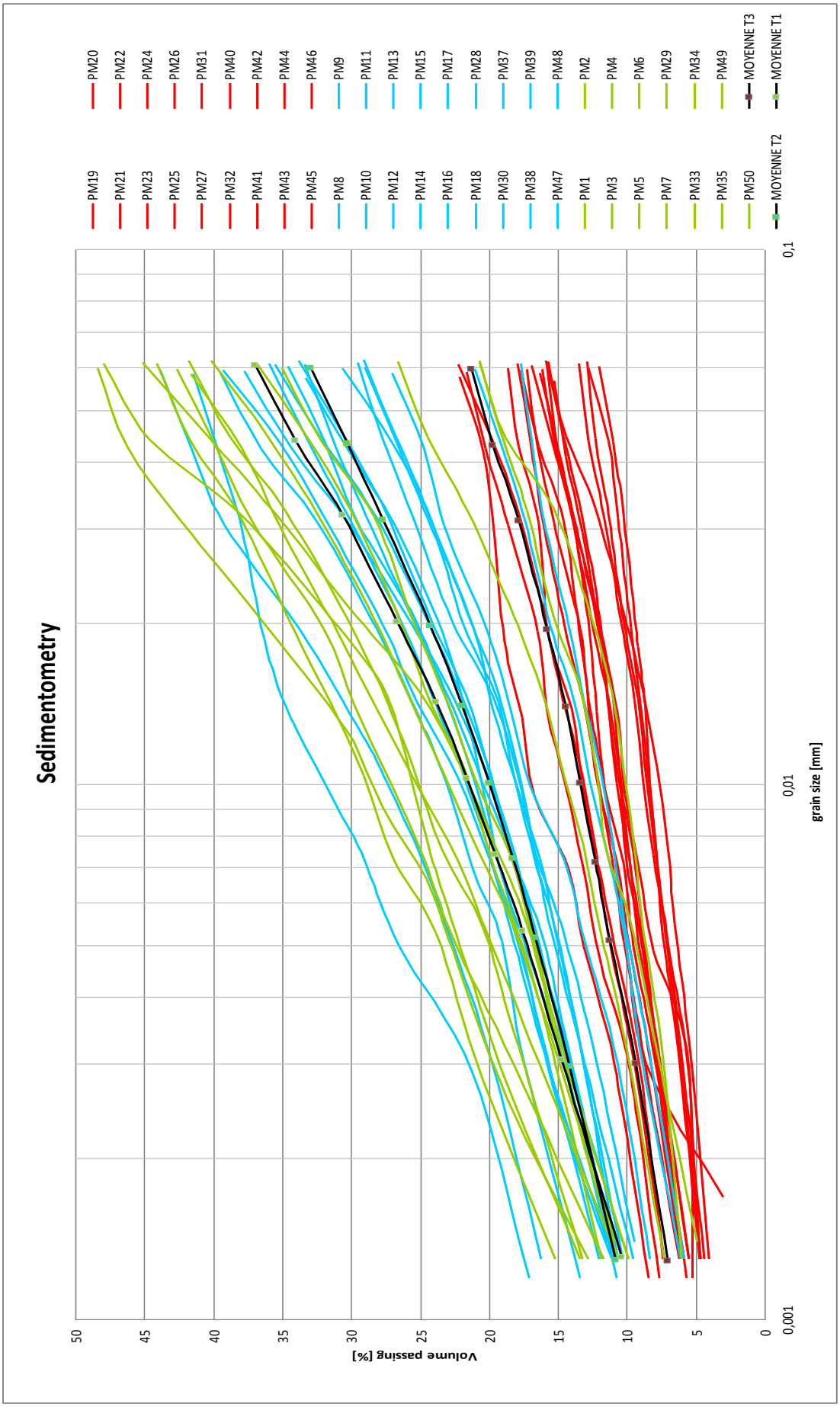

Figure 4. 3 Sedimentometry of the sandy silt layer.

Moisture content and methylene blue value

Moisture content is a fundamental parameter that influences the behaviour of a soil. It is a rapport between the mass of water of a sample and the dry mass of the same sample; it is express in percentage (NF P94-050). The values of P1 and P2 are similar (respectively 14,48% and 14,00%) whereas the P3 has a lower average value of 11,93%.

The methylene blue value VBS is a parameter that permit to define the content of clay part in soil. Infect, clay absorb a quantity of methylene blue proportional to its specific surface. Soil could shows different values (NF P 94-068) :

- 0,1 : limit under which the soil could be considered water insensible. Beside, passing at 80µm have to be ≤ 12 % (not clayey soil).
- 0,2 : limit under which the soil start to be considered water insensible.
- 1,5 : limit between silty sand soil and clayey sand soil.
- 2,5 : limit between silty soil with low plasticity and with average plasticity.
- 6 : limit between silty soil and clayey soil.
- 8 : limit between clayey soil and highly clayey soil.

The methylene blue values confirm what it has been seen with the granulometry. The VBS of P1 shows higher volume of fine part (VBS=1,11), P2 has a similar value (0,9), P3 on the contrary has a lower value (0,62). Therefore it is observed that the fine part content is higher in the two first parts.

Plastic index

Plastic index, derived from Atterberg limits, characterizes the clay content of a soil, infect it is directly dependent to clay fraction present in a soil. Liquid limit w_L represents the moisture content between an liquid and plastic behaviour; plastic limit w_P identifies the limit between plastic and solid conditions. Plastic Index is calculated as the difference between plastic limit and liquid limit of a soil, in other words, it is the range between a moister content that makes soil deformable and a moister

content that makes it more resistant. Soil could shows different values (NF P 11-300) :

- 12 : upper limit of a lightly clayey soil,
- 25 : upper limit of a average clayey soil,
- 40 : limit between clayey soil and very clayey soil.

From our tests we found out that all our soil is lightly clayey (Table 4.2).

P 1		P 2		P 3	
W_L	29,61	W_L	32,03	W_L	31,24
W_P	21,80	W_P	22,76	W_P	22,43
IP	7,83	IP	9,29	IP	8,79

Table 4. 2 Atterberg limits and plastic index of the three part.

GTR

The French norma divide the soil into six categories, in relation to nature, components and mechanical properties (NF P 11-300):

- A : fine soil,
- B : sandy and coarse soil with fine part,
- C : soil with fine and coarse elements,
- D : water insensible soil.
- R : rocks,
- F : organic soils.

Moreover, there are sub categories in which the soil is classified according to his nature, condition and behavior (granulometry, VBS value and plastic index, moisture content, Los Angeles and Micro-Deval index).

P1 and P2 have been classified as C1A1, instead P3 is composed of soil C1B5. The following pictures (Figure 4.4) show the difference between the materials of P1, P2 and P3 respectively.

Figure 4. 4 Example of soils respectively from part 1 (P102), part 2 (P110) and part 3 (P116).

Proctor test

The similarity of the results of tests for P1 and P2, suggests to mix samples from the two parts. Proctor test was carried out on the mixture.

Different tests were carried out for different moisture content, in order to design the compaction curve. The value of optimum moisture content results 11,4%, with a dry density of 19,2 kN/m^3, as shown in Figure 4.5.

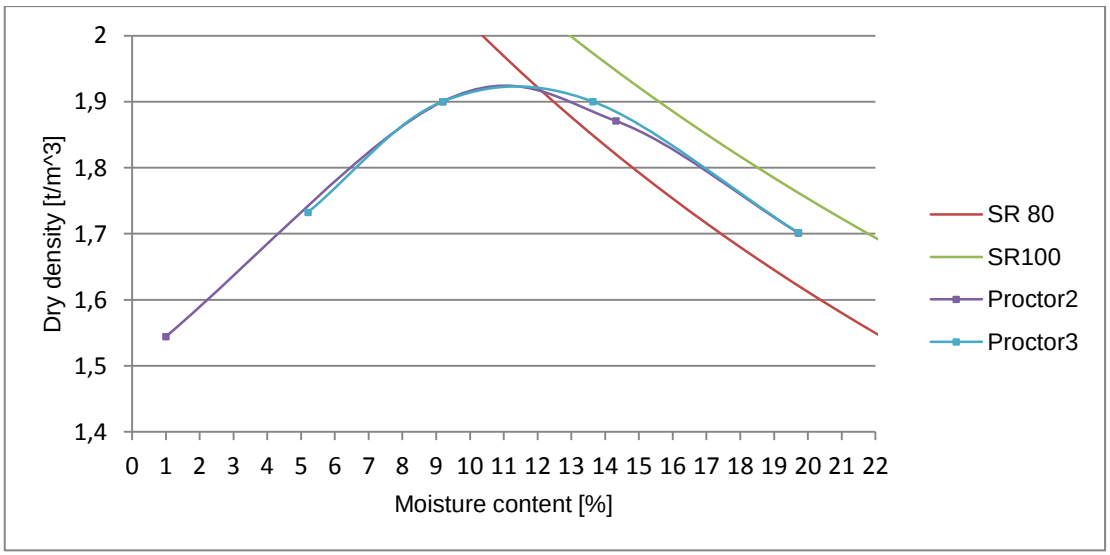

Figure 4. 5 Compaction curves, saturation curves for S=80% (red line) and saturation curve for S=100%.

4.2. Study on permeability

Permeability is highly important: hardly determinable with certainty, it is fundamental in the field of impermeable natural barrier.

At first, an oedometer was set. Two samples were taken from the mixture of soil coming from Part 1 and Part 2. The samples were compacted with the Standard Proctor procedure, with a moisture content of w_{opt}+3% (Sample 1) and w_{opt}+4% (Sample 2); their dimensions were 2,5cm of thickness and 7cm of diameter (Figure 4.6).

Figure 4. 6 Sample 1 after testing.

Loading and unloading cycles were applied, and displacements at different loads were registered. The void ratio has been evaluated in function of the different loading charge, giving the output represented in Figure 4.7. Results are not very representative, in fact pre-consolidation curve and consolidation point are not identifiable. This is quite unusual, even more thinking at the compacting phase operated when the soil has been set up. Pre-consolidation and consolidation coefficients, C_c and $C_{r,}$ were calculated, resulting respectively 0,014 and 0,002 for

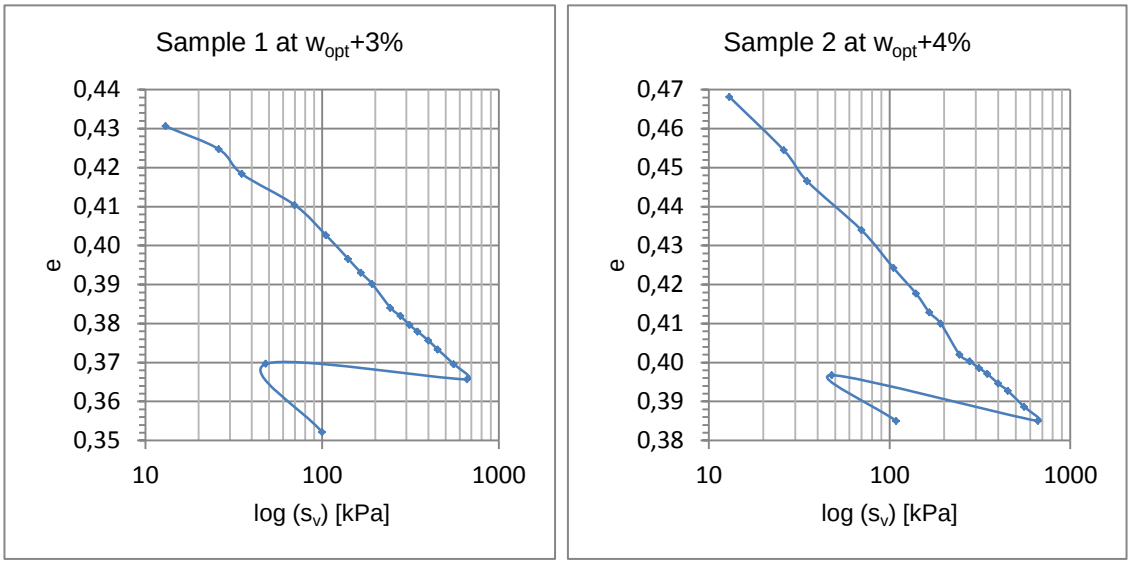

Figure 4. 7 Oedometer test results for sample 1 and sample 2.

sample 1, and 0,028 and 0,0019 for sample 2.

Both the samples do not show a great tendency to deform, as it can be seen in Figure 4.8 and Figure 4.9.

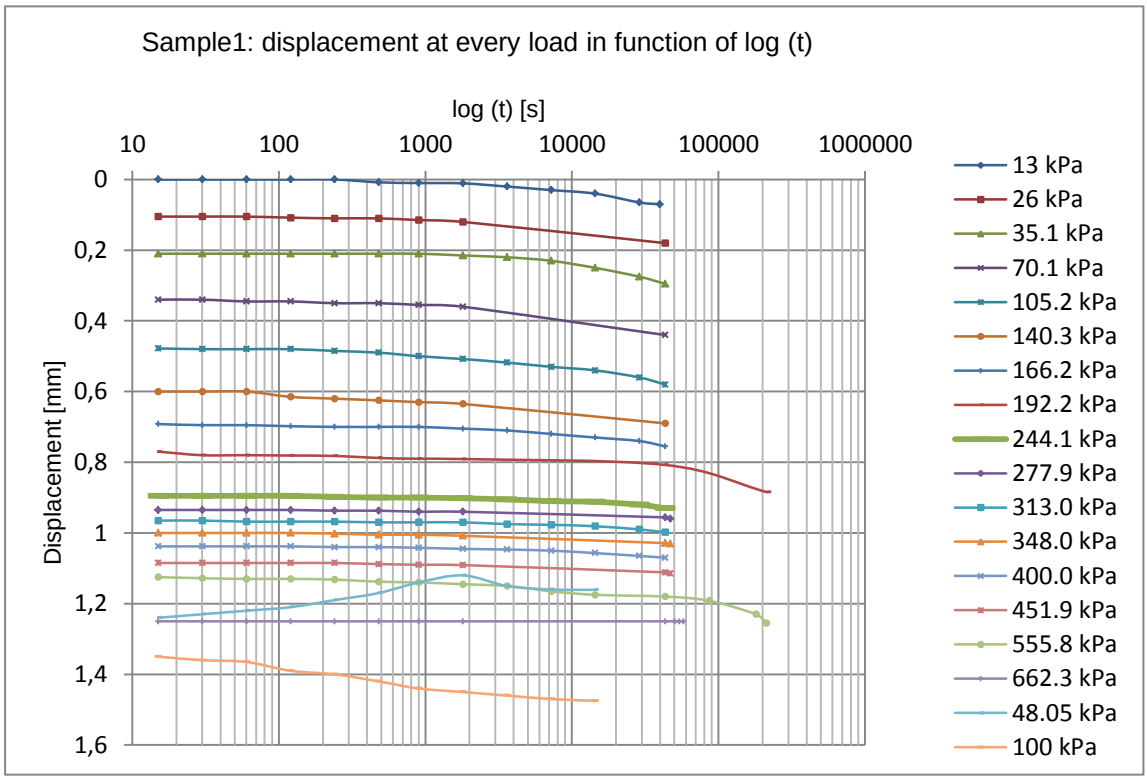

Figure 4. 8 Displacement trend in function of time for every load step for sample 1.

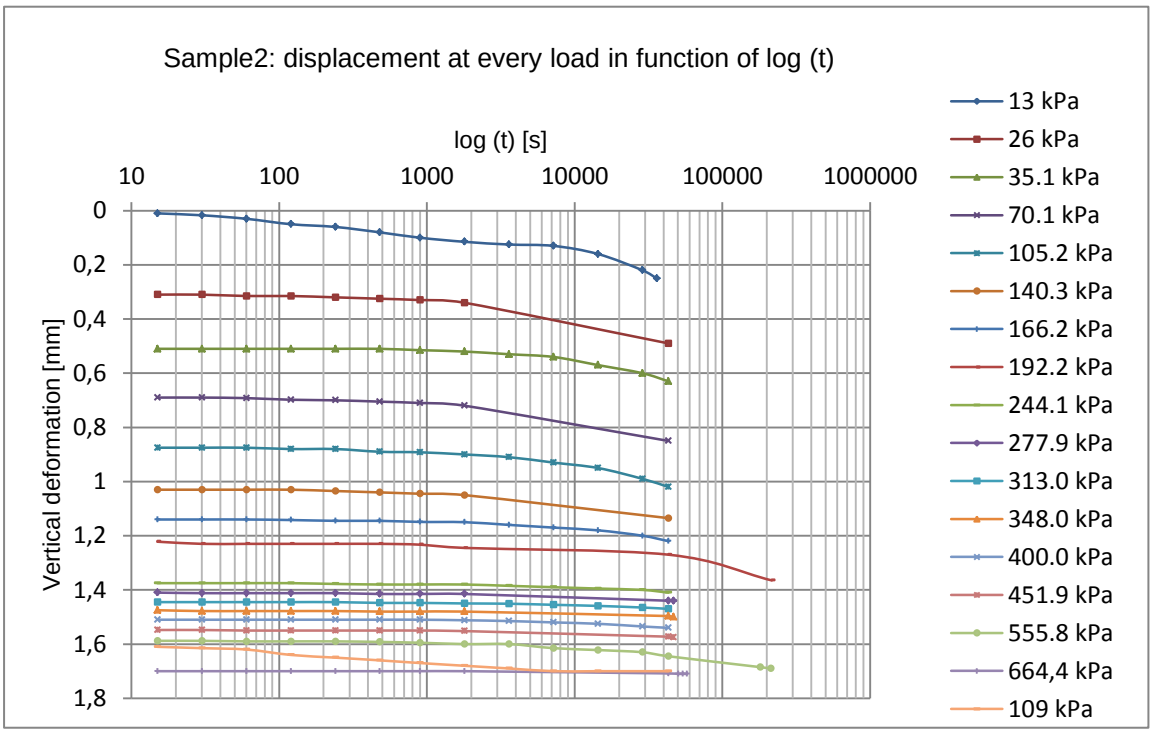

Figure 4. 9 Displacement trend in function of time for every load step for sample 2.

Permeability was then evaluated. The molds hosting the samples subjected to a load of 20kPa were linked to a tube in order to apply an hydraulic charge. It was registered the variation in time of the hydraulic charge (height of water column) applied at the samples (Figure 4.10). After a period for saturation of the sample, the time to dissipate an hydraulic charge of 50cm was registered. It takes 5 hours for sample 2, whereas it takes 2,5 hours for sample 1. Sample 1, characterized by a lower moisture content, shows higher permeability.

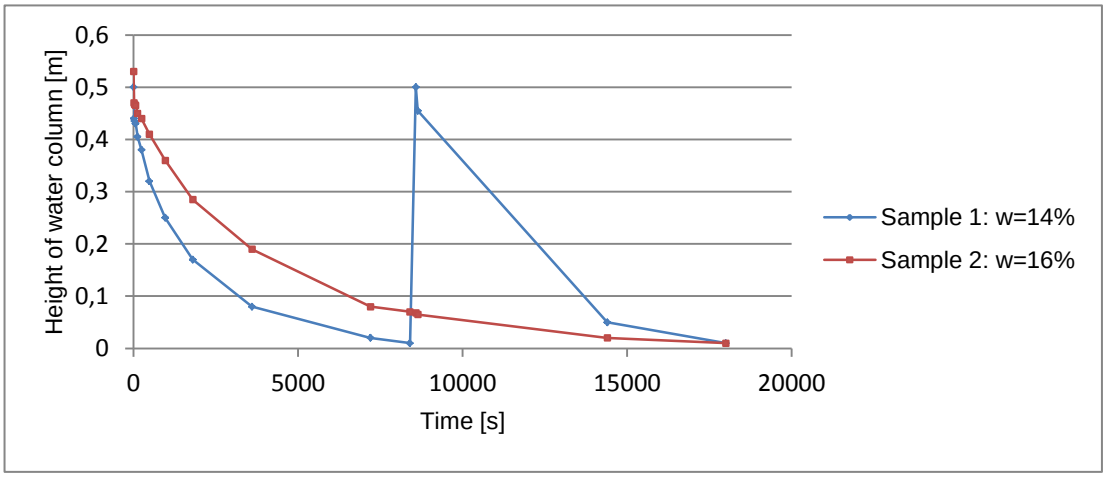

Figure 4. 10 Hydraulic charge in time.

Permeability is than calculated as following. Schematically representing our system as shown in Figure 4.11, a balance could be evaluated between the incoming and outgoing volumetric flow rate (Equation 4.1).

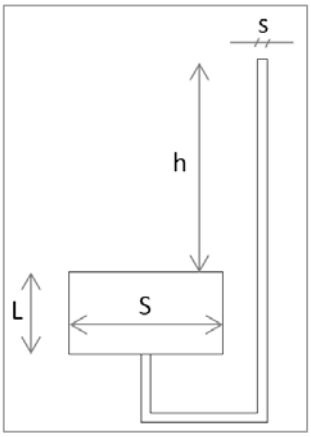

Figure 4. 11 Scheme of a oedopermeameter.

$$Q_{in} = Q_{out} \tag{4.1}$$

With two different definition of incoming and outgoing flow rate, they are treated differently: the first one linked to the considered volume of fluid in time, the second one linked to cross-sectional surface and velocity of the fluid (Equations 4.2a and 4.2b). Afterwards Equations are linked to Darcy law (Equation 4.3).

$$Q_{in} = \frac{dV}{dt} \quad Q_{out} = v \cdot S \tag{4.2a; 4.2b}$$

$$Darcy \rightarrow v = k \cdot i = k \cdot \frac{h}{L} \tag{4.3}$$

Integrating in time, it results Equation 4.4:

$$k = \left(\frac{1}{t_2 - t_1}\right) \cdot \frac{s \cdot L}{S} \cdot \ln\left(\frac{h_1}{h_2}\right) \quad (4.4)$$

Where:

- s is the section of the tube [m^2]
- L is the height of the sample [m]
- S is the section of the sample [m^2]
- t_1 and t_2 [s] initial and final instant, corresponding to initial and final height of water in the tube, respectively h_1 and h_2 [m]

Permeability for sample 1 results to be *3,80 x 10^{-8}* m/s, whereas permeability for sample 2 results to be *1,80 x 10^{-8}* m/s. These values do not confirm the permeability required for a top cover barrier. The permeability was after evaluated every time-step, results agree with previous calculations (Figure 4.12).

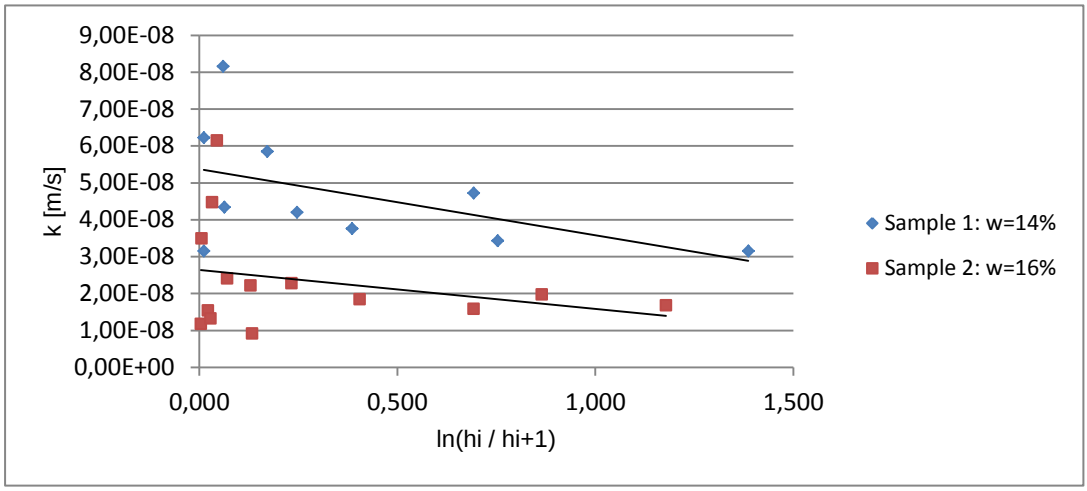

Figure 4. 12 Permeability represented every time step registered, from the maximum height of the water in the tube, until its emptying.

.

After that other two oedopermeability tests were carried out. Sample 3 was set with a moisture content of 14% and sample 4 with 12%. Unfortunately, sample 3 did not give reliable results due to air infiltrations in the system.

Results of oedometer test were comparable. Permeability was then evaluated on sample 4. In Figure 4.13, the curves represent the emptying of the tube from water, at subsequent cycles of hydraulic charge. The necessary time to void the tube decreased, varying in a range from 3,33 hours to 2,08 hours, anyway it follows the same trend: initial steep fall, followed by a trend more feeble.

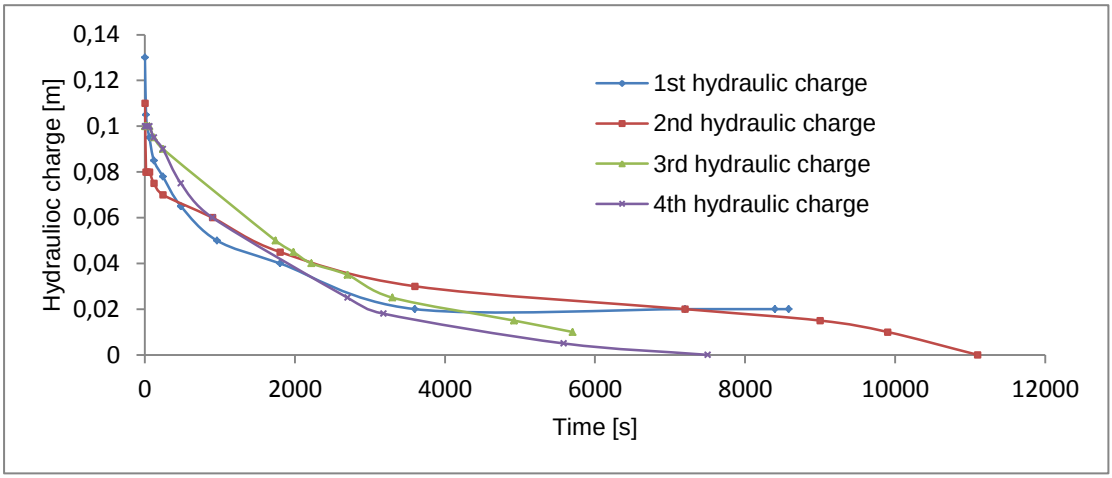

Figure 4. 13 Hydraulic charge in time at different charge cycles.

Through Equation 4.4, permeability of sample 4 results to be 3,30 x 10^{-8} m/s. This value does not confirm another time the permeability required for a top cover barrier. The permeability was after evaluated every time-step, resulting graph in Figure 4.14, that confirms previous calculations.

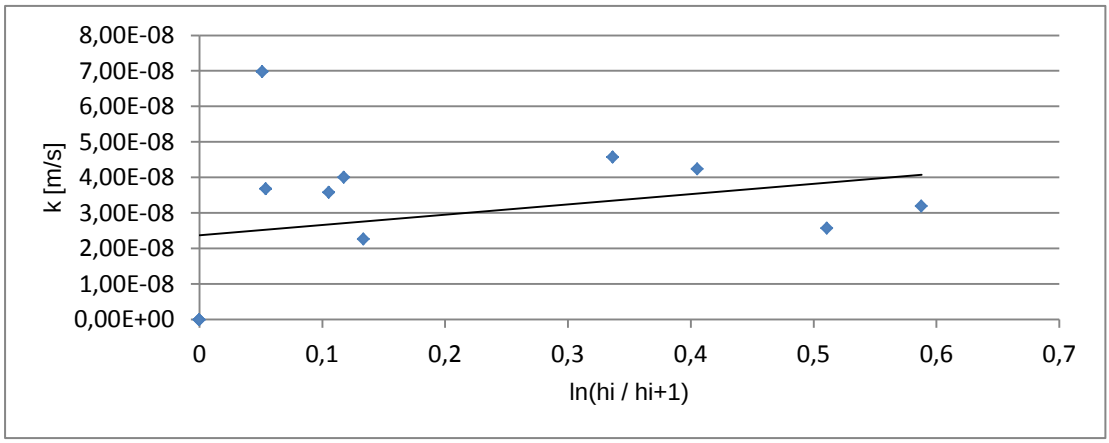

Figure 4. 14 Permeability represented every time step registered, from the maximum height of the water in the tube, until its emptying.

In this study, sandy silt layer of CSM disposal facility, has not the issue of impermeable barrier, which is accomplished by bituminous geomembrane. In the perspective that the differential settlements damaged geomembrane, as claimed,

compromising its sealing power, sandy silt layer could help geomembrane role. Thanks to the values of permeability obtained, it can be claimed that sandy-silt layer does not contribute in sealing issues, infect generally accepted minimum permeability coefficient is $k=10^{-9}$m/s (Heerten and Koerner, 2008).

4.3. Unconfined compression test

Compression tests on samples were carried out (Figure 4.15). Samples came from the site, precisely from the mixature of P1 and P2. They were compacted with Standard Proctor procedure, characterized by two different moisture content: $w=w_{opt}+3\%=14\%$ (test 1) and $w=w_{opt}+1\%=12\%$ (test 2); the samples showed the following dimensions: height of 7,2cm and diameter of 2cm. The test has been carried with constant monitored displacement of 0,6mm/min; the force applied was

Figure 4. 15 Sample during (left) and after (right) the unconfined compression test.

registered in time.

Outputs of test at two different moisture content are reported in Figure 4.11. The sample with lower moisture content shows higher resistance but less capability to deform; on the contrary, the sample with higher moisture content shows higher deformation but less resistance. Test 1, characterized with high moisture content (w=14%), reaches deformation of approx. 9,8% before resistance fall, whereas Test 2, with moisture content value of 12%, collapses at a deformation of 6%. Moreover, sample of Test 1 is characterized by a stress resistance of 56,8kPa, besides, sample of Test 2 of 47,9kPa. This is a proof of the high influence of water content: a

variation of 2% in moisture content implies a variance of 38,8% in vertical deformation and a variance of 15,7% in stress resistance.

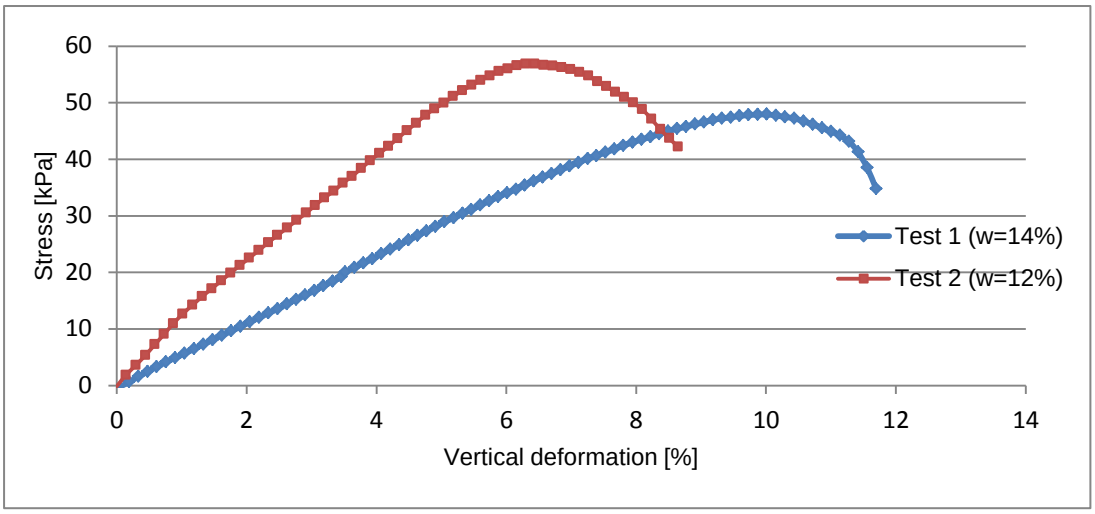

Figure 4. 16 Comparison of two unconfined compression tests.

Influence of moisture content is highlighted in the previous lines in relations to stress resistance and deformation; anyway, its influence has to be considered from different points of view, facing also with permeability. Many studies (Plé et al., 2011; Rajesh et al., 2011; Barral, 2008; Camp, 2010; Cuevas et al, 2009; Moon et al., 2007) relate moisture content with crack occurrence: the more deformable is a soil (that means, the higher moisture content is), the more cracks formation is delayed. In this perspective water content positively affects permeability. However, on the contrary, a too high moisture content implies high permeability, which is obviously a negative aspect in the outlook of soil barriers (Rajesh et al., 2011; Moon et al., 2007; Wickramarachchi et al., 2011). For these reasons water content has to be carefully taken in account in designing a soil barrier.

4.4. Bending test and Particle Image Velocimetry method

A study with PIV method of the flexural behaviour of a soil beam in a bending test (described in Section 2.2) has been carried out. During the experience, a PENTAX

(OPTIO WG-1) digital camera takes pictures every 10 seconds, in order to study with the digital images the deformation through PIV method.

A Matlab program developed by H. Pinard (2012) at first (1) changes the images format from .png to .jpg for its better manipulation, then (2) the images were treated to improve the readability, brightening up the image but not the beam. After, (3) the software Openpiv, open source Matlab software for PIV analysis, is used to evaluate the length of the lower fiber of the beam, assessing its deformability. Besides, Openpiv was used to identify occurrence of cracks on the beam, comparing an image without displacement (the first one, usually) and each of the following image, characterized by an increasing displacement. In the end, the deformation is evaluated by the open-source software Openpiv. The setting of part (2) of the Matlab experience requires a precise disposition of white supports in order to make as uniform as possible the image, without shadows, and also a precise disposition of halogen lamps (Figure 4.17).

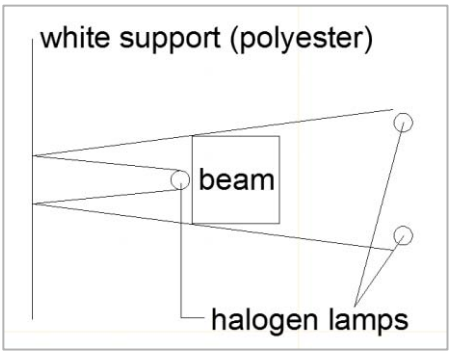

Figure 4. 17 Lightening disposition

As already pointed out, the precise occurrence of the first crack is evaluated with image analysis of Openpiv. The software Openpiv compare every image with the first one and it gives a file .txt as output. It consists in a series of data organized in four columns, the first two columns identify the pixel coordinate (x; y) of every pixels that form the beam, the third and fourth columns represent the displacement in direction x and direction y of every pixel. After loading this data-set in Openpiv, it could calculate the deformation of the beam. More options are available, deformation in x or y direction could be study separately, or together. The latter seems to be the more representative.

The soil in exam, sieved at 5mm, has been mixed with water to reach the moisture content of 14% ($w_{optimum\ proctor}$ +3%, in situ original moisture content). It was kept stored in hermetic bags at constant temperature for 48h in order to make hydration

uniform. After, 8,78kg of soil were compacted on both sides, with constant velocity rate of 0,99mm/min, obtaining a beam with dimensions of 0,40m x 0,10m x 0,10m. The surface texture of the beam does not give good results in the PIV analysis, for this reason the surface was spread of painted sand: sand with diameter between 8mm and 7mm was coloured in black with paint, and after it was applied to the beam surface. The freshness of the paint was enough to paste the sand on the soil, with the aid of a little pressure. The beam was placed on the bending test apparatus. It has two pairs of rollers: the lower one (movable) is spaced 300mm joined to the lower part of the device, whereas the upper pair (fixed) is spaced 100mm and it is joined with the upper part of the apparatus. The beam is placed on the lower rollers, with the sand surface facing the operator (Figure 4.18). The lower part was risen with constant velocity rate imposed by the operator (in this case 0,12mm/min), in this way the beam is put in contact with the upper roller and a flexural stress is applied to the beam itself. Finally, the deformation brings the sample to rupture.

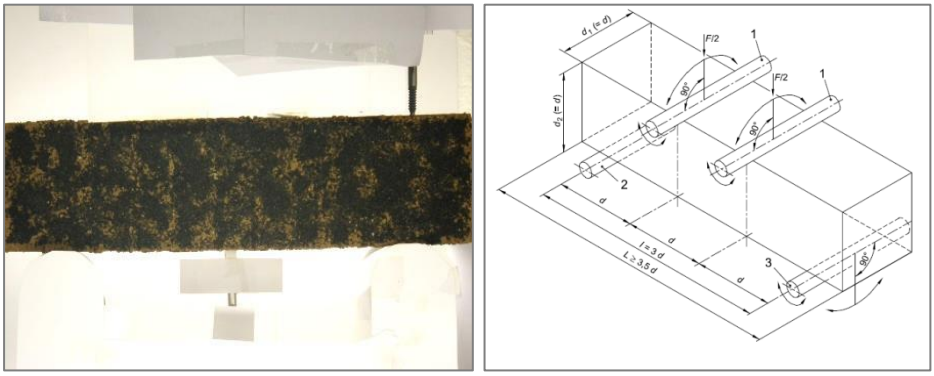

Figure 4. 18 Soil beam disposed in the bending test apparatus (left) and scheme of a bending test apparatus proportions.

The great importance of this test lays in different aspects. At first, it well represents the situation occurred in the CSM top cover: bending test simulates the stress condition induced by differential settlements occurred in the landfill site; in addition, the utilisation of the soil coming from the site, give more detailed information, precisely on CSM top barrier. Moreover, crack appearance is an important parameter related to permeability, which plays a key role in cap barriers in helping geomembrane sealing capacity.

The occurrence of the first crack could be seen in Figure 4.19, pointed by the arrow. Openpiv was used to identify crack formation between all images. The output pointed out crack formation at image 182. In red colour the higher deformations. A

clarification has to be made: due to program settings, the image in Figure 4.19 reports the beam overturned.

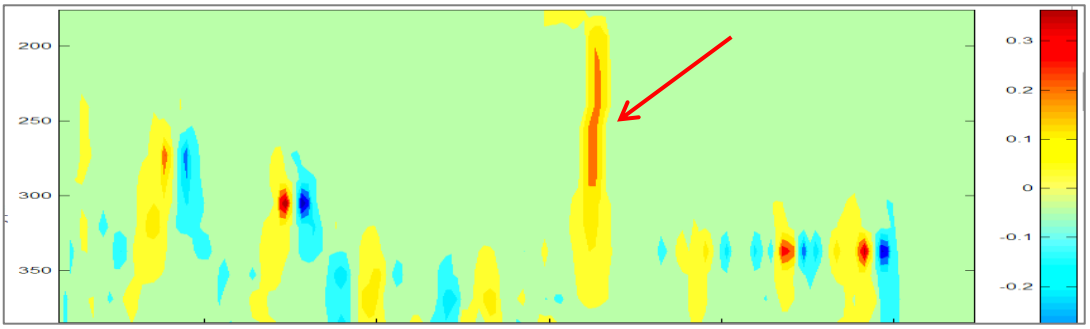

Figure 4. 19 OpenPiv output, occurrence of the first crack.

As it is shown in Figure 4.19, the first crack appeared in a central position. This is an important result because it confirms that the experience was well-set: the beam has been placed in the right position relatively to the supports, the supports themselves were placed correctly, the soil was homogenously hydrated and compacted.

The output represented in Figure 4.20 shows that a deformation of 1,13% brings to crack appearance. Locally, in CSM site, as described in Section 3.2, deformation of the lower fibre of the sandy silt layer reaches the values of 2,32%. It is reasonable to claim that cracks could have been occurred in the sandy silt layer. This could be a problem in the long timescale: geomembrane deterioration could bring to loss of sealing capacity and in this perspective an opportune soil layer could help geomembrane in keeping low permeability.

However, the outputs of this test affirm that the present soil could not solve this assignment, because of its modest deformability.

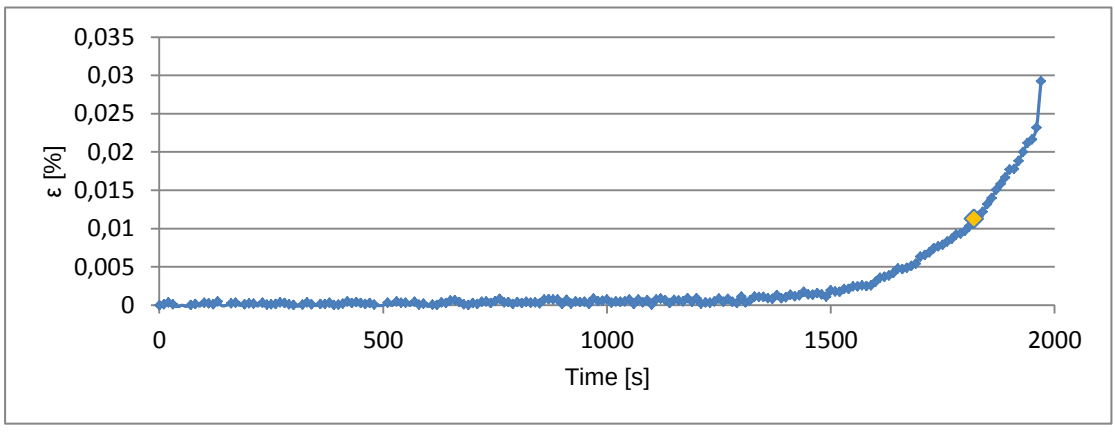

Figure 4. 20 Deformation of the lower fiber, in time.

It is worthy to note that some prescriptions could be taken into account to decrease deformation potential and consequently increase permeability:

- Augmentation of the thickness of the sandy silt layer from 1m up to 1,5m. According to centrifuge laboratory tests conducted by Gourc et al (2010) and Vishwanadham et al (2011) on a clay layer, an increase of thickness from 0,6m up to 1,2m could lead to an increase of 25-30% of maximum outer fiber strain.
- Augmentation of compaction energy: augmentation of 30% of the compaction energy decrease from 0,20% to 0,04% the strain necessary for the first crack formation (Camp, 2008);
- Overburden of 25kN/m^2 delays opening cracks on a clay barrier in laboratory test (Viswanadham and Rajesh, 2008). Placing an additional layer as overburden could be taken in account;
- Moisture content of the sandy silt layer up to w_{opt}+5% could improve deformability. According to the Bureau de Recherches Géologiques et Minières, a moisture content value included between w_{opt}+2% and w_{opt}+6% could positively improves deformability without compromising mechanical stiffness (Camp, 2008);
- Setting up of a geogrid layer in the tension zone (Viswanadham and Rajesh, 2008) for further settlements;
- Adjusting original soil adding a clay portion, paying attention because of the high sensibility of clay to dehydration and swelling capacity;
- Fiber reinforcement in soil layer. Many studies (Gourc et al., 2010; Rajesh et al., 2011; Viswanadham et al., 2011) affirm that mixing soil layer with fiber reinforcement sensibly delays opening cracks. 90-mm-fiber content of 0,5% of dry weight of the soil allows higher deformations: limiting distortion varies from 1,01% for unreinforced soil to 1,31% for reinforced soil. Moreover, delaying occurrence of cracks, postpones loss of sealing efficiency. Despite the fact that a fiber in the soil body could be a preferential path for fluids, permeability is not influenced. In addition, several studies affirm that fiber reinforced soil behaviour is not sensibly influenced by layer thickness (Viswanadham et al., 2011);
- Substitution of the entire layer with a sand-bentonite-polymers layer. Its characteristics seems to accomplish all the problems with high deformation

and low permeability. It is a new feature used in northern Europe, expecially in the Netherlands. It seems to give good results.

According to the writer, fiber reinforcement seems the best solution: it improves deformability of the soil layer, facing the problem of differential settlements, without damaging the sealing efficiency. Anyway, a study on mixing a clay fraction with the sandy-silt layer could give good results.

Conclusions

The opportunity of carrying out a great quantity of observations on the behaviour of a top cover of a disposal facility for low and intermediate short life radioactive wastes plays an important role both in an universal perspective and specifically in the case in exam. The unexpected occurrence of differential settlements entails a loss of integrity of the barrier, causing damage to sealing property and mechanical resistance. Hence, the issue of this study focusses on the response of the main means composing the top cover in the area subjected to settlements: bituminous geomembrane and mineral (sandy-silt) barrier.

At first, considering percentage elongation of the surface and percentage elongation of the bituminous geomembrane, it came out that the membrane show a sensibly higher deformation than the surface (2,32% vs 0,5%). This fact was strengthened by a study on the volumes involved in the area before and after settlement: a volume increase was registered (approx. 6,4% on the entire settled area). These observations led to justify the occurred settlements with a crushing of the waste body, due to a rearrangement of the backfill. A specific research on geomembrane samples taken from the area in exam pointed out a loss in resistance, in spite visible damage were not remarked.

All the results that came out involved a possible damage to the sealing power of the bituminous geomembrane. In this perspective a geotechnical research on the mineral barrier was carried out, in order to understand if it could cooperate in terms of resistance to deformability and waterproofness with the membrane, facing with eventual further differential settlements. Permeability of the sandy-silt layer was evaluated; its value ($1,8 \div 3,8 \times 10^{-8}$ m/s) resulted to be too high (min. 10^{-9} m/s) to cope with a loss on sealing power of the geomembrane. Flexural resistance and maximum deformation before cracking were assessed with bending test, coupled with Particle Image Velocimetry method analysis, on a soil beam. Cracking potential infect affects both mechanical resistance and permeability. The maximal possible deformation of the outer fiber of the beam, indentified with the occurrence of the first crack, was estimated as 1,13%. The comparison of this value with the maximal deformation registered in situ (2,32%) led to state that crack formation occurred in the settled area. In particular, it can be claimed that measures should be taken into

account to deal with problem of gas emission and water infiltration specifically for the landfill under study.

It is worthy to note that managing radioactive waste is an issue of increasing importance world-wide. Different alternatives could be considered i.e. augmentation of the sandy-silt layer thickness, setting up an overburden, adding clay portion to the mineral layer, increase of moisture content of the sandy-silt layer. In the perspective of this rapport the more attractive reinforcement seems to be the addition of polymer fibers in the mineral layer. In fact it coupled different features as high mechanical resistance, delay in opening cracks, and non-influence on sealing efficiency. Many other means are still under study and finding the best solution could be a future aim.

Acknowledgments

Un primo doveroso ringraziamento è indirizzato al Prof. Carrubba, senza il quale non avrei potuto vivere l'esperienza di studiare all'estero, imparare una nuova lingua e confrontarmi con una realtà differente dalla nostra contando sulle mie forze. A Prof. Gourc per il suo sostegno, la sua disponibilità e il suo modo di fare così familiare. A Matthieu Verstaevel, mio tutor, per tutto ciò che si impara confrontandosi con una persona diversa da se stessi.

Un immancanbile e interminabile grazie alla mia famiglia: a mamma, papà e Vale, senza senza i cui insegnamenti, sostegni, consigli, scontri e confronti non sarei arrivata dove sono e soprattutto come sono; alle zie e a Pino per il loro affetto (che più di loro non mi vizia nessuno) e il loro considerarmi a volte ancora la loro piccolina; a tutte quelle persone che sono famiglia più lontana o acquisita per la loro allegria e differenti punti di vista. Grazie.

Un grazie alla mia 'famiglia padovana' per tutte le avventure passate insieme, per i momenti condivisi, per le risate, per le cene, per gli interminabili aperitivi, per i concerti, per il nostro crescere assieme, un grazie a tutti quegli amici che, chi più, chi meno, chi più in passato, chi più nel presente, chi è solo passato, chi invece resta, hanno segnato il loro passaggio nella mia vita, lasciando una impronta che sommata alle altre ha portato a costruire la persona che sono. Quindi un super grazie e un abbraccio stretto (dei miei) a Albi perché mi sopporta come neanche i miei genitori riescono a fare, Arianna la mia sorella acquisita perché non esiste al di fuori di lei nessuno con cui io sia sempre così d'accordo, la mia Giuli e la sua autoironia, Andrea e gli scambi di paranoie e di risate, Paolo e la pace che infonde, il mitico Gegio e la mitica Fede per la costanza con cui la nostra amicizia va e andrà avanti, Franceschina la mia più fedele compagna di studi, Pietro e i nostri scambi culturali, Alicina e il suo entusiasmo, e poi Aurora, Mitia, DavideB, DavideDB, Alessio, Melanie, Elena, Bettina, Giulietta, Tal, Alessandro, Elisa, Ciccio, Claire (on est pas coupines pour rien), e tutti quelli che nel bene e nel male sono stati miei compagni nell'avventura della vita fino ad ora, che non ho segnato ma a cui spero si scaldi il cuore a sentirsi chiamati in causa in queste righe.

Un ciclo finisce, e con la gioia di tutto ciò che mi ha dato, ne faccio tesoro per tutti quelli che si apriranno nell'avvenire, da vivere con consapevolezza e ironia.

References

1. RJ. Adrian (1991), **Particle imaging techniques for experimental fluid mechanics**. Ann. Rev. Fluid Mech. 23, 261-304.
2. Andra (2008), **Rapport annuel 2008 du Centre de stockage de la Manche.**
3. Andra (2011), **Rapport d'information sur la sureté nucléaire et la radioprotection du Centre de stockage de la Manche.**
4. Andra (2012), **National Invenctory of Radioactive Material and Waste 2012 – The Essential**
5. Dr D.Aronsson, **Shallow land repositories for very low level waste.**
6. R.D. Baird, C.D. Pedersen, G.B. Merrell, L.S. Berta, B.S. Mason, (2007), **Barnwell Low-Level Radioactive Waste Disposal Facility; Conceptual Design for Low-Volume Operations. DRAF Report.**
7. C. Barral (2008), **PhD Thesis: Etude des transferts d'eau et de gaz dans les geomateriaux argileux utilises dans les couvertures des installations de stockage de dechets non dangereux** .
8. C. H. Benson, I. E. Kucukkirca, J. Scalia (2010), **Properties of geosynthetic exhumed from a final cover at solid waste landfill.** Geotextiles and Geomembranes 28, 536e546
9. F. Bouchelaghem, N. Jozja (2009a), **Multi-scale study of permeability evolution of a bentonite clay owing to pollutant transport. Part I: Model derivation**. Engineering Geology 108, 119–132
10. F. Bouchelaghem, N. Jozja (2009b), **Multi-scale study of permeability evolution of a bentonite clay owing to pollutant transport. Part II: Application to an MG-bentonite**. Engineering Geology 108, 286–294
11. A. Bouazza (2002), **Geosynthetic clay liners.** Geotextiles and Geomembranes 20, 3–17
12. S. Camp (2008), **PhD Thesis: Comportament sous flexion d'une argile: application a la couverture d'une Installation de Stocage de Dechets Tres Faiblement Active.**

13. S. Camp, J.P. Gourc, O. Ple (2010), **Landfill clay barrier subjected to cracking: Multi-scale analysis of bending tests**. Applied Clay Science 48, 384–392

14. J. Cuevas, S. Leguey, A. Garralon, MR. Procopio, MT. Sevilla, N. Sànchez Jimenez, RR. Aabad, A. Garrido (2009), **Behaviour of kaolinite and illite-based clay as landfill barriers**. Applied Clay Science 42, 497–509

15. J. Cuevas, A. I. Ruiz, I. S. de Soto, T. Sevilla, J. R. Procopio, P. Da Silva, J. Gismera, M. Regadío, N. S. Jiménez, M.R. Rastrero, S. Leguey (2011), **The performance of natural clay as a barrier to the diffusion of municipal solid waste landfill leachates**. Journal of Environmental Management 95, S175 e S181

16. ENRESA, (2009), **Almacén centralizado de residuos radiactivos de maja y media actividad. El Cabril.**

17. "GAO: Death of Yucca Mountain Caused by Political Manoeuvring". New York Times. May 9, 2011.

18. JP. Gourc (1982), **PhD Thesis: Quelques aspects du comportement des Geotextiles en Mécanique des Sols.**

19. JP. Gourc, S. Camp, B.V.S. Viswanadham, S. Rajesh (2010), **Deformation behaviour of clay cap barriers of hazardous waste containment system: full-scale and centrifuge test**. Geotextiles and Geomembranes 28, 281–291

20. R. Gurka, A. Liberzon, D. Hefetz, D. Rubinstein, U. Shavit (1999), **Computation of pressure distribution using PIV velocity data**, 3rd International Workshop on Particle Image Velocimetry, Santa Barbara, California.

21. G.Heerten, R.M. Koerner (2008), **Cover systems for landfills and brownfields.** Land Contamination & Reclamation, 16 (4), 343-356.

22. International Atomic Energy Agency (2005), **Radioactive Waste Menagement. Status and Trends. Issue#4.**

23. International Atomic Energy Agency (2007), **IAEA Safety Glossary: Terminology Used in Nuclear Safety and Radiation Protection**. Vienna: IAEA.

24. S. Inazumi (2003), **PhD Thesis: Waste Sludge Barrier for a Landfill Cover System.**

25. Y. Jung, P. T. Imhoff, D. Augenstein, R. Yazdani (2011), **Mitigating lethane emissions and air intrusion in heterogeneous landfills with a high permeability layer**. Waste Management 31, 1049–1058

26. J.-B. Kang, C. D. Shackelford (2011), **Consolidation enhanced membrane behaviour of a geosynthetic clay liner**. Geotextiles and Geomembranes 29, 544e556

27. G.F. Knoll (2010), **Radiation detection and measurement**, 4th ed. John Wiley and Sons Inc., Hoboken.

28. D. McNaught, A. Wilkinson (1997), **IUPAC. Compendium of Chemical Terminology**, 2nd ed. Blackwell Scientific Publications, Oxford.

29. AK. Mishra, M. Ohtsubo, L. Li, T. Hihashi (2011), **Controlling factors of the swelling of various bentonites and their correlation with the hydraulic conductivity of soil-bentonite mixtures**. Applied Clay Science 52, 78–84

30. S. Moon, K. Nam, J. Y. Kim, S. K. Hwan, M. Chung (2007), **Effectiveness of compacted soil liner as a gas barrier layer in the landfill final cover system**. Waste Management 28, 1909–1914

31. DH. Phillips, G. Sinnathamby, MI. Russel, C. Anderson, A. Paksy (2011), **Mineralogy of selected geologicaldeposit from United Kingdom and Republic of Ireland as possible capping material for a low-level radioactive waste disposal falicities.** Applied Clay Science 53, 395–401

32. H. Pinard (2012), Rapport de stage: **Mise au point d'un protocole de mesure des deformations par PIV lors d'un essai de flexion.**

33. O. Plè, JP. Gourc, P. Villard, S. Camp, and TNH. Lè. (2011), **Special Industrial Waste Repository: Experimental and Numerical Study of the Cap Cover**.

34. S. Rajesh, JP. Gourc, B.V.S. Viswanadham (2011), **Evaluation of gas permeability and mechanical beahviour of soil barriers of landfill cap cover through laboratory test**.

35. Scholey, G. K., Frost, J. D., Lo Presti, D. C. F. & Jamiolkowski, M. (1995). **Review of instrumentation for measuring small strains during triaxial testing of soil specimens.** ASTM Geotech. Test. J. 18, No. 2, 137–156.

36. CC. Smith, JC. Cripps, MJ. Wymer (1999), **Permeability of compacted colliery spoil. A parametric study.** Engineering Geology 53, 187–193.

37. CS. Tang, B. Shi, C. Liu, WB. Suo, L. Gao (2010), **Experimental characterization of shrinkage and dessication cracking in clay layer**. Applied Clay Science 52, 69–77

38. N. Touze-Foltz, C. Dunquennoi, E. Gaget (2006), **Hydraulic and mechanical behaviour of GCLs in contact with leacheate as part of a composite liner**. Geotextiles and Geomembranes 24, 188–197

39. G. Turk, J. Logar, B. Majes, (2001), **Modelling soil behaviour in uniaxial strain conditions by neural networks.** Advances in Engineering Software, 32, 805–812.

40. Vattenfall (2009), **Technical information on Ringhals.**

41. M. Verstaevel, JP. Gourc, A. Marchiol, D. Rey (2012), **The French surface disposal facilities for nuclear wastes presentation, survey and research**.

42. M. Verstaevel, JP. Gourc (2012), **Specificity of the cap cover for French landfill dedicated to nuclear wastes of low activity.**

43. JP. Vervialle (2011), **The Centre de la Manche disposal facility.** KHNP, October 25th, 2011.

44. M. V. Villar, A. Lloret. (2008), **Influence of dry density and water content on the swelling of a compacted bentonite**. Applied Clay Science 39, 38 – 49.

45. B.V.S. Viswanadham, S. Rajesh, P.V. Divya, JP, Gourc (2011), **Influence of randomly distribuited geofibers on the integrity of clay-based landfill cover: a centrifuge study**.

46. B.V.S. Viswanadham, S. Rajesh (2008), **Centrifuge model tests on clay based engineered barriers subjected to differential settlements**. Applied Clay Science 42, 460–472.

47. DJ. White, WA. Take, MD. Bolton, SE. Munachen, (2001a), **Measuring soil deformation in geotechnical models using digital images and PIV**

analysis. Proocedings of the 10th international conference on computer methods and advanced geomechanics. Tucson, Arizona.

48. DJ. White, WA. Take, MD. Bolton, SE. Munachen, (2001b), **A deformation measurement system for geotechnical testing based on digital imaging, close-range photogrammetry, and PIV image analysis.** 15th International Conference on Soil Mechanics and Geotechnical Engineering. Istanbul, Turkey. pp 539-542. pub. Balkema, Rotterdam.

49. DJ. White, WA. Take, MD. Bolton, (2003). **Soil deformation measurement using particle image velocimetry (PIV) and photogrammetry.** Geotechnique 53, No. 7, 619–631.

50. P. Wickramarachchi, K. Kawamoto, S. Hamamoto, M. Nagamori, P. Moldrup, T. Komatsu (2011), **Effects of dry bulk density and particle size fraction on gas transport parameters in variably saturated landfill cover soil**. Waste Management 31, 2464–2472.

Standards:

51. NF P 11-300: Classification des matériaux utilisables dans la construction des remblais et des couches de forme d´infrastructures routières.

52. XP P 94-011: Description — Identification — Dénomination des sols.

53. XP P 94-010: Glossaire géotechnique.

54. NF P 94-050: Détermination de la tenueur eu eau pondérale des matériaux.

55. NF P 94-056: Analyse granulometrique. Méthode par étuvage.

56. NF P 94-057: Analyse granulometrique. Méthode hydrometrique.

57. NF P 94-068: Essai au bleu de méthylène sur un sol par l'essai à la tâche.

58. XP P 94-090-1: Essais de compressibilité sur matériaux fins quasi saturés avec chargement par paliers à l'oedomètre.

59. NF P 94 093: Essai de compactage Proctor- essai Proctor normal et modifié.

60. NF P 94-077: Essai de compression simple.

Web pages

1. www.andra.fr
2. www.enresa.es
3. www.geosyntheticssociety.org
4. www.iaea.org
5. http://insc.ans.org/
6. www.nrc.gov
7. www.trisoplast.nl
8. www.vettenfall.se
9. www.word-nuclear.org